HELMHOLTZ
CENTRE FOR
ENVIRONMENTAL
RESEARCH – UFZ

PhD Dissertation 08/2008

Radon as a natural geochemical tracer for study of groundwater discharge into lakes

Axel Schmidt

ISSN 1860-0387

Radon as a natural geochemical tracer for study of groundwater discharge into lakes

Inaugural-Dissertation

zur

Erlangung des Doktorgrades

der Mathematisch-Naturwissenschaftlichen Fakultät

der Universität zu Köln

vorgelegt von

Axel Schmidt

aus Naumburg/Saale

Leipzig 2008

Berichterstatter:	Prof. Dr. Martin Melles
	Prof. Dr. Michael Schlüter
	PD Dr. habil. Michael Schubert
Tag der mündlichen Prüfung:	27. Juni 2008

+ = −

Je mehr
die Sonne scheint
desto mehr
Wasser verdunstet
es entstehen
mehr Wolken
und
die Sonne
scheint weniger

Je weniger
die Sonne scheint
desto weniger
Wasser verdunstet
es entstehen
weniger Wolken
und
die Sonne
scheint mehr

da capo

Josef Albers

Zusammenfassung

In der vorliegenden Arbeit wurde die Eignung des natürlich vorkommenden, radioaktiven Edelgas-Isotops Radon-222 (^{222}Rn) zur qualitativen und quantitativen Beschreibung von Grundwassereinträgen in Seen untersucht.

Als Grundlage für die Untersuchungen wurden zwei neuartige Techniken zur Vor-Ort Bestimmung von Radon in Wässern entwickelt. Eine Methode erlaubt eine Detektion von Radon außerhalb (ex-situ), die andere eine Bestimmung von Radon innerhalb (in-situ) des entsprechenden Wasserkörpers. Bei der ex-situ Messung wird Wasser aus dem Untersuchungsgewässer durch eine Austauschzelle geleitet. Innerhalb dieser Zelle wird das im Wasser gelöste Radon durch Diffusion in einen entgegengesetzt verlaufenden, geschlossenen Luftstrom überführt und anschließend in einem Rado[illegible] detektiert. Bei der in-situ Radonbestimmung wird ein aus einer semipermeablen Membran bestehendes Modul in die Wassersäule eingebracht. Ein angeschlossenes Radonmessgerät erzeugt einen Luftstrom, der durch dieses Modul geleitet wird. Das in der Wassersäule gelöste Radon diffundiert anschließend durch die Membran in den entsprechenden, geschlossenen Luftstrom und wird durch diesen in das Radonmessgerät geleitet und dort detektiert.

Beide Verfahren wurden zur Verifizierung mit herkömmlichen Standardmethoden zur Messung von Radon in Wässern verglichen. Alle Methoden zeigen in ihrer Effizienz und zeitlichen Abhängigkeit in Bezug auf die Detektion von Radon-222 eine sehr gute Übereinstimmung.

Durch Kombination der neu entwickelten, mobilen Radonextraktionstechniken mit einem geeigneten tragbaren Messgerät ist es möglich, das Radon-222 in Grund- sowie Oberflächenwässern, d.h. innerhalb eines breiten Konzentrationsspektrums, mit hinreichender Genauigkeit (2σ-Fehler: ≤ 20 %) zu detektieren.

Radon-222 wurde anschließend eingesetzt, um die Grundwassereinträge in einen meromiktischen und in einen dimiktischen See zu charakterisieren, d.h. es wurden zwei Seentypen untersucht, die sich durch ihre jeweilige Wasserzirkulation grundsätzlich voneinander unterscheiden. Grundlage für die Beschreibung von Grundwassereinträgen in Seen mit Hilfe von Radon-222 als geochemischer Tracer bildet die Bilanzierung sämtlicher Quellen und Senken des Edelgases in Bezug auf eine repräsentative

Wassersäule des entsprechenden Oberflächengewässers. An beiden Untersuchungsstandorten konnte gezeigt werden, dass es basierend auf der Detektion von Radon-222 möglich ist, sowohl eine qualitative Beeinflussung des Seewasserkörpers durch Grundwasser nachzuweisen, als auch eine quantitative Abschätzung der Grundwasserzuflussmengen durchzuführen.

Zusammenfassend lässt sich sagen, dass die Nutzung des Edelgas-Isotops Radon-222 als geochemischer Tracer die Anwendung von Vor-Ort Detektionstechniken möglich macht und somit eine schnelle, zuverlässige und kostengünstige Beschreibung der Grundwasseranbindung von Seen erlaubt.

Abstract

In the presented work the suitability of the naturally occurring radioactive noble gas isotope radon-222 (^{222}Rn) for qualitative and quantitative description of groundwater discharge into lakes was studied.

Basis of these investigations was the development of two innovative techniques for the on-site determination of radon in water. One method allows the detection of radon outside the water body involved (ex-situ), the other within the said body (in-situ). In the ex-situ radon measurement procedure, water from the source concerned is taken up in an exchange cell used for this purpose. Inside this cell, the radon dissolved in water is transferred via diffusion into a closed counter-flow of air and subsequently detected by a radon-in-air monitor. Where the in-situ radon determination is concerned, a module composed of a semipermeable membrane is introduced into a water column. Subsequently, the radon dissolved in the water body diffuses through the membrane into the corresponding air flow, by means of which it is transferred into a radon-in-air monitor and is detected.

For verification purposes, both procedures were compared with conventional standard methods for the measurement of radon in water. All methods used show very good consistency in terms of their efficiency and the time required for the detection of radon-222.

Combination of the developed mobile radon extraction techniques with a suitable and portable radon monitor allow the detection of radon-222 with sufficient accuracy (2σ-error: ≤ 20 %) in groundwater as well as in surface waters, i.e., within a broad range of concentrations.

Radon-222 was subsequently used to characterize groundwater discharge into a meromictic and a dimictic lake, i.e., two types of lake basically distinct from each other with respect to their water circulation properties were investigated. Underlying basis of the description of groundwater discharge into lakes using radon-222 as a geochemical tracer is the balancing of all sources and sinks of the noble gas with reference to the water column of the respective surface water body. It could be shown at both investigation sites that it is possible to reveal a qualitative effect of groundwater on the lake water as well as a quantitative estimation of the groundwater discharge rates based

on the detection of radon-222.

In general, it can be stated that the use of the noble gas isotope radon-222 as a geochemical tracer makes the application of on-site detection techniques possible and that this in turn permits a rapid, reliable, and cost-effective assessment of groundwater discharge rates into lake water bodies.

Table of Contents

Danksagung

Die vorliegende Arbeit wäre ohne die Unterstützung unzähliger Personen nicht zustande gekommen – allen sei an dieser Stelle herzlich gedankt!

Ein großer Dank gebührt Herrn Professor William C. Burnett. Er war es, der mich bei meinem ersten Aufenthalt in seiner Arbeitsgruppe im Jahr 2002 von den Vorzügen des Radons überzeugte und dazu bewegte, dieses Edelgas im Bereich von Seen anzuwenden. Ebenso bedanke ich mich bei Natasha Dimova, Henrieta Dulaiova, Rick Peterson, Isaac Santos und Christina Stringer für die großartige Zusammenarbeit und die wunderschöne, gemeinsame Zeit.

Herrn Professor Martin Melles sei gedankt für seine Bereitschaft, sich mit dem Thema „Radon" auseinanderzusetzen, für die Betreuung dieser Arbeit und seine immerwährende Unterstützung während meiner Studien- und Promotionszeit.

Ein ganz besonderer Dank gebührt Herrn Dr. Michael Schubert. Er hat durch richtungsweisende Impulse viel zum Gelingen dieser Arbeit beigetragen, ohne mich dabei jedoch in deren Ausgestaltung einzuschränken. Ebenso bedanke ich mich für die Unterstützung und gute Zusammenarbeit bei meinen derzeitigen und ehemaligen Kollegen der Arbeitsgruppe Umweltradioisotope: Antje Böhnke, Daniel Geppert, Steve Gomell, Stefanie Härtel, Steffen Lau, Katja Lehmann, Nico Meye, Hanns-Christian Treutler und Nadine Zimmer.

Für die Bereitstellung von Felddaten zum Waldsee danke ich Severine Dietz und Uwe Kiwel. Anne Seebach sei gedankt für die angenehme Zeit in der Lausitz und anderswo.

Besonderer Dank kommt den Herrn Steffen Lau, Nils Reiche, Professor Michael Schlüter, Kevin Tattrie und Dr. Rainer Wennrich für ihre kritische Durchsicht früherer Manuskripte dieser Arbeit zu.

Der Studienstiftung des deutschen Volkes danke ich für die großartige finanzielle und ideelle Unterstützung während meiner Promotion. Erst hierdurch war es mir möglich, das vorliegende Thema nach meinen Wünschen und Vorstellungen gestalten und ausführen zu können.

Susan Krause danke ich für ihr Verständnis, ihre Geduld und Rücksichtnahme, sowie ihrer Fähigkeit, mir zu zeigen, dass Wissenschaft nicht alles ist.

Ein besonderer Dank gilt meinen Eltern, Manfred und Sigrid Schmidt. Die vorliegende Arbeit wäre nie entstanden ohne ihre immerwährende Unterstützung, ihr Vertrauen und ihre Liebe.

List of Figures

List of Tables

1 Introduction

Lakes are integral parts of the global hydrological system. Even though they just represent a small part of the entire water volume on earth, lakes are of great importance to humanity for water supply, as a source of power, for recreation, and for aesthetic value, as well as to ecology for providing unique habitat for diverse communities of flora and fauna.

Much interest in the hydrology of lakes is centred on water budgets. Water budgets are needed in order to manage lake water volumes, to determine chemical budgets, and to predict future development of the respective water resources. Water budgets are in general defined by input and output terms. Potential sources of water to lakes are direct precipitation, inflowing streams, diffusive surface run-off, and discharging groundwater. Losses occur due to evaporation, streams, and subsurface outflow. Although the relative importance of these input and output terms may vary greatly according to physiographic and climatic settings, each term has the potential to essentially influence the quality of the lake water.

However, historically groundwater discharge has been considered a minor component of a lake's overall water budget, and, as a result, it was often ignored (Harvey et al. 2000). In recent years the importance of groundwater discharge into surface waters has been increasingly recognized because of its potential significance as a source of natural and anthropogenically–derived dissolved chemical components. Since the concentrations of dissolved species in groundwater are often higher than in surface waters, even small amounts of groundwater input into surface waters may have important effects. Furthermore, the exchange of water between aquifers and lakes potentially provides a major pathway for chemical transfer between these hydraulically connected water bodies. For instance, the migration of dissolved carbon, oxygen, and/or nutrients coupled to such exchange processes must be considered a main driver for biogeochemical processes on both sides of the groundwater/surface water interface (Moore 2006, Swarzenski et al. 2006, Santos et al. 2008a, Santos et al. 2008b). Nutrients, for example, if transported by discharging groundwater into a lake water body can strongly influence the ecosystem of the lake (Shaw et al. 1990c, Gallagher et al. 1996, Hayashi and Rosenberry 2002, Sebestyen and Schneider 2004) as well as the

nitrogen/phosphorus ratio of the lake water (Hagerthey and Kerfoot 1998). While nutrient input and the potentially resulting eutrophication are mainly an issue in heavily fertilized areas, groundwater/lake water interactions are also important in other regions, e.g. in former lignite mining areas. As shown by many authors, groundwater discharge into open-pit lignite mining lakes is often associated with particular geochemical reactions which are likely to have significant negative impact on the quality of the lake water body (Evangelou and Zhang 1995, Göttlicher and Gasharova 2000, Knöller and Strauch 2002, Knöller et al. 2004, Blodau 2006). Lake water acidification due to oxidation of sedimentary iron sulfides (pyrite, FeS_2) can be exemplified as a hydrochemical problem typically connected to such aquatic systems. Poor ecological conditions of the lake and a resulting negative impact on the general economic value of the entire post mining area are likely consequences. Furthermore, in the vicinity of urban areas or industrial mega sites, dissolved contaminants such as pharmaceuticals (Wiegel et al. 2004, Reinstorf et al. 2008) and heavy metals (Gandy et al. 2007) are not only influential on the aquatic life and the biological properties of an affected water body, but also on its overall water quality.

The relative impact of groundwater to a particular water body is controlled by the underlying strata and the source of groundwater-derived constituents (Kishel and Gerla 2002, Swarzenski et al. 2007, Weinstein et al. 2007). The increase of groundwater discharge into surface water is caused by natural, e.g. high precipitation rates, relief, and hydraulic conductivity (Zektser and Loaiciga 1993) as well as anthropogenic factors, e.g. pumping and irrigation (Santos et al. 2008b). These parameters can change the pressure head, the most important single factor controlling groundwater flow and hence groundwater discharge. Since alterations in either groundwater quantity or quality could result in deterioration of lake (eco-)systems, knowledge of the complete water budget, including groundwater contributions, is essential for the development of sustainable water management strategies (Schneider et al. 2005). Thus, comprehensive understanding of groundwater/lake water interaction and tracing of pathways between these hydraulically connected systems are essential for the protection and the future development of the respective water resources and are a significant contribution for environmental protection.

Groundwater discharge is often patchy, diffuse, temporally-variable, and may respond

to multiple driving forces (Shaw and Prepas 1990b, Sebestyen and Schneider 2001, Burnett et al. 2003a, Schneider at al. 2005, Weinstein et al. 2007). Basically, there are three approaches for measuring groundwater discharge: hydrologic modeling, direct physical measurement with seepage meters, and use of geochemical tracers. Since seepage meters only allow a spot measurement of the rate and the quality of discharging groundwater (Lee 1977), many seepage meters are needed in order to evaluate the spatial and temporal variability of groundwater discharge (Shaw and Prepas 1990a, Taniguchi et al. 2006). On the other hand, geochemical tracer signals, which are coming into the surface water with the groundwater, are integrated by the water column. Because smaller-scale variations are smoothed out that way, the tracer approach is a very good way to deal with large spatial heterogeneity problems that are associated with groundwater pathways (Cook et al. 2003, Burnett et al. 2006, Swarzenski 2007). Therefore, naturally occurring substances, such as certain unstable (e.g. radium; Moore 1996, Kraemer 2005) or stable isotopes (e.g. ^{2}H, ^{18}O; Yehdegho et al. 1997, Gibson et al. 2002), dissolved noble gases (e.g. helium; McCoy et al. 2007), or anthropogenic compounds such as SF_6 or CFC's (Cook et al. 1995, Gooddy et al. 2006) are commonly applied as geochemical tracers for the investigation of groundwater/surface water interactions.

The naturally occurring radon-222 has also been applied successfully for assessment of groundwater discharge into surface waters. For example, it has widely been used for the study of groundwater interactions with coastal water (Cable et al. 1996, Burnett et al. 2003a, Chanton et al. 2003, Schlüter et al. 2004, Crusius et al. 2005, Burnett et al. 2008, Cable and Martin 2008), as well as river water (Ellins et al. 1990, Cook et al. 2003, Wu et al. 2004, Cook et al. 2006, Mullinger at al. 2007). However, just a few studies report on using radon-222 as a tracer for the estimation of groundwater discharge into lake water bodies (Corbett et al. 1997, Tuccimei et al. 2005, Kluge et al. 2007).

The research described in this dissertation aimed to assess the applicability of radon-222 as a geochemical tracer for the qualification and quantification of groundwater discharge into lakes.

Radon is a radioactive noble gas. In Chapter 2 the processes of natural radioactivity, statistics of radioactive decay as well as physical and chemical properties of radon are

presented. Further on, the origin and the behavior of radon-222 in the (aquatic) environment is reported and the applicability of the noble gas as a geochemical tracer is discussed.

The usefulness of radon-222 as a tracer is limited by the time consuming nature of collecting discrete water samples and conventional (laboratory) analysis procedures. In Chapter 3 new approaches for the on-site determination of radon in water are presented. Section 3.1 deals with continuous and discrete detection of radon in ground- and surface waters by means of an ex-situ extraction cell. Section 3.2 reports a method for in-situ determination of radon activity concentrations in surface waters by means of hydrophobic membrane tubing.

Chapter 4 demonstrates the application of radon-222 as a geochemical tracer of groundwater discharge into different lake environments. Section 4.1 reports on groundwater discharge into an exemplary lignite mining lake. The lake is meromictic, i.e., the water body is subdivided horizontally into two separate layers – the upper mixolimnion (with seasonal mixing) and the lower monimolimnion (without seasonal mixing). Section 4.2 presents a study on the assessment of groundwater discharge into a dimictic lake, i.e., a water body with biannual mixing.

2 Theoretical background

2.1 Physical and chemical background

2.1.1 Basics of radioactive decay

Radioactivity is a natural and spontaneous process by which unstable atomic nuclei emit particles or radiate excess energy. These processes result in a transforming of an atom (isotope, radionuclide) of one type, called the parent nucleus, to an atom of a different type, called the daughter nucleus. The radioactive decay is a random process and is subject to the laws of statistics.

Activity

The decay rate of an unstable nucleus is described by its activity, i.e., by the number of atoms that decay per time unit. The unit of activity is the Becquerel (Bq), defined as one decay per second: 1 Bq = 1 s^{-1} (Turner 2007).

The activity of a substance related to its mass is called specific activity (Bq kg^{-1}); the activity related to its volume is called activity concentration (Bq l^{-1} or Bq m^{-3}).

Decay law

The activity can be described by a linear differential equation, the so called decay law (Eq. 2-1), where the number of atoms (dN) decaying in a given time interval (dt) is proportional to the number of radioactive atoms present (N). The proportionality constant is called the decay constant.

$$A(t) = -\lambda N(t) = \frac{dN}{dt} \qquad \text{Eq. 2-1}$$

$A(t)$	activity	[Bq]
λ	decay constant	[s^{-1}]
$\left(\frac{dN}{dt}\right)$		[-]

The negative sign of the decay constant signifies a decreasing number of radionuclides with time. The solution of Eq. 2-1 after integration with respect to time provides the following relation.

$$N(t) = N_0 e^{-\lambda t} \qquad \text{Eq. 2-2}$$

$N(t)$	number of atoms at time t	[-]
N_0	number of atoms at time t = 0	[-]
λ	decay constant	[s^{-1}]
t	time	[s]

The decay constant is dependent on the half-life of the respective radionuclide and can be calculated by the transformation of Eq. 2-2 with respect to λ.

$$\lambda = \frac{\ln 2}{t_{1/2}} \qquad \text{Eq. 2-3}$$

λ	decay constant	[s^{-1}]
$t_{1/2}$	half-life	[s]

The half-life is the time required for a quantity of atoms to decay to half of its initial value, i.e., after one half-life 50 % of the initially present atoms will have decayed, according to the statistic. The decay constant statistically refers to the probability of the number of nuclei that will undergo radioactive transformation in a certain time interval. Half-life and decay constant are characteristic properties of each radioactive isotope.

2.1.2 Modes of radioactive decay

In the following the three main types of radioactive transitions, i.e., alpha, and beta decay, and gamma radiation are presented. A common feature in all described modes is

the release of ionizing radiation, i.e., the energy of the released particles or radiation is sufficiently high enough to remove electrons from atoms and molecules, respectively (Turner 2007).

Alpha decay

Alpha decay is a process by which a so called alpha particle is emitted. The alpha particle is structurally equivalent to the nucleus of a helium atom and consists of two protons and two neutrons. It is emitted with discrete, element specific energies as a decay product of many radionuclides; predominantly with an atomic number higher than 82. For example, the radionuclide polonium-216 decays by alpha particle emission to yield the daughter nuclide lead-212:

$$^{216}_{84}\mathrm{Po} \rightarrow ^{212}_{82}\mathrm{Pb} + ^{4}_{2}\mathrm{He} + 6.78\,\mathrm{MeV} \qquad \text{Eq. 2-4}$$

Beta decay

In beta decay a beta particle (an electron or a positron) is emitted. In the case of electron emission, the process is referred to as "beta minus" (β^-), while in the case of positron emission it is referred to as "beta plus" (β^+) decay.

In β^- decay, a neutron (n^0) is converted into a proton (p^+) while emitting an electron (e^-) and an anti-neutrino ($^0_0\overline{\nu}$). In β^+ decay, a proton is converted into a neutron while emitting a positron (e^+) and a neutrino ($^0_0\nu$).

Gamma radiation

The daughter nuclides produced by alpha and beta decay are often obtained in an excited energy state. The energy associated with this excited state is released when the nucleus returns to its ground state by emitting a photon. The emitted electromagnetic radiation is called gamma radiation. Thus, the emission of gamma radiation is not a mode of radioactive decay (such as alpha and beta decay), it is rather a mechanism by which excess energy is emitted from certain radionuclides, i.e., highly energetic

electromagnetic radiation emitted from the nucleus of the atom.

2.1.3 Statistics of radioactive decay

Measurements always have errors, i.e., differences between the actually measured value of a physical quantity and the true value of the same physical quantity cannot be avoided. Therefore the estimation of measurement uncertainties is central to the concept of measurement. In statistics two types of measurement errors are distinguished: systematic and random errors.

A systematic error is any biasing effect in the environment, in the methods of observation or in the instruments used, which introduces error into an experiment in a way that it always shifts the results of an experiment in the same direction. All measurements are prone to systematic error. Constant systematic errors are very difficult to deal with, because their effects cannot be dealt with by just repeating measurements or averaging large numbers of results. A common means to remove a systematic error is the observation of a known process, i.e., through calibration.

Random errors, on the other hand, are mainly due to the statistical nature of processes observed, as for instance in the case of radioactive decay. Thus, random errors can be evaluated by methods of statistics, in contrast to systematical errors. In general, random errors affect the precision of measurements while systematic errors influence the accuracy of measurements (Menditto et al. 2007).

Radioactive decay as a random process is subject to the laws of statistics. Counting statistics provides the means to describe the average behavior of nuclear decays in a certain sample and is used to express the probability of obtaining a given count within a certain confidence interval. If radioactive decay occurs within a certain time interval the process can be described by a continuous probability distribution (Gaussian distribution). This distribution is characterized by two independent parameters: the arithmetic mean and the standard deviation. The arithmetic mean of all counts within a certain time interval can be calculated by following equation (Turner 2007).

$$\bar{x} = \frac{1}{n}\sum_{i=1}^{n} x_i \qquad \text{Eq. 2-5}$$

$\bar{x}$ arithmetic mean

n n-Measurements

x_i measurement value

The standard deviation of values is a measure of the spread of its values compared to the arithmetic mean and can be calculated applying Eq. 2-6 (Turner 2007).

$$\sigma = \sqrt{\frac{1}{n}\sum_{i=1}^{n}(x_i - \bar{x})^2} \qquad \text{Eq. 2-6}$$

σ standard deviation

n n-Measurements

x_i measurement value

$\bar{x}$ arithmetic mean

By applying of these two parameters the Gaussian distribution can be written as the probability density for the continuous random variable x (Eq. 2-7, Turner 2007). The application of Gaussian distribution leads to confidence intervals (σ), which are very important for counting measurements. Confidence intervals are divided between $\pm 1\sigma$, $\pm 2\sigma$, and $\pm 3\sigma$, i.e., 1σ covers 68 %, 2σ 95 %, and 3σ 99 % of all values within the Gaussian distribution (Figure 2-1).

$$p(x) = \frac{1}{\sigma\sqrt{2\pi}} \exp\left[-\frac{(x-\bar{x})^2}{2\sigma^2}\right] \qquad \text{Eq. 2-7}$$

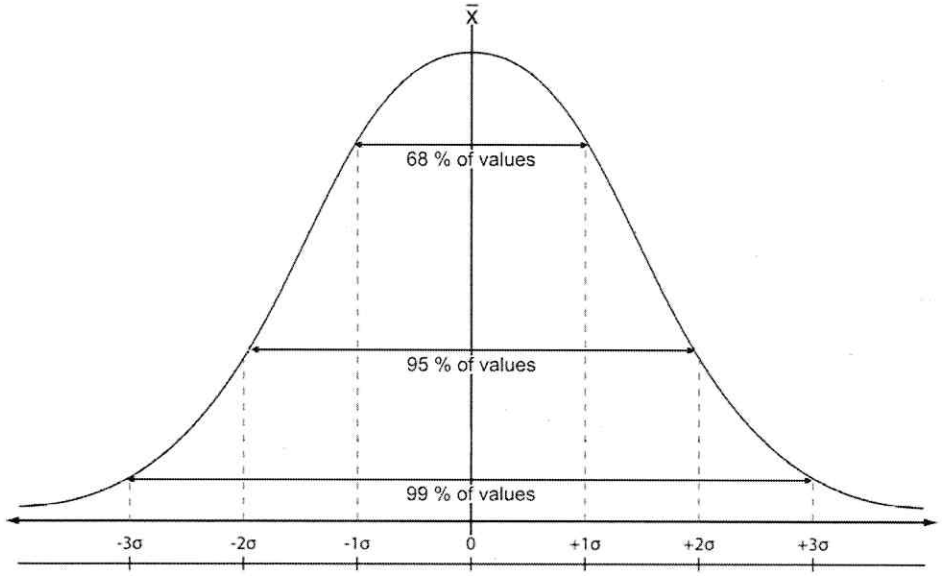

Figure 2-1: Gaussian distribution with specific confidence intervals (Turner 2007, modified).

2.1.4 Physical and chemical properties of radon

Radon (Rn) is an element of the noble gas group. It is monomolecular, colorless, odorless, and savorless. With a density of 9.73 g l^{-1} it is the heaviest and with 202.15 and 211.35 K it has the highest melting and boiling points, respectively, of all noble gases (Weigel 1978). Some characteristic properties of radon are summarized in Table 2-1.

In spite of its noble gas properties and the resulting stable electron configuration, which leads to a chemically inert behavior, some chemical compounds of radon are known. In laboratory tests (unstable) compounds between radon and fluoride (RnF_2, RnF_4, RnF_6; Avrorin et al. 1981) and the solution of radon in different fluoride compounds as well as a fixation of radon as clathrates were observed (Weigel 1978, Stein 1983). Likewise an adsorptive fixation of radon on activated carbon (Cohen and Nason 1986, Bocanegra and Hopke 1988, Gaul and Underhill 2005) and silica gel (De Jong et al. 2005) was reported.

Table 2-1: Properties of radon-222 under standard state (T = 273.15 K, p = 101 325 Pa; Weigel 1978, Stein 1983, Cothern 1987, Wilkening 1990).

Atomic mass (relative)	222 g mol^{-1}
Atomic radius (calculated)	120 pm
Atomic volume	50.5 cm^3 mol^{-1}
Density	9.73 g l^{-1}
Electron configuration	[Xe] $4f^{14}$ $5d^{10}$ $6s^2$ $6p^6$
Electrons per energy level	2, 8, 18, 32, 18, 8
Electronegativity (absolute)	5.1 eV
First ionization energy	1037 kJ mol^{-1}
Conductivity (thermal)	0.00364 W m^{-1} K^{-1}
Molar volume	50.5 × 10^{-6} m^3 mol^{-1}
Radius (covalent)	145 pm
Enthalpy of fusion	2.89 kJ mol^{-1}
Melting point	202.15 K
Boiling point	211.35 K
Enthalpy of evaporation	16.40 kJ mol^{-1}
Specific heat capacity	94 J kg^{-1} K^{-1}

Besides the mentioned chemical and adsorptive compounds radon also dissolves in aqueous and non-aqueous phase-liquids. For the description of the solution behavior of radon in aqueous liquids and the resulting partition behavior of the noble gas between the aqueous liquid and the surrounding air the "theory of regular solutions" can be applied (Hildebrand 1929, Scatchard 1931). This theory uses as parameters for the inter-molecular forces in the liquid phase the so called "cohesive energy density". This term is defined as the ratio of the enthalpy of evaporation and the respective molar volume of the liquid phase (Eq. 2-8).

The square root of the cohesive energy density is called the Hildebrand solubility parameter (δ) - named after the physicist Joel Hildebrand. If a liquid phase characterized by a high Hildebrand parameter is mixed with a liquid phase characterized by a low Hildebrand parameter (and vice versa), much more energy is required for mutual dispersion than can be gained by the actual mixing process resulting in immiscibility. On the other hand, two liquid phases with similar Hildebrand parameters gain sufficient energy on mutual dispersion to result in an energy balance that allows miscibility.

$$c = \frac{\Delta H_V - RT}{V_m} \qquad \text{Eq. 2-8}$$

c	cohesive energy density	[J l^{-1}]
ΔH_V	enthalpy of evaporation	[kJ mol^{-1}]
R	general gas constant	[J mol^{-1} K^{-1}]
T	temperature	[K]
V_m	molar volume	[l mol^{-1}]

The Hildebrand solubility parameter is used for the thermodynamic description of liquid phases. If gases, such as radon, are considered, i.e., if the Hildebrand parameters of liquids are to be compared to those of gases, the gases have to be treated as hypothetically liquid solutes at atmospheric pressure (Prausnitz et al. 1986). If a gas has a Hildebrand parameter close to that of a liquid, gas and liquid show good mutual solubility (Steinberg and Manowitz 1959).

By using Eq. 2-8 and the data given in Table 2-1 the Hildebrand parameter for radon amounts to about 18.1 $MPa^{1/2}$. Water, on the other hand, shows a Hildebrand parameter of about 47.9 $MPa^{1/2}$. The resulting specific solubility of radon in water can be expressed by the temperature dependent partition coefficient of radon ($k_{w/air}$) between water and the surrounding air (Eq. 2-9)

$$k_{w/air} = \frac{C_{Rn}^{w}}{C_{Rn}^{air}} \qquad \text{Eq. 2-9}$$

$k_{w/air}$	radon partition coefficient between water and air	[-]
C_{Rn}^{w}	radon activity concentration - water	[Bq m^{-3}]
C_{Rn}^{air}	radon activity concentration - air	[Bq m^{-3}]

Weigel (1978) developed an empirical regression equation (Eq. 2-10) for the estimation of the radon partition coefficient between water and air by using Eq. 2-9. This temperature dependent partition coefficient ($k_{w/air}$) expresses the ratio of the equilibrium

radon activity concentration between water and air. For instance, the partition coefficient of radon in water for a temperature of 25°C is 0.25.

$$k_{w/air} = 0.105 + 0.405\ e^{-0.0502\ T} \qquad \text{Eq. 2-10}$$

$k_{w/air}$	radon partition coefficient between water and air	[-]
T	water temperature	[°C]

Non-aqueous phase-liquids (NAPL's), like toluene, benzene, or xylene have Hildebrand parameters which are similar to radon (Table 2-2), i.e., the solubility of radon in NAPL is much better than in water. The resulting radon retardation by NAPL allows the use of radon activity concentration patterns for localizing and assessing residual NAPL contamination of aquifers (Semprini et al. 2000, Hoehener and Surbeck 2004, Lau et al. 2004, Schubert et al. 2007a, Schubert et al. 2007b).

Table 2-2: Hildebrand parameter (δ) of selected liquid phases and their partition coefficients ($k_{w/air}$) at 25°C (Barton 1991).

Liquid phase	δ [$MPa^{1/2}$]	Partition coefficient [-]
Water	47.9	0.25
Hexane	14.9	16.56
Benzene	18.8	12.82
Toluene	18.2	13.24
Xylene	18.0	15.40
Methanol	29.6	5.71
Ethanol	26.0	6.17
Isopropanol	24.3	6.16
2-Butanol	22.1	7.58
Glycerol	33.7	0.21
Acetone	20.2	6.30
Diethyl ether	15.1	15.08
Formic acid	24.7	1.05
Acetic acid	20.7	4.43
Butyric acid	21.5	7.52

2.2 Geological background

2.2.1 Radon as part of the natural decay chains

Radon occurs naturally in five different isotopes. The three most important are actinon (radon-219), thoron (radon-220), and radon (radon-222). These isotopes are members of the natural radioactive decay chain of uranium-235, thorium-232, and uranium-238, respectively, in which radon is produced via α-decay from its parent nuclide radium (Ra) and decays to polonium (Po). End members of each decay chain are stable isotopes of lead (Table 2-3).

Table 2-3: Selected members of the naturally decay chains of uranium-238, thorium-232, and uranium-235, their respective half-lives, and decay modes. The short-lived radon progeny is marked in grey (Schubert 2006, modified).

	Uranium-238-chain	Thorium-232-chain	Uranium-235-chain
Origin isotope	U-238	Th-232	U-235
Half-life $t_{1/2}$	4.47×10^9 a	1.41×10^{10} a	7.04×10^8 a
Decay	α	α	α
	•	•	•
Radium	Ra-226	Ra-224	Ra-223
Half-life $t_{1/2}$	1600 a	3.66 d	11.44 d
Decay	α	α	α
Radon	Rn-222	Rn-220	Rn-219
Half-life $t_{1/2}$	3.82 d	55.6 s	3.96 s
Decay	α	α	α
Polonium	Po-218	Po-216	Po-215
Half-life $t_{1/2}$	183 s	0.15 s	1.78 ms
Decay	α	α	α
Lead	Pb-214	Pb-212	Pb-211
Half-life $t_{1/2}$	26.8 min	10.64 h	36.1 min
Decay	β	β	β
Wismuth	Bi-214	Bi-212	Bi-211
Half-life $t_{1/2}$	19.9 min	60.55 min	2.14 min
Decay	β	β	β
Polonium	Po-214	Po-212	Po-211
Half-life $t_{1/2}$	164.3 µs	0.29 µs	0.52 s
Decay	α	α	α
	•	•	•
Lead as stable endmember	Pb-206	Pb-208	Pb-207

The four daughter nuclides of radon-222 (polonium-218, lead-214, wismuth-214, and polonium-214) are characterized by very short half-lives, i.e., they decay virtual instantly in relation to radon. In a so called secular equilibrium the quantity of the four daughter nuclides remains constant because its production rate (due to the decay of radon) is equal to its decay rate. Hence, between the four daughter nuclides and radon a radiogenic decay equilibrium is built up, which achieves 97 % after 150 min (cf. Eq. 2-2, Eq. 2-3), i.e. after five half-lives of lead-214 ($t_{1/2}$ = 26.8 min), as the longest-lived of the four.

With respect to the very short half-lives of radon-219 ($t_{1/2}$ = 3.96 s) and radon-220 ($t_{1/2}$ = 55.6 s), only radon-222 ($t_{1/2}$ = 3.82 d) is predestinated for the investigation of (hydrological) processes which occur within a time scale of up to four half-lives, i.e., about 16 days (Hoehn and von Gunten 1989). Hence, all investigations described in this thesis are concerned only with the isotope radon-222, which is from here on solely referred to by the term "radon".

2.2.2 Radon as an omnipresent component of groundwater

Radon is the daughter nuclide of radium-226, which, in turn, derives from the decay of uranium-238. In all igneous, sedimentary, and metamorphic rocks uranium and radium are ubiquitous elements. The quantity of radon produced within rocks and, hence, in the grain framework of an aquifer depends directly on the specific activity of radium-226 (A_{Ra}) within the mineral matrix. A few examples for mean specific radium-226 activities of different rocks species are shown in Table 2-4.

Within the mineral matrix of an aquifer radon is produced continuously because of the α-decay of radium within the ion grid. The liberated kinetic energy during this process (~ 90 keV, Sun and Semkow 1998) leads to a vectored acceleration of the radon atom. For minerals, the recoil range of radon atoms varies between 0.02 and 0.07 µm (Tanner 1980, Sun and Semkow 1998, Cecil and Green 1999).

A diffusive emission of a radon atom from the mineral matrix into the surrounding pore space is negligible (Cecil and Green 1999), because of the half-life of radon and its small diffusion coefficient in crystal media of around 10^{-24} m^2 s^{-1} (Tanner 1980). Half-

life and diffusion coefficient allow diffusion lengths[1] in crystal media of about 10^{-7} to 10^{-26} µm (Nazaroff 1992).

Table 2-4: Mean specific radium-226 activities of rock species (Nazaroff et al. 1988).

Rock classification	Rock	A_{Ra-226} (mean) [Bq kg^{-1}]	Number of samples
Alkali-Feldspar-Pluton	Syenite	692	75
Alkali-Feldspar-Volcanic rock	Phonolite	368	138
Acid Pluton	Granite	78	569
Acid Volcanic rock	Rhyolite	71	131
Intermediate Pluton	Diorite	40	271
Intermediate Volcanic rock	Andesite	26	71
Alkaline Pluton	Gabbro	10	119
Alkaline Volcanic rock	Basalt	11	77
Metamorphic Igneous rock	Gneiss	50	138
Metamorphic Sedimentary rock	Slate	37	207
Evaporite	Limestone	25	141

Because of the insignificant diffusive part the only way for radon to leave the mineral matrix is recoil by the decay of radium. Only radon atoms which are produced in close vicinity to the grain surface area (within the recoil range), and which are accelerated into the direction of the grain surface have a chance to reach the pore space (Figure 2-2: A, B, E). In the pore space the radon atom is less braked than in the mineral, hence, recoil lengths within the pore space are much larger. If the pore space is saturated with water recoil distances are around 0.1 µm (Tanner 1980), in the unsaturated pore space recoil length can reach up to 63 µm (Tanner 1980, Sun and Semkow 1998, Cecil and Green 1999).

The escape of radon from the mineral matrix into the pore space is called radon-emanation. The ratio of the amount of radon, which leaves the mineral matrix, and the total radon, which is produced within the mineral matrix, is described by the emanation

[1] Diffusion length is a distance on which the concentration of a radioactive material is reducing about the factor e^{-1} by the diffusion through a non-radioactive media (Bonotto and Andrews 1997).

coefficient (Eq. 2-11, Tanner 1980). Emanation coefficients of different mineral materials are shown in Table 2-5.

$$\varepsilon = \frac{N^e}{N^p} \qquad \text{Eq. 2-11}$$

ε	emanation coefficient	[-]
N^e	number of radon atoms which emanate into the pore space	[-]
N^p	number of radon atoms which are produced in the mineral grain	[-]

Table 2-5: Emanation coefficient (ε) of mineral materials.

Material	ε	Reference
Bedrock (hackled)		
Gneiss (4 % water saturation)	0.05 - 0.60	Przylibski 2000
Granite (4 % water saturation)	0.05 - 0.15	Przylibski 2000
Basalt (unknown moistness)	0.03 - 0.08	Barretto 1975
Conglomerate (unknown moistness)	0.02 - 0.10	Barretto 1975
Sandstone (unknown moistness)	0.03 - 0.12	Barretto 1975
Argillite (water saturated)	0.04 - 0.16	Ferry et al. 2002
Soil (unknown moistness)		
Sand	0.06 - 0.18	Nazaroff et al. 1988
Loam	0.17 - 0.23	Nazaroff et al. 1988
Clay	0.18 - 0.40	Nazaroff et al. 1988
Different soils	0.06 - 0.32	Greeman and Rose 1996
Minerals (hackled, unknown moistness)		
Plagioclase	0.02	Krishnaswami & Seidemann 1988
Hornblende	0.03	Krishnaswami & Seidemann 1988
Biotite	0.03 - 0.07	Barretto 1975
Monazite	0.002	Barretto 1975

Besides the radium content of the mineral matrix the spatial distribution of radium within a mineral grain and the resulting radon emanation coefficient are responsible for the radon activity concentration in the intra- and intergranular pore space.

In natural aquifers mineral grains are often characterized by an inhomogeneous radium distribution, because radium can be preferential enriched in secondary mineral phases,

e.g. in surface coatings (Andrews and Wood 1972, Tanner 1980, Ball et al. 1991, Purtscheller et al. 1995). Especially iron- and manganese oxides as well as manganese hydroxides are adapted to precipitate radium (and uranium) from a liquid solution and enrich those on mineral grains in a form of coatings. Furthermore, reducing conditions within an aquifer leads to precipitation and enrichment of uranium at mineral surfaces (Michel 1987, Schumann and Gundersen 1996, Porcelli and Swarzenski 2003). On the other hand, oxygen rich aquifers lead to a (re-)mobilization of uranium from the secondary minerals. Hence, although secondary minerals enlarge the radon emanation, other parameters, like redox- and temperature conditions and pH values influence the radon emanation of the grains within an aquifer (Abdelouas et al. 1998, Almeida et al. 2004).

Additionally, size and shape as well as the resulting specific surface area are important parameters for the emanation power of a mineral grain (Rama and Moore 1984, Schumann and Gundersen 1996, Bonotto and Andrews 1997). In general, an increase in the specific surface area of a grain leads to an increase of the emanation coefficient (Figure 2-2: C; Bossus 1984, Semkow and Parekh 1990, Semkow 1991, Maraziotis 1996, Przylibski 2000, Porcelli and Swarzenski 2003).

Further on, a key parameter for the activity concentration of radon within a pore space is the dry density of the matrix. The higher the porosity within an aquifer, i.e., the lower the dry density of the mineral matrix, the lower the number of the emanating radon atoms into the pore space. At the same time it has to be considered that at high packing density emanated radon atoms can drive into adjacent grains and hence are lost for the radon balance of the groundwater (Figure 2-2: D).

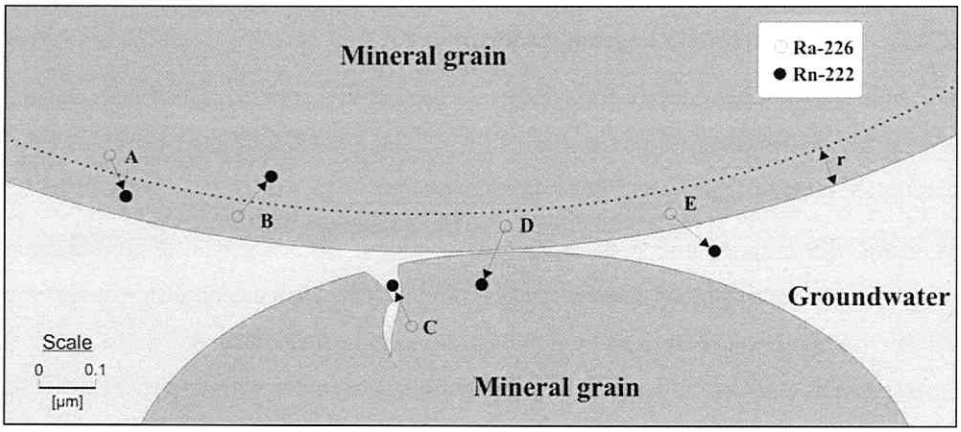

Figure 2-2: Schematic illustration of emanation processes (Tanner 1980, modified).

Two mineral grains are in contact with water. Radium-226 atoms decay yielding a radon-222 atom. r: maximal recoil range of radon atoms within the mineral grain. A, B: The radon atoms lie at greater depth within the mineral grain than the recoil range. C: The radon atom escapes from the mineral grain into a saturated pore space and is free to diffuse through the pores. D: The radon atom escapes from the grain and buries itself into an adjacent grain. E: The radon atom escapes from the mineral grain and loses the remainder of its recoil energy in the water and is free to diffuse through the pores.

Considering all mentioned parameters the radon activity concentration of groundwater can be quantified using Eq. 2-12 (Andrews and Wood 1972).

$$C_{Rn}^{gw} = \frac{\varepsilon A_{Ra} \rho_{dry}}{\Phi} \qquad \text{Eq. 2-12}$$

C_{Rn}^{gw}	radon activity concentration - groundwater	[Bq m^{-3}]
ε	emanation coefficient	[-]
A_{Ra}	specific radium-226 activity	[Bq kg^{-1}]
ρ_{dry}	dry density	[kg m^{-3}]
Φ	porosity	[-]

2.2.3 Radon migration in groundwater

An aquifer is a multi-component system: unconsolidated rocks and bedrocks are the spatial fixed subsystem; the pore space filling fluids (water: saturated; water and air: unsaturated) are the corresponding mobile subsystem.

As it was shown in the last section radon is an omnipresent component of groundwater. However, the radon activity concentration of groundwater depends on different specific aquifer parameters, as described by Eq. 2-12. Hence, in geochemical and petrographical homogeneous aquifers a homogeneous distribution of the radon activity concentration is expected. In contrast, in geochemical and petrographical heterogeneous aquifers the radon activity concentration is also non-uniform distributed. The build-up of lateral radon distribution patterns are the result of different local changes within the aquifer composition. Further on, in dependence on groundwater velocity abduction processes of the radon activity concentration from one aquifer area to another petrographical different are possible. The decay equilibrium of radon between the aquifer matrix and contacting groundwater justifies after 20 days to 97 % (cf. Eq. 2-2, Eq. 2-3), i.e., the distances over which a significant disequilibrium between radon activity concentration of the groundwater and the specific radium activity of the aquifer material is preserved is even in the case of high groundwater velocities only a few meters.

Changes in the hydrostatic potential field within an aquifer lead to an advective transport of radon. This process can be described by Darcy's law, which formulates the flow of groundwater volume per time and drained cross sectional area as function of the groundwater velocity. Hence, the advective radon transport is dependent on the groundwater velocity and can be described as follows.

$$J_{adv} = \frac{N_{adv}}{F_{eff}\, t} = v_{gw}\, C_{Rn}^{gw} \qquad \text{Eq. 2-13}$$

J_{adv}	advective mass flow	[Bq m^{-2} s^{-1}]
N_{adv}	advective particle flow	[Bq]
F_{eff}	available (effective) area	[m^2]
t	time	[s]
v_{gw}	groundwater velocity	[m s^{-1}]
C_{Rn}^{gw}	radon activity concentration - groundwater	[Bq m^{-3}]

The groundwater velocity is proportional to the attached pressure gradient (Eq. 2-14). The proportionality constant is defined by the permeability of the aquifer material and the dynamic viscosity of the groundwater. By the application of a one dimensional approach the particle flow is orientated from the higher to the lower pressure, on the other hand, the pressure gradient is vice versa. Hence, the proportionality constant shown in Eq. 2-14 has a negative sign.

$$v_{gw} = -\frac{k}{\eta}\left(\frac{\partial p}{\partial z}\right) \qquad \text{Eq. 2-14}$$

v_{gw}	groundwater velocity	[m s^{-1}]
k	permeability - aquifer	[m^2]
η	dynamic viscosity - groundwater	[kg m^{-1} s^{-1}]
$\left(\frac{\partial p}{\partial z}\right)$	pressure gradient	[kg m^{-1} s^{-2} m^{-1}]

Concentration differences within an aquifer lead to a radon migration. This process is based on Brownian motion and can be explained by molecular diffusion. Diffusion is the movement of particles of a substance from an area of high concentration to an area of low concentration, resulting in the uniform distribution of the substance. Hence, it is a vectorial movement mechanism, which is independent from water movement. The

diffusion process can be described mathematically by the diffusion equation. This equation is derived from Fick's law, which states that the net movement of diffusing particles per unit area of section ("flux") is proportional to the concentration gradient, and is towards lower concentration (Eq. 2-15). The constant of proportionality is the molecular diffusion coefficient of radon (D_m, $D_m = 1.14 \times 10^{-9}$ m^2 s^{-1} at 18°C, Rona 1917).

$$J_{diff} = -D_m \frac{\partial C}{\partial z} \qquad \text{Eq. 2-15}$$

J_{diff}	diffusive flux	[Bq m^{-2} s^{-1}]
D_m	molecular diffusion coefficient - radon	[m^2 s^{-1}]
$\left(\frac{\partial C}{\partial z}\right)$	concentration gradient	[Bq m^{-3} m^{-1}]

The positive diffusive flux is directed from the higher to the lower concentrations. The concentration gradient, on the other hand, shows vice versa. Hence, the proportionality constant shown in Eq. 2-15 has a negative sign.

Diffusion is a flux through a medium, i.e., the material in which diffusion takes place is an essential parameter for the characterization of the diffusion coefficient. Hence, diffusion within a surface water body and diffusion within a saturated sediment matrix are two different processes.

The diffusion coefficient within sediments (D_S) describes the limited diffusive movement of material within the saturated sediment matrix because of the interaction between aquatic and solid phases (e.g. physicochemical properties of the solid phase, ionic strength of the liquid phase at the pore space). D_S is mainly characterized by the geometry of the pores. The geometry of the pore network, on the other hand, is described by the parameter tortuosity. Tortuosity is defined as the ratio of the distance that an ion or molecule travels around particles (e.g. grains) and the direct path towards lower concentration (Maerki et al. 2004). The relation between D_S and tortuosity is given by Eq. 2-16 (Maerki et al. 2004).

$$D_S = \frac{D_W}{\theta^2} \qquad \text{Eq. 2-16}$$

D_S	diffusion coefficient - sediment	[$m^2\ s^{-1}$]
D_W	diffusion coefficient - water	[$m^2\ s^{-1}$]
θ	tortuosity	[-]

The directly determination of tortuosity is difficult and time consuming (Van Rees et al. 1991, Iversen and Jørgsen 1993, Maerki et al. 2004). Therefore, for the determination of D_S a mathematical approach introduced by Ullman and Aller (1982) can be used (Eq. 2-17).

$$D_S \approx D_W \Phi \qquad \text{Eq. 2-17}$$

D_S	diffusion coefficient - sediment	[$m^2\ s^{-1}$]
D_W	diffusion coefficient - water	[$m^2\ s^{-1}$]
Φ	sediment porosity	[-]

The diffusion coefficient of radon in surface water (D_W) can be calculated using an empirical temperature dependency expression developed by Peng et al. (1974).

$$-\log D_W = \left(\frac{980}{T}\right) + 1.59 \qquad \text{Eq. 2-18}$$

D_W	diffusion coefficient - water	[$m^2\ s^{-1}$]
T	temperature	[K]

By using D_S the non-steady-state, i.e., the spatial and temporal dependent diffusive radon flux within a porous sediment matrix can be described by using Fick's second law.

$$J_{diff} = \frac{\partial C(z,t)}{\partial t} = -D_S\left(\frac{\partial^2 C}{\partial x^2} + \frac{\partial^2 C}{\partial y^2} + \frac{\partial^2 C}{\partial z^2}\right) \qquad \text{Eq. 2-19}$$

J_{diff}	diffusive flux	[Bq m^{-2} s^{-1}]
D_S	diffusion coefficient - sediment	[m^2 s^{-1}]
$\left(\frac{\partial^2 C}{\partial (v)^2}\right)$	concentration gradient in x-, y-, z-direction	[Bq m^{-3} m^{-1}]

Besides advection and diffusion, radon migration within an aquifer is also influenced by dispersion. Dispersion describes the solute spreading about the mean motion caused by local fluctuations in groundwater velocity (Freeze and Cherry 1979, Jensen at al. 1993). Hence, this parameter is an additional flux dependent contribution to the radon migration within an aquifer. The dispersion flux can be described mathematically by Fick's first law. In the according equation (Eq. 2-20) the constant of proportionality is defined as the dispersion coefficient.

$$J_{disp} = -D_D \frac{\partial C}{\partial z} \qquad \text{Eq. 2-20}$$

J_{disp}	dispersion flux	[Bq m^{-2} s^{-1}]
D_D	dispersion coefficient - groundwater	[m^2 s^{-1}]
$\left(\frac{\partial C}{\partial z}\right)$	concentration gradient	[Bq m^{-3} m^{-1}]

The dispersion coefficient is directly related to groundwater velocity and can be calculated with the term dispersivity (Eq. 2-21).

$$D_D = \tau v_{gw} \qquad \text{Eq. 2-21}$$

D_D	dispersion coefficient - groundwater	[m^2 s^{-1}]
τ	dispersivity	[m]
v_{gw}	groundwater velocity	[m s^{-1}]

Dispersivity is a property of the porous medium. It is connected to the heterogeneous of the aquifer and to the scale on which the transport takes place. Dispersion is an anisotropic process even if the medium in which the process takes place shows isotropic properties. Thus, in a three dimensional room the dispersion coefficient can be described mathematically by a tensor, which simplifies to identity matrix, if the flux is one dimensional directed, e.g. in the case of groundwater movement.

Using the advection, diffusion, and dispersion terms (Eq. 2-13, Eq. 2-19, Eq. 2-20) and in consideration of continuous radon decay and radon production the radon migration within an aquifer can be described by a one dimensional advective-diffusive-transport model. However, considering that within an aquifer, pressure- and concentration gradients are one dimensional directed, dispersivity, porosity, specific radium-226 activity, and radon activity concentration are constant and the radon migration is not influenced by the diffusion of other substances, the general radon transport model simplifies to Eq. 2-22 (Craig 1969).

$$\frac{\partial C}{\partial t} = D_S \frac{\partial^2 C}{\partial z^2} + v_{gw} \frac{\partial C}{\partial z} + \lambda C_\infty - \lambda C = 0 \qquad \text{Eq. 2-22}$$

D_S	diffusion coefficient - sediment	$[m^2\ s^{-1}]$
$\left(\frac{\partial^2 C}{\partial z^2}\right)$	diffusive concentration gradient	$[Bq\ m^{-3}\ m^{-1}]$
v_{gw}	groundwater velocity	$[m\ s^{-1}]$
$\left(\frac{\partial C}{\partial z}\right)$	advective concentration gradient	$[Bq\ m^{-3}\ m^{-1}]$
λC_∞	radon production - aquifer	$[Bq\ m^{-3}\ s^{-1}]$
λC	radon decay - aquifer	$[Bq\ m^{-3}\ s^{-1}]$

In general a diffusive migration of radon within an aquifer is negligible because of its small diffusion coefficient. Thus, the transport of radon in groundwater is controlled by the advective migration only, i.e. it is directly dependent on the groundwater velocity.

2.3 Applicability of radon as a natural geochemical tracer for study of groundwater discharge into lakes

The high potential of radon for being used as a naturally occurring geochemical tracer for the study of groundwater discharge into surface water is generally due to three main characteristics.

The first property to be named is the ubiquitous occurrence of radon in the environment. As direct decay product of radium-226, being part of the natural uranium-238 decay chain, radon is produced in and emanated by virtually all kinds of mineral material. Radon that is emanated by an aquifer matrix enters the groundwater that occupies the aquifer pore space. Depending on the specific radium-226 activity and other aquifer material properties radon activity concentrations in groundwater generally vary between about 1 and 50 Bq l^{-1} (cf. section 2.2.2).

Surface waters contain radon as well. However, activity concentrations are typically two to three magnitudes below the activity concentrations found in groundwater. The low radon activity concentration that is characteristic for surface waters is due to (1) the limited contact of surface water bodies to radon emanating mineral material, (2) the usually low activity concentrations of dissolved radium-226 in the water, and (3) the radon half-life of 3.8 days. This half-life causes a radon diffusion length in (ground-) water of only about 2 cm (Tanner 1964), which normally results in a very sharp activity concentration gradient at the groundwater/surface water interface.

The second property, which has to be named as advantageous for the use of radon as a geochemical tracer, is its biologically and chemically inert behaviour. Due to its noble gas configuration radon does neither interact with mineral material or microorganisms, nor does its mobility depend on the chemical conditions present in the aquifer. Although some chemical radon compounds have been observed in laboratory experiments (cf. section 2.1.4), radon dissolved in groundwater is virtually not retarded while migrating with the groundwater through the aquifer even in very reactive environments (Treutler et al. 2007). The only exception here is the significant decrease of radon activity concentration in the groundwater if residual non-aqueous phase-liquid (NAPL) is present, a characteristic which is due to the in general very good solubility of radon in NAPL (cf. section 2.1.4).

The third reason predestining radon as a geochemical tracer is the fact that radon, in contrast to other geochemical tracers such as stabile isotopes or SF_6, does not merely allow tracing of groundwater migration pathways; it can also be used for assessing groundwater migration processes as a function of time. If surface water enters an aquifer, radioactive equilibrium between the water and the aquifer matrix will not be reached before about four radon half-lives have passed. Hence, the short half-life of radon permits the investigation of hydrological processes occurring within a time scale of up to 16 days (Hoehn and von Gunten 1989).

3 On-site techniques for determination of radon in water

3.1 Continuous and discrete on-site ex-situ determination of radon in ground- and surface waters

3.1.1 Introduction

Radon-in-water activity concentrations are conventionally detected by means of liquid scintillation counting (LSC) applying either water soluble scintillators or organic scintillation liquids after radon extraction into these organics (Pates and Mullinger 2007). A disadvantage of this conventional detection method is the fact that, if radon activity concentrations are low, background noise, precision, and accuracy of mobile LSC equipment is in most cases insufficient. Hence, laboratory measurements are required, an approach that is rather time consuming. Since large surface waters bodies, such as rivers or lakes, lack considerable contact to radon emanating mineral surfaces, they show significantly lower radon activity concentrations than groundwater and sediment pore waters. Hence, conventional LSC is not the method of choice if extensive radon surveys or on-site measurements of radon in groundwater wells or along track lines at surface waters are required.

Due to the limited on-site applicability of conventional LSC and the need of continuous and discrete radon-in-water measurements several alternative detection methods have been developed (Key et al. 1979, Mathieu et al. 1988, Stringer and Burnett 2004, Schubert et al. 2006a). They are based on stripping of radon from the water into a carrier gas and measuring the respective radon-in-gas activity concentration using a Lucas scintillation cell or a mobile radon-in-gas monitor. For example, Burnett et al. (2001) and Burnett and Dulaiova (2003) introduced a detection technique, in which the water is sprayed through a nozzle into the head space of an air filled extraction chamber ("RADAqua", Durridge Company, Inc.) that is combined with a mobile radon-in-air monitor. In the extraction chamber a part of the radon degasses from water sprayed into the air volume. The radon activity concentration equilibration between water and air is facilitated by the very fine droplets leaving the nozzle, i.e., by the large and continuously renewed water/air interface.

In general radon activity concentration equilibrium between water and air is determined by the respective partition coefficient. This coefficient depends on the temperature in the system as it was given in Eq. 2-10 (Weigel 1978).

In the following chapter a robust and straightforward method for on-site ex-situ

determination of radon activity concentrations in water is presented. The methodical approach is based on the principle of liquid-gas-membrane-extraction. The used extraction cell, which consists of hollow polypropylene fibres, allows radon stripping from the water of interest into a connected closed air loop. The resulting radon-in-air activity concentration, which can easily be re-converted into the original radon-in-water activity concentration is measured by means of a standard mobile radon-in-air monitor. The experimental setup allows radon detection in discrete water samples as well as in continuous water pump streams.

The study discussed in the following section has been published in a modified form as:

Schmidt, A., Schlueter, M., Melles, M., Schubert, M. (2008). Continuous and discrete on-site detection of radon-222 in ground- and surface waters by means of an extraction module. *Applied Radiation and Isotopes,* doi:10.1016/j.apradiso.2008.05.005.

3.1.2 Material

Equipment

The equipment applied for the measurement of radon activity concentrations in both, pump streams of continuously running water and discrete samples, consists of two main parts: a standard mobile radon-in-air monitor and a hollow fibre membrane extraction cell applicable for radon membrane extraction.

Mobile radon-in-air monitor

For all experiments the RAD-7 (Durridge Company, Inc.) was used as mobile radon-in-air monitor. The monitor consists of a one litre half-spherical detection chamber. It allows determination of radon-in-air activity concentrations by detecting the short-lived α-emitting radon progeny polonium-218 ($t_{1/2}$ = 3.05 min; α-energy 6.00 MeV) and polonium-214 ($t_{1/2}$ = 164 ms; α-energy 7.69 MeV) using a passivated implanted planar silicon alpha detector (PIPS). The detection system allows energy discrimination and hence distinguishing between polonium-218 and polonium-214 decays. Both polonium nuclides can be used as proxy for the radon activity concentration in the air that is pumped through the RAD-7 detection chamber. The air stream is maintained with an internal air pump. Since an air moisture content of less than 10 % is mandatory for operating the PIPS detector, an external air drying unit has to be implemented in the air

stream. However, while radioactive equilibrium between radon and polonium-218 is reached within about 15 min (i.e., after about five polonium-218 half-lives), nearly 3 h are required for radioactive equilibration between radon and polonium-214. That longer equilibration time is due to the half-life of lead-214 ($t_{1/2}$ = 27 min), which precedes polonium-214 in the decay chain.

Extraction cell

For radon extraction a Teflon hollow-fibre degassing cartridge (MiniModule®, Membrana) was employed. The cell consists of a fabric of knit hollow fibres, each of which has a diameter of about 300 µm, and consists of hydrophobic polypropylene. The polypropylene itself shows a porous sponge-like structure with a nominal pore size of 0.04 µm. Gas transfer through the fibre hence takes place not by permeation through the actual polypropylene material but solely by diffusion through the membrane pores.

The extraction cell has a length of about 18.1 cm and a diameter of about 4.25 cm. The active surface within it, allowing water-gas extraction of radon, amounts to 0.58 m^2. The lumenside and shellside volume is about 53 and 78 cm^3, respectively. The maximal allowed water pressure to be applied is about 410 kPa; the maximal water flow rate is about 2.5 l min^{-1}.

Because of the fine porous structure of the membrane it is possible that the material gets clogged with time when the sampled water is dirty. Hence, if clogging is to be expected the water should pass a filter before it enters the extraction cell.

3.1.3 Laboratory and field experiments

Laboratory and field experiments were carried out in order to evaluate the applicability of the experimental setup including the RAD-7 and the extraction cell for continuous monitoring of radon-in-water activity concentrations as well as for analysis of discrete water samples. Continuous measurements are required if spatial and temporal differences of radon activity concentrations are of interest, e.g. for the localization (Stieglitz 2005) or the quantification of groundwater discharge into surface water bodies (Burnett and Dulaiova 2006). The measurement of discrete samples is the method of choice if only a limited amount of water is available or if temporal and spatial radon variations are of no relevance.

3.1.3.1 Continuous measurements

For the determination of the radon-in-water activity concentration in a continuously flowing water pump stream the water passes the extraction cell followed by an attached probe that allows continuous temperature recording (HOBO data logger, Onset Computer Corporation) and is finally discharged (Figure 3-1). In reverse flow a stream of air (~ 1 l min^{-1}) is pumped through the extraction cell, a desiccant column (for maintaining the air humidity at less than 10 %), and the RAD-7 detection chamber in a closed air loop. The air stream is maintained by the RAD-7 internal pump.

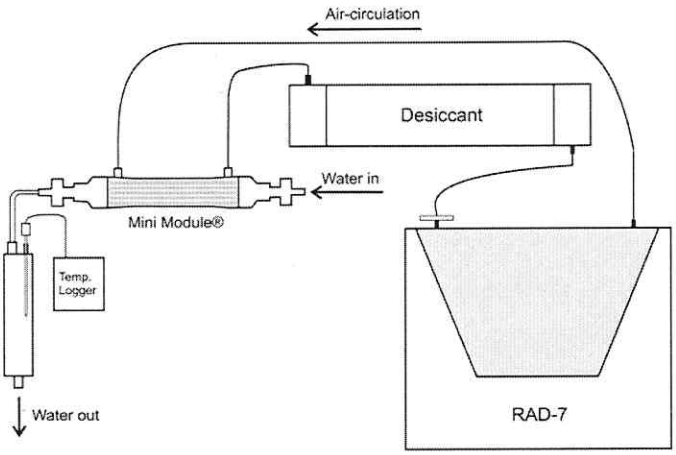

Figure 3-1: Schematic sketch of the experimental setup for continuous radon-in-water measurement.

The response time of the RAD-7 to abrupt changes in the radon activity concentration in the closed air loop is controlled by the decay equilibration time between radon and polonium-218, which is used as radon proxy. Hence, the half-life of polonium-218, which is about 3 minutes, sets the theoretical lower limit for the response time of the whole experimental setup to about 15 minutes. Other important system-independent parameters influencing the response time of the experimental setup are the volume of the circling air (which is given by the volumes of the detection chamber of the RAD-7, the desiccant column, extraction cell, and tubing), the kinetics of radon degassing from the water to the air (which mainly depends on the active surface within the extraction cell and can thus not be modified significantly), and the flow rate of the water through the extraction cell. The dependence of the response time on the water flow rate is discussed in the results and discussion section below (cf. section 3.1.4).

State of the art for continuous measurements of radon-in-water activity concentrations is the method introduced by Burnett et al. (2001), and Burnett and Dulaiova (2003) using the RADAqua for radon extraction as mentioned above. For the characterization of the system efficiency of the experimental setup discussed here all measurement results achieved by using the extraction cell were compared to results of measurements carried out simultaneously with the RADAqua. The respective RADAqua experiments were carried out as described by Burnett and Dulaiova (2003).

3.1.3.2 Measurement of discrete samples

For the determination of radon activity concentrations in discrete water samples the extraction cell is applied as part of a closed water circle (Figure 3-2). All water samples were collected in HDPE (high density polyethylene)-bottles equipped with a three port screw-on-cap (Stringer and Burnett 2004). Through one of the ports the water sample was filled carefully into the bottle from the bottom up without much turbulence, allowing for water overflow through a second port. At the third port a pump (Immersion pump Elegant, Comet-Pumpen Systemtechnik GmbH) was attached inside the bottle. Hence, the whole experimental setup consisted of two inverse closed flow cycles: a water loop and an inversely running air loop. The water cycle is driven by the pump inside the bottle, which moves the water continuously through the inlet port of the extraction cell and back to the sample bottle. The built-in air pump of the RAD-7 circulates the air in reverse flow through the extraction cell, a desiccant column, and back to the RAD-7 detection chamber.

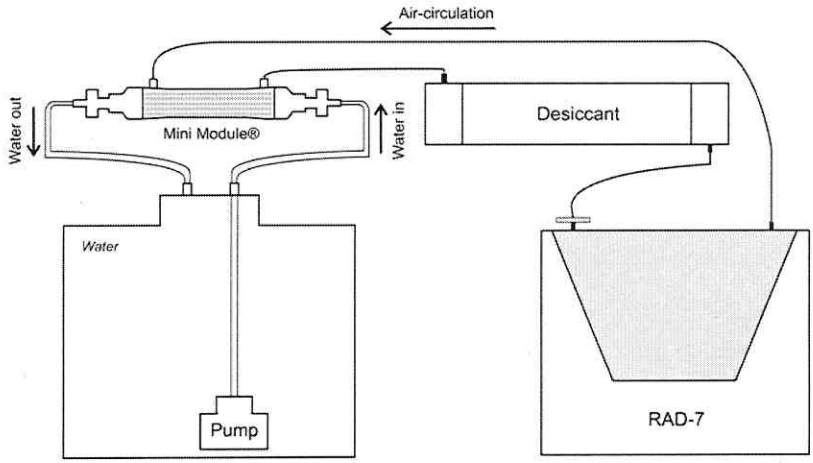

Figure 3-2: Schematic sketch of the experimental setup for radon measurement in discrete water samples.

3.1.4 Results and discussion

Since no loss or retardation of radon while crossing the membrane material has to be taken into account the detection limit of the experimental setup depends only on the detection limit of the chosen radon-in-air monitor. All experiments described here were carried out with the RAD-7 being run at a 10 min counting cycle. The RAD-7 chamber sensitivity is reported to be 1 cpm (count per minute) at 75 Bq m^{-3}. The lower radon-in-air detection limit is about 2 Bq m^{-3} (Durridge Company, Inc.2000). All laboratory experiments were carried out with tab water from the laboratory, which is known to show an essentially steady radon activity concentration of about 1 000 Bq m^{-3} (Table 3-1) yielding radon-in-air activity concentrations well above the RAD-7 detection limit.

3.1.4.1 Continuous measurements

For investigation of the dependence of the radon-in-water/radon-in-air equilibration time on the water flow rate through the extraction cell laboratory experiments were carried out with four different water flow rates (1.0, 1.5, 2.0, 2.5 l min^{-1}). In the case of a continuous pump stream the water reservoir, which degasses into the circling air, is effectively unlimited. Therefore, the radon-in-air activity concentrations determined can easily be converted into radon-in-water activity concentrations by multiplication with the (temperature dependent) radon partition coefficient (cf. Eq. 2-10). After calculation and correcting for temperature dependence the recorded time series of radon-in-water activity concentrations were plotted for each flow rate (Figure 3-3). The obtained mean equilibrium activity concentrations achieved with the extraction cell (and the RADAqua for comparison) are summarized in Table 3-1.

Generally it can be stated, that at higher water flow rates less time is needed to reach radon activity concentration equilibrium between water and gas phase. For example, this effect becomes obvious if the 1 l min^{-1} and the 1.5 l min^{-1} results are compared: at 1 l min^{-1} equilibrium is reached after about 40 to 50 minutes; at a flow rate of $\geq$ 1.5 l min^{-1} equilibration takes only about 30 to 40 minutes. At all flow rates insignificant differences were observed between the results detected with extraction cell and RADAqua. Hence, both experimental approaches lead to virtually the same results.

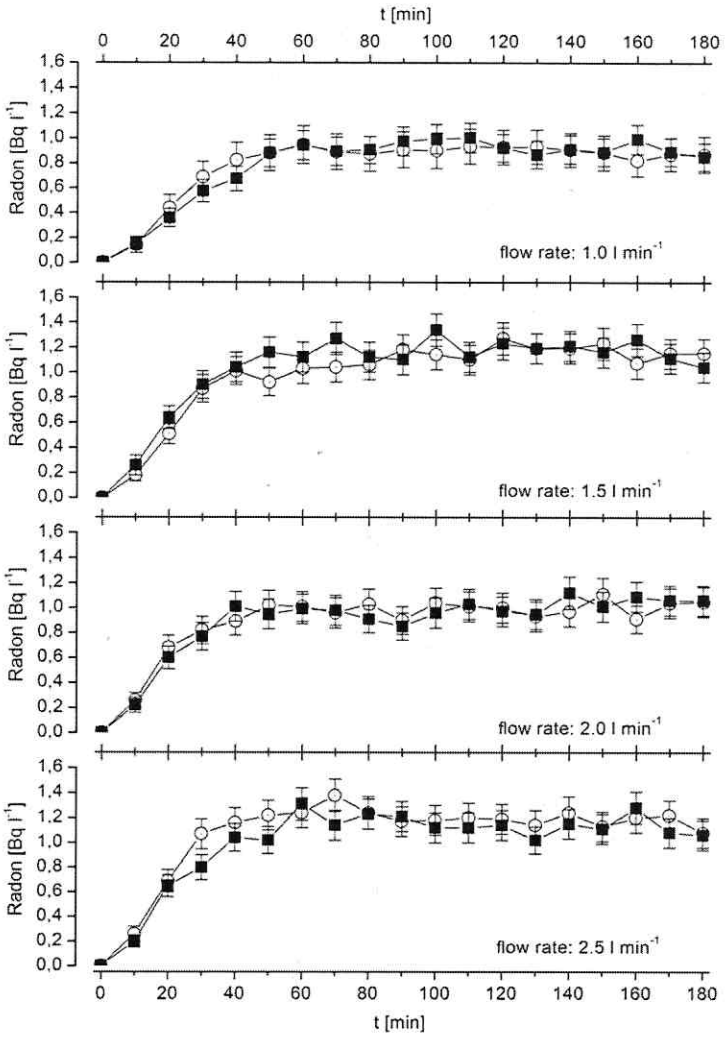

Figure 3-3: Comparison of radon-in-water activity concentrations at different water flow rates. Open circles label the extraction cell, black squares the RADAqua results.

Table 3-1: Comparison of equilibrium activity concentrations achieved with extraction cell and RADAqua; uncertainties (2σ-error) are based on counting statistics.

Flow rate [l min^{-1}]	Extraction cell [Bq l^{-1}]	RADAqua [Bq l^{-1}]
1.0	0.90 ± 0.14	0.92 ± 0.11
1.5	1.13 ± 0.12	1.16 ± 0.12
2.0	1.00 ± 0.12	0.99 ± 0.12
2.5	1.19 ± 0.12	1.13 ± 0.12

In order to test the applicability of the extraction cell for continuous on-site measurements in natural waters a radon survey was conducted in the large harbour area

off Bremerhaven (Germany). According to the German Geological Survey parts of this harbour are influenced by the intrusion of freshwater (unpublished data). Figure 3-4 shows the results recorded for a near-shore transect. All the equipment was installed on the research vessel "Heincke". Water was pumped continuously from 1.5 m below sea surface through the extraction cell with a water flow rate of ~ 2 l min^{-1}. Again the results of the two detection approaches, extraction cell and RADAqua are in very good agreement. The observed maximum radon activity concentrations at 10:00 o'clock (Figure 3-4) coincides with a region where submarine groundwater discharge into the harbour is assumed (German Geological Survey, unpublished data).

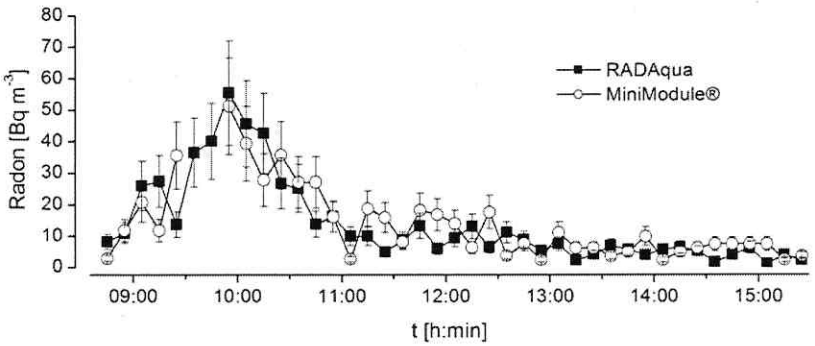

Figure 3-4: Comparison of results achieved with extraction cell and RADAqua for radon activity concentrations along a transect through a harbour area off Bremerhaven.

3.1.4.2 Measurement of discrete samples

As shown in section 3.1.4.1, the time needed to reach radon activity concentration equilibrium between water and air depends on the water flow rate. It was shown that higher flow rates yield shorter equilibration times (cf. Figure 3-3). Hence, for all experiments carried out to examine discrete water samples a constant flow rate of 2.5 l min^{-1} was applied (which is the maximum allowed for the extraction cell).

Since the water volume that releases radon into the circling air is limited by the chosen sample size, determined radon-in-air activity concentrations cannot be converted into radon-in-water activity concentrations by just applying the radon partition coefficient discussed above. The air and water volumes involved have to be taken into account. After air/water equilibrium is achieved the original radon activity concentration of the water sample can be determined by applying Eq. 3-1.

$$C_{Rn}^{w} = \frac{C_{Rn}^{air} V_{air} + k_{w/air} C_{Rn}^{air} V_{w}}{V_{w}} \qquad \text{Eq. 3-1}$$

C_{Rn}^{w}	radon activity concentration - water	[Bq l^{-1}]
C_{Rn}^{air}	radon activity concentration - air	[Bq l^{-1}]
V_{air}	air volume	[l]
V_{w}	water volume	[l]
$k_{w/air}$	partition coefficient (cf. Eq. 2-10)	[-]

As evident from Eq. 3-1 air and water volume are important parameters for accurate determination of C_{Rn}^{w}. The larger water volume and the less air volume, the higher is the resulting radon inventory in the closed air loop and the better are counting statistics. Lee and Kim (2006) reported that if the air volume increases linear relative to the water volume, counting efficiency of the radon-in-air activity concentrations decreases exponentially.

In the experiments the system temperature and hence $k_{w/air}$ was held constant at 20°C and 0.26, respectively. The circling air volume (detection chamber of the RAD-7, desiccant column, extraction cell, and tubing) was also kept invariable at about 1.4 litre for all measurements. The only variable parameter influential to the results (according to Eq. 3-1) was the volume of the water sample.

In order to characterize the dependency of the detection efficiency on the volume of the water sample applied, experiments with three different water volumes (6, 10, 20 litre) were carried out. All water samples showed the same radon activity concentration of about 1 000 Bq m^{-3} (tap water). Figure 3-5 shows the resulting time series of the recorded polonium-218 decays (in counts per minute, cpm) for each experiment. As expected, the count rate (i.e., the radon inventory in the circling air volume) increases with increasing volume of the water sample. That implies that the uncertainty of the radon activity concentrations derived from the recorded polonium-218 decays increases with decreasing sample volume. Hence, it can generally be concluded that, if low radon activity concentrations are to be expected larger water volumes should be sampled and used for measurement.

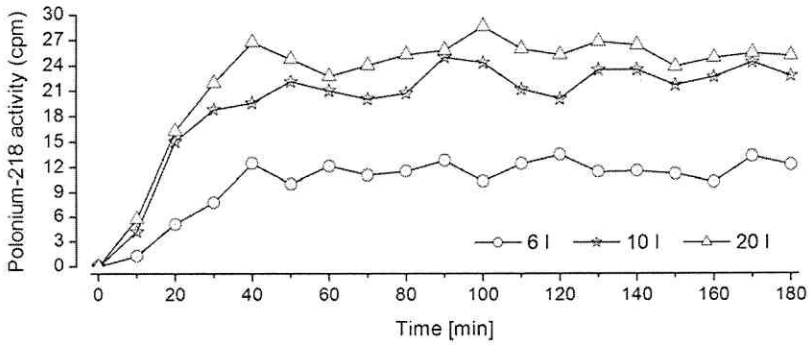

Figure 3-5: Polonium-218 count rates for different water sample volumes. For each measurement radon-in-water activity concentrations and circling air volumes are the same.

In order to test the applicability of the extraction cell for on-site analysis of discrete samples of natural waters, groundwater and surface water samples were taken from several sites in Germany. As shown in Table 3-2 the results achieved with the extraction cell agree within 10 % uncertainty with the results achieved with the RADAqua.

Table 3-2: Comparison of extraction cell results and RADAqua results for water samples taken from different sites in Germany.

Water type	Location	Radon activity concentration [Bq l^{-1}]					
		Extraction cell			RADAqua		
Groundwater	Leipzig Lowland	21.5	±	0.6	21.3	±	0.3
	Lusatia region	6.1	±	0.4	5.9	±	0.4
	Goitzsche, Bitterfeld region	1.3	±	0.3	1.2	±	0.1
River water	Schachtgraben, Bitterfeld region	0.9	±	0.08	0.9	±	0.09
	Schaugraben, Falkenberg	1.2	±	0.4	1.1	±	0.08
Lake water	Lake Ammelshainer See, Leipzig	0.05	±	0.004	0.05	±	0.002
	Lake Waldsee, Lusatia	0.01	±	0.003	0.01	±	0.003
	Goitzsche, Bitterfeld region	0.1	±	0.03	0.11	±	0.02
	Restloch 111, Lusatia	0.002	±	0.0003	0.002	±	0.0001

The counting time of the RAD-7 necessary to guarantee statistically reliable results depends on the radon activity concentration in the circling air. In the case of small water sample volumes the radon activity concentration in the circling air, which is supported

by the radon degassing from the water sample, expanded counting times might become necessary. For a 6 litre water sample with a radon-in-water activity concentration of ≥ 0.03 Bq l^{-1} a counting time of 7 h or less is sufficient for achieving an uncertainty (2σ-error) of less than 20 %. For activity concentrations of ≤ 0.03 Bq l^{-1} a longer counting time must be allowed. As reported by Lee and Kim (2006) at low radon-in-water activity concentrations (< 0.001 Bq l^{-1}) statistically reliable results might require counting times that exceed 24 h.

3.1.5 Conclusion

In the study discussed a newly developed method for the measurement of radon-in-water activity concentrations by means of a small-size easy to handle extraction cell is presented. The technique is based on extracting radon from the water into a closed air-stream und measuring the radon-in-air activity concentration by means of a customary mobile radon-in-air monitor.

The results obtained with the extraction cell were evaluated against the results of the comparable and well established method for the continuous measurement of radon-in-water activity concentrations applying the RADAqua. All results match closely.

The extraction cell, which is applicable to a wide activity concentration range, is in particular advantageous for on-site ex-situ measurements of discrete and continuous radon-in-water activity concentrations. The main advantage of the extraction cell compared to the RADAqua is that the developed and presented experimental set-up can be handled more easily. This is of particular advantage under rough on-site conditions. Hence, the extraction cell has to be considered an equivalent alternative to the well established RADAqua.

3.2 Continuous on-site in-situ determination of radon in surface waters

3.2.1 Introduction

One of the major obstacles of on-site radon-in-water determination is the potential loss of radon during water sampling, sample handling, or while purging the radon from the water sample using an ex-situ stripping unit (cf. section 3.1). Experimental setups for on-site radon-in-water measurements use the distinct partitioning behaviour of radon between water and air (Weigel 1978, Clever 1979) and are all based on the same principle: radon is extracted from a water sample (or a continuous water pump stream) by stripping it from the water into a closed circuit air stream where its activity concentration is measured by means of a radon-in-air monitor. In most cases radon stripping is done by bringing water and air stream in direct contact, i.e., by bubbling the air through the water (Lee and Kim 2006, Schubert et al. 2006) or by spraying the water into the air stream (Burnett and Dulaiova 2003). Some authors suggested membrane extraction (Surbeck 1996, Freyer et al. 2003). Although detection limits of less than 0.01 Bq l^{-1} can be reached with that stripping approach, the potentially significant radon loss during water sampling and sample handling still poses a considerable risk. An alternative way of representative radon detection is in-situ extraction of radon directly from the water body of concern without any water sampling involved. This approach, discussed in the following section, is in particular advantageous if large surface water bodies, such as lakes or rivers, are subject of investigation.

The study discussed in the following section has been published in a modified form as:

Schubert, M., Schmidt, A., Paschke, A., Lopez, A., Balcázar, M. (2008). In situ determination of radon in surface water bodies by means of a hydrophobic membrane tubing. *Radiation Measurements* 43: 111-120.

3.2.2 Methodology

3.2.2.1 Equipment setup

The equipment applied for in-situ radon extraction and measurement consists of two main parts, a commercially available mobile radon-in-air monitor including a radon-tight air pump and a "radon extraction module" developed as part of the study presented in this section.

Mobile radon-in-air monitor

Two different radon-in-air monitors were used for the various experiments carried out during the study: the "AlphaGuard" and the "RAD-7".

The RAD-7 has been described in detail in section 3.1. The AlphaGuard (Genitron Instruments) works in a complete different way. It uses a 0.62 litre pulse ionization chamber for direct detection of radon alpha decays. The chamber sensitivity is 1 cpm at 20 Bq m^{-3}. The lower detection limit depends on the length of the chosen counting cycle, which can be set to 1 min, 10 min, or 60 min. A 60 min cycle allows a detection limit of 2 Bq m^{-3}.

The response time of the detector to abrupt changes in radon-in-air activity concentration depends on the chosen operation mode specified by the way of radon entry (either by diffusion or by pumping with an adjustable pump rate) and by the chosen length of the counting cycle. With a pump rate of 1 l min^{-1} in connection with the 1 minute counting cycle, a configuration which was used for all described experiments involving the AlphaGuard, the response time, i.e., the time needed to completely exchange and measure the air in the ionization chamber, is about 3 minutes (Schubert et al. 2007a). The air stream is maintained with an external air pump ("AlphaPump", Genitron Instruments).

Both, the "AlphaGuard" and the "RAD-7" are radon-in-air monitors. If radon-in-water activity concentrations are to be determined by extracting the radon from the water into a closed circuit air stream and measuring its activity concentration in the circling air, the time needed to reach radon activity concentration equilibrium between air and water adds considerably to response time of both monitors. For the AlphaGuard Schubert et al. (2006) reported a total response time to abruptly changing radon-in-water activity concentrations of about 10 minutes (radon extraction by bubbling the circling air through the water). For the RAD-7 response times of about 30-40 minutes were reported by Burnett and Dulaiova (2003) (using polonium-218 as radon proxy; radon extraction by spraying the water into the circling air).

Radon extraction module

The radon extraction module, developed as part of the presented study, forms the second part of the used equipment. It is shown in Figure 3-6a. The module mainly consists of a robust hydrophobic tubular capillary membrane (Accurel® PP V8/2 HF,

Membrana) made of polypropylene, a material which guarantees strong hydrophobic properties even under water pressures of up to 350 kPa (i.e., approximately 35 m water column). The inner diameter of the tubing is 5.5 mm, the wall thickness amounts to 1.55 mm. The membrane material itself shows a sponge-like structure with a nominal pore size of 0.2 µm (Figure 3-6b).

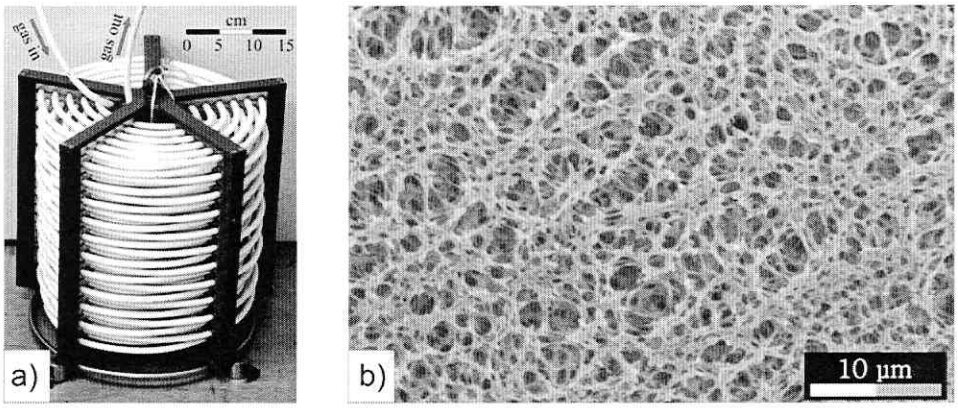

Figure 3-6: a) Radon extraction module; b) scanning electron microscope image of the membrane material (photo by Membrana).

The mode of radon transfer through the membrane is not a permeation through the polypropylene material but solely diffusion through the pores. Due to the hydrophobic nature of the polypropylene the pores are air-filled even if the tubing is put under water. For the prototype of the radon extraction module a 50 m piece of the membrane tubing was coiled up in 22 layers with 6 loops each. The mean distance between the loops is about 2 cm allowing water to be constantly exchanged easily by slowly moving the module in the investigated water volume.

3.2.2.2 Detection limit, data reproducibility, and response time

Since no loss or retardation of radon while migration through the membrane has to be taken into consideration the detection limit of the equipment depends solely on the detection limit of the chosen radon-in-air monitor being run in a certain operation mode. For all experiments carried out with the AlphaGuard the "1 min flow mode" in connection with an air pump rate of 1 l min^{-1} was applied, a configuration for which a radon-in-air detection limit of 1 000 Bq m^{-3} is reported (Genitron Instruments 2002).

Hence, with a water/air partition coefficient of $k_{w/air} = 0.3$ (valid for a temperature of 15°C, Clever 1979, Figure 3-9) radon-in-water activity concentrations down to about 300 Bq m^{-3} can be measured.

While such detection limit is sufficient for groundwater analysis, radon activity concentrations of surface waters are in general a magnitude below that value. Hence, for analyzing radon activity concentrations in surface water the RAD-7 was chosen as radon-in-air monitor. The RAD-7 was run in a ten minutes counting cycle. In that mode the monitor allows detection of radon-in-air activity concentrations of down to 4 Bq m^{-3}, i.e., radon-in-water activity concentrations that are about a magnitude below the range of radon activity concentrations normally found in natural surface waters.

In case of both radon detectors the data reproducibility, i.e., the precision of the achieved results, increases with an increasing number of single readings after activity concentration equilibrium between water and air has been reached in the system. The laboratory experiments, which are discussed in the following section in more detail, revealed for the AlphaGuard a standard deviation of 4.5 % (1σ-error) if ten single equilibrium activity concentration readings are taken for calculation of a mean equilibrium activity concentration. For the RAD-7 a respective uncertainty of 2.8 % (2σ-error) was achieved.

While the response time of the RAD-7 reported by Burnett and Dulaiova (2003) is 30-40 minutes, as mentioned above, the equilibration time applicable in connection with the radon extraction module is about 50 min, i.e., somewhat longer. That difference can be explained as follows. The equilibration time for radon-in-water measurement is controlled by two equilibria that have to be established: first the activity concentration equilibrium between water and circulating air followed by the radioactive equilibrium between radon in the air and polonium-218 attached to the PIPS detector. The time needed to reach activity concentration equilibration is governed by the kinetics of radon migration from the water into the circulating air. Burnett and Dulaiova (2003) used the RADAqua module for ex-situ radon extraction. The RADAqua is based on the principle of stripping radon from the water by spraying the water into the air stream allowing a large and continuously renewed interface between water and air, which enhances radon exchange by turbulent convection. In case of the radon extraction module, however, radon migrates through the air-filled membrane pores, which is an additional mass transfer step, leading to the slightly longer response time. Furthermore, in case of the radon extraction module existence of a thin aqueous boundary layer at the outside the

membrane tubing has to be taken into consideration. That stagnant layer slows down the radon exchange because here molecular diffusion and not advective transport is the dominant radon migration process.

3.2.3 Experimental

3.2.3.1 Influence of selected membrane properties and membrane dimensions

Various laboratory experiments were carried out in order to investigate the properties of the tubular capillary membrane concerning radon diffusion through its wall. An essential parameter here is the time that is needed to reach radon activity concentration equilibrium between both sides of the membrane after an abrupt activity concentration change has occurred on one side of it. Experiments were carried out with the aim to investigate the dependence of the activity concentration equilibration time (a) on the radon activity concentration gradient across the membrane and (b) on the length of the membrane tubing used. A third set of experiments was carried out in order to (c) investigate potentially occurring anisotropic properties of the membrane material concerning radon diffusion, i.e., to examine if the "outside → inside" radon permeability of the material is different from its "inside → outside" permeability. The setup for the three sets of experiments are discussed below in more detail.

For analyzing the membrane properties concerning radon diffusion air-air exchange experiments were carried out; i.e., instead of choosing a water-air setup, air was put inside and outside of the membrane tubing. Main reason for that experimental approach was that air-air exchange experiments lead (in the given context) to the same results as water-air exchange experiments but are much easier to be carried out. If the radon extraction module is used in practice, both, the water sitting on the outside of the membrane tubing wall and the air circling inside of the tubing are kept in constant motion. Hence, radon diffusion is only occurring in the air-filled pores of the membrane material (and to a minor degree in the very thin boundary layer being attached to its outside wall). Since radon diffusion through the air-filled wall of the membrane tubing was to be investigated with the experiments discussed in this section, the chosen air-air setup represented the most efficient experimental approach.

Due to its short response time to activity concentration changes (only 3 min) the AlphaGuard was used for all experiments that focussed primarily on material properties.

(a) Dependence on the radon activity concentration gradient

In order to investigate the dependence of the activity concentration equilibration time on the radon activity concentration gradient across the membrane seven single experiments were carried out. All experiments were performed in the same way under the same physical conditions.

A sealed 20 litre stainless steel barrel was equipped with a 0.5 m piece of membrane tubing (Figure 3-7). The membrane tubing was installed inside the barrel, the ends being attached to an input and an output port in its lid. A radon-tight air pump and the AlphaGuard, both containing radon free air, were attached to the same ports in the lid outside the barrel. After assembling the equipment a closed circuit air stream through the membrane tubing, the AlphaGuard, and the pump was started. Next a certain volume of air was taken from the barrel and instantly replaced by the same volume of air rich in radon by means of a syringe via an injection valve in the lid of the barrel. The radon-rich air was taken from a radon source chamber in which a known and constant radon activity concentration is maintained. By transferring a certain air volume from the source chamber into the barrel, a certain radon activity [kBq] was added to the barrel. That allowed the setup of experiments with certain radon activity concentrations inside the barrel chosen individually for each experiment. The radon activity concentrations in the barrel ranged from 2 to 30 kBq m^{-3}. After injection of the radon-rich air the closed circuit air stream was maintained for 20 more minutes.

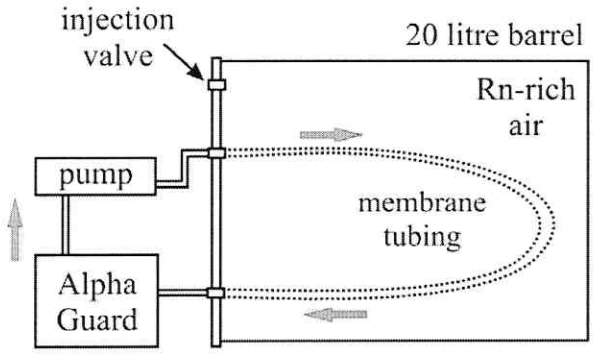

Figure 3-7: Experimental setup for varying radon activity concentration in the donor phase; the air stream is indicated by arrows.

The tubing used for connecting barrel, AlphaGuard, and pump outside the barrel was Tygon R-3603. It guarantees minimal diffusive radon loss through the walls of the tubing. The air pump rate was set to 1 l min^{-1}. The radon activity concentration measured in the closed circuit air stream, which increased steadily due to radon diffusion through the membrane until equilibrium with the activity concentration inside the barrel was reached, was monitored as time series every minute. After each experiment the whole system was flushed with radon free air.

(b) Dependence on the length of the tubing

In order to investigate the dependence of the activity concentration equilibration time on the length of the membrane tubing, five sets of experiments with three experiments each were carried out. The five investigated tubing lengths ranged from 5 to 300 cm. The experiments were carried out the same way as described above, where a 50 cm piece of membrane tubing had been used (cf. Figure 3-7). For all experiments a radon activity concentration of about 20 kBq m^{-3} was applied.

(c) Potential direction-dependent membrane permeability

In order to check for the occurrence of directional anisotropy of membrane permeability the experimental setup described above was principally reversed (Figure 3-8). The AlphaGuard was put into the 20 litre stainless steel barrel, its outlet being connected to one of the ports in the lid of the barrel. Outside the barrel the input and the output port in the lid were connected using Tygon tubing enclosing the gas pump. That direct flow path could be shut with a gate valve (Figure 3-8: "A"). After closing the barrel a certain radon activity was injected into to the barrel as described above. Then the pump was switched on to homogenize the radon activity concentration in the whole system. To ensure homogeneity the closed circuit air flow was kept running until the radon activity concentration detected by the AlphaGuard was constant (ca. 5 min). Subsequently the gate valve "A" was closed and the air stream was led through a 0.5 m piece of the membrane tubing by opening the gate valves "B" and "C".

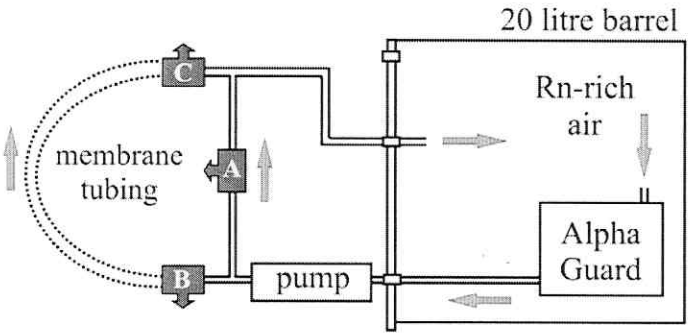

Figure 3-8: Experimental setup for inversion of radon transport direction; the air stream is indicated by arrows.

The whole experiment was set up inside a small sized closed fume hood, the ventilation of which was not switched on before the experiment was finished to avoid any air pressure gradient that could potentially influence the radon migration through the membrane. The drop of activity concentration due to radon loss from the system by diffusion through the wall of the membrane tubing into the fume hood was measured as a function of time every minute. The time needed for reaching activity concentration equilibration (i.e., until nearly all radon had left the system) was compared to the results achieved with the reverse experiments described above (a). A set of four identical experiments was carried out. For each of the experiments the initial radon activity concentration in the system was set to about 12 kBq m^{-3}.

3.2.3.2 Test of the radon extraction module

Because radon activity concentrations, which have to be expected in lakes, are below the detection limit that can be reached with the AlphaGuard being run in the 1 min flow mode, the RAD-7 was chosen as radon monitor for examining the performance of the developed radon extraction module for in-situ radon-in-water determination. A disadvantage of the setup applying the RAD-7 is its considerably longer response time to abrupt changes in radon activity concentration (cf. section 3.1.3.1).

For testing the characteristics of the radon extraction module two different laboratory experiments and one on-site experiment were carried out. The laboratory experiments focussed on the performance of the module in case of (d) increasing and (e) decreasing radon activity concentrations in the water. The on-site survey was carried out to confirm

the practical manageability of the device in the field (f).

The experimental procedure applied for all experiments was essentially the same. The radon extraction module was connected to the RAD-7 with sufficient length of Tygon tubing in a way, that the "gas in" port of the extraction module (cf. Figure 3-6a) was linked to the outlet of the RAD-7 and the module "gas out" port was connected to the drying unit and the inlet of the RAD-7. After connection the radon extraction module was lowered into the water volume of interest, i.e., in case of the lab experiments into a 100 litre water-filled stainless steel barrel (which was closed afterwards) or, in case of the on-site survey, into the water body of a lake fed mainly by groundwater. Finally the RAD-7 internal gas pump was set to a continuous air flow of 1 l min^{-1} and the closed circuit air stream was maintained until a stabile activity concentration plateau was reached. The RAD-7 was run in a 10 minutes counting cycle.

(d) Radon extraction module test with increasing activity concentrations

For the first lab experiment the radon activity concentration in the barrel was increased in four steps. First the barrel was filled with tap water. The barrel was filled from the bottom up by means of a hose without much turbulence. The radon extraction module was completely submersed into the water volume and connected to the RAD-7 via a gas inlet and a gas outlet port in the lit of the 100 litre barrel. A battery-operated submersible water pump, which was switched on to keep the water in the barrel in motion, was put into the barrel as well. Than the lid of the barrel was closed, the air pump was switched on and one hour was allowed to reach activity concentration and decay equilibrium between radon in the water, radon in the circling air, and polonium-218 attached to the PIPS detector. After equilibrium was reached a further hour was allowed to record at least six single equilibrium readings (one per ten minutes).

Subsequently the radon activity concentration in the water was increased in three single steps. For each of the steps one litre of water was pumped off the barrel and replaced by one litre of water rich in radon[2]. The water pumped off the barrel was used for LSC analysis of the radon activity concentration in the barrel as described by Freyer et al. (1997).

[2] The radon rich water was taken from the radon spa Bad Schmiedeberg/Saxony-Anhalt, Germany.

(e) Radon extraction module test with decreasing activity concentrations

For testing the performance of the extraction module in case of decreasing radon activity concentrations a second laboratory experiment was carried out. For that experiment the 100 litre barrel was filled with water that showed a radon activity concentration of about 6 kBq m^{-3} (confirmed by LSC). After setting up the equipment as described above the air pump was switched on and the increase in radon activity concentration in the closed air loop was recorded by means of the RAD-7. After 90 minutes the air pump was stopped, the barrel was opened, about half of the water was exchanged with virtually radon free water, the barrel was closed again, and the closed circuit air flow re-started. The radon activity concentration in the water in that second step of the experiment was 3.4 kBq m^{-3} (detected by LSC). Now the decrease in radon activity concentration in the closed circuit air stream was monitored and the equilibration time was compared to the equilibration time determined with the activity concentration increase experiment described above.

(f) Field test of the radon extraction module

The on-site test of the exchange module was carried in May 2007 at a lake in a homogeneous gravel aquifer (the former gravel mining pit Lake Ammelshainer See), located close to the city of Leipzig/Germany (51°, 18' N; 12°, 36' E). The lake shows a maximum depth of 24 metres and a surface area of about 530 000 m^2. Depth profiles of electrical conductivity, pH, and temperature determined at the lake revealed virtually constant values of 790 µS cm^{-1}, 7.6, and 13.1°C, respectively, indicating a well-mixed water body. The radon extraction module was lowered into the lake from a small boat, fixed to a location in the approximate middle of the lake, to depths of 0.3, 4, 7, and 9 m. In each depth the radon activity concentration was recorded by means of the radon extraction module applying the RAD-7 as radon monitor as described above. After finishing the measurement in one depth (about two hours) the whole set of equipment (radon extraction module, radon monitor, and drying unit) was flushed with outside air, the radon extraction module was lowered into the next depth, and the procedure started anew. Additionally, from each depth a 6 litre sample was taken and analyzed for its radon activity concentration in the laboratory as described by Lee and Kim (2006).

For the laboratory and the on-site experiments alike the radon activity concentration determined in the closed air stream had to be converted into a radon-in-water activity

concentration. Since in both experimental setups the radon inventory of the examined water volume (100 litre barrel or lake) was very large compared to the radon inventory that partitioned into the air stream (i.e., into the detection system), the radon-in-water activity concentration (C_{Rn}^{w}) could easily be converted from the determined radon-in-air activity concentration (C_{Rn}^{air}) by applying Eq. 3-2.

$$C_{Rn}^{w} = C_{Rn}^{air} k_{w/air} \qquad \text{Eq. 3-2}$$

C_{Rn}^{w}	radon-in-water activity concentration	[Bq m^{-3}]
C_{Rn}^{air}	radon-in-air activity concentration	[Bq m^{-3}]
$k_{w/air}$	partition coefficient	[-]

In Eq. 3-2 $k_{w/air}$ is the temperature dependent water/air partition coefficient for radon (cf. Eq. 2-10). The temperature dependence is illustrated in Figure 3-9 (Clever 1979). Note that the temperature dependence is most pronounced between temperatures of 0 and about 20°C. For evaluation of the laboratory results (lab temperature: 20°C) a $k_{w/air}$ of 0.26 and for the on-site experiment (lake temperature: 13.1°C) a $k_{w/air}$ of 0.32 was used.

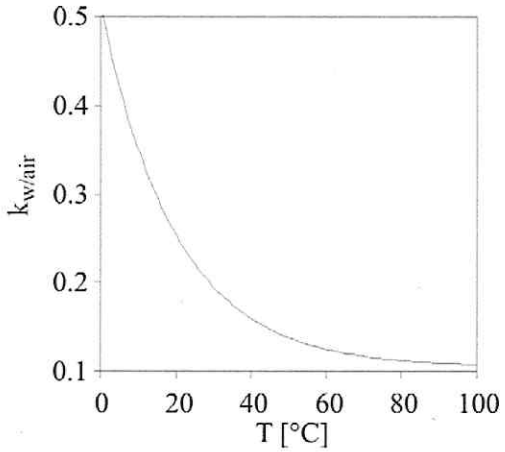

Figure 3-9: Temperature dependence of $k_{w/air}$.

3.2.4 Results and discussion

3.2.4.1 Influence of selected membrane properties and membrane dimensions

(a) Dependence on the radon activity concentration gradient

The experimental results related to the dependence of the activity concentration equilibration time on the radon activity concentration gradient across the membrane are illustrated in Figure 3-10. For the experiments radon activity concentrations of 2, 13, 17, 20, 25, and 30 kBq m^{-3}, respectively, were applied. The experiment with 30 kBq m^{-3} was repeated for the sake of direct data comparability. All activity concentrations were recorded as time series in 1 minute steps. With the aim to allow better comparability between the data series all activity concentrations in Figure 3-10 are shown as percentage values. The respective equilibrium activity concentration was represented by 100 %. An additional set of experiments, which was carried out with the aim to show that the air circling through the system did not equilibrate at an activity concentration lower than the actual activity concentration in the barrel, confirmed the 100 % efficiency of the membrane material concerning radon diffusion.

All the curves plotted show virtually the same time dependence (f (t)). Differences are due to the statistic nature of radioactive decay. A dependence of the activity concentration equilibration time on the activity concentration gradient was not observed. That becomes in particular obvious if the results of the two experiments carried out with 30 kBq m^{-3} are compared to each other (both curved are plotted in bold). The two curves cover the whole range of experimental results displayed, confirming the statistical nature of the differences between the individual curves.

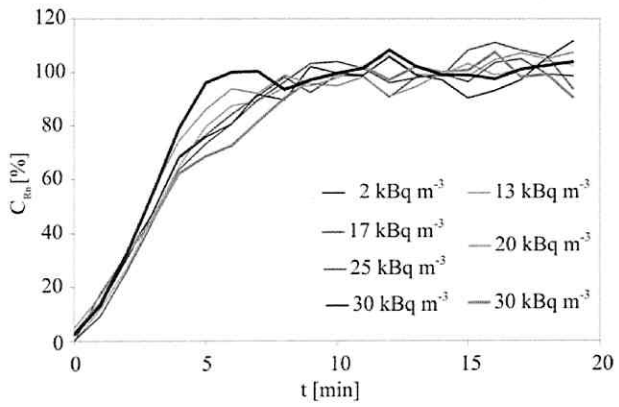

Figure 3-10: Increase in radon activity concentration as f (t) for six different concentration levels; the experiment with 30 kBq m^{-3} was carried out twice.

As it can be seen in Figure 3-11, which summarizes the results displayed in Figure 3-10 by showing the mean relative activity concentrations of all seven experiments at each time step, activity concentration equilibrium between the air volume in the barrel and the closed circuit air stream was generally reached after about 10 minutes. Since the response time of the AlphaGuard (in the 1 min flow mode with an air flow rate of 1 l min^{-1}) is, as mentioned above, about 3 minutes, it can be stated that the activity concentration equilibration process between the two gas phases takes only about five minutes. This conclusion is in accordance with results of experiments that focussed on radon partitioning from water samples into an air stream bubbling through the water carried out by Schubert et al. (2007a).

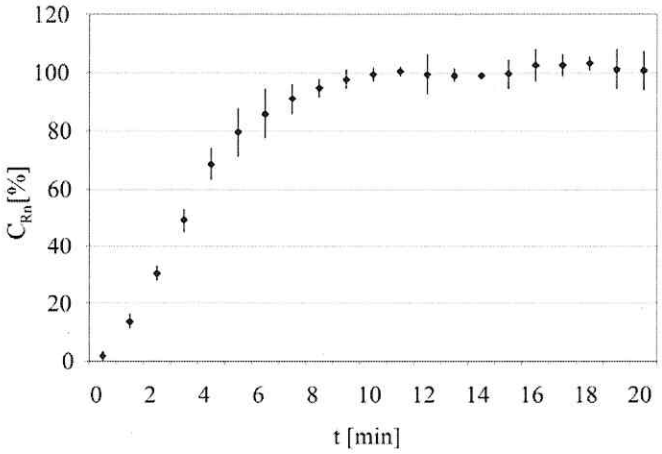

Figure 3-11: Increase in radon activity concentration as f (t); mean values of the data sets displayed in Figure 3-10.

(b) Dependence on the length of the tubing

Each of the plots displayed in Figure 3-12 summarizes the results of a set of three identical experiments (except the data shown for 50 cm, which are adopted from Figure 3-11, i.e., represent seven individual experiments). Each set of experiments was carried out under the same conditions with a different length of membrane tubing. The plots show a distinct dependence of the activity concentration equilibration time on the length of the membrane tubing applied. Generally it can be said, the longer the membrane tubing, i.e., the larger the membrane area available for diffusion, the faster activity concentration equilibrium is reached. Yet, it can also be concluded from the data, that the determined dependence is most pronounced with tube lengths of less than 75 cm.

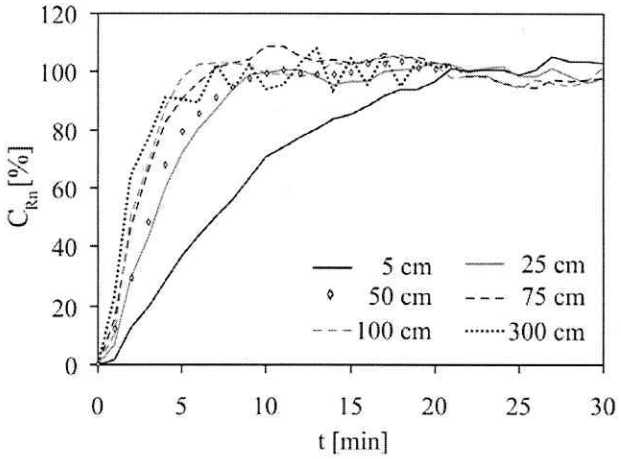

Figure 3-12: Increase in radon activity concentration as f (t) for six different lengths of the membrane tubing.

The experiments suggest that a membrane tubing length of about 1 m is sufficient for a reasonably short activity concentration equilibration time (< 10 min). However, it has to be kept in mind that all experiments were carried out under laboratory conditions. Under on-site conditions, e.g. in a lake or a river, a certain share of the pores of the membrane may get clogged over time (e.g. by clay particles or biofilms) potentially reducing the radon permeability of the membrane material. For this reason a long membrane tubing has generally to be considered advantageous in particular with regard to its long term on-site use. Hence, and besides the requirement of a tube length of more that 1 m, the main aspect for the construction of the radon extraction module was its practical way of handling, i.e., size, shape, weight, and fragility.

(c) Potential direction-dependent membrane permeability

Figure 3-13 illustrates the results of a set of four identical experiments, i.e., the mean relative activity concentrations detected at each time step during the experiments (comparable to Figure 3-11). The experimental scenario was essentially reverse to the scenario discussed above (a) and allows the assessment of radon diffusion from the inside to the outside of the membrane tubing. Hence, comparison of the experimental results of (a) and (c) (Figure 3-11 and Figure 3-13) reveals information about a potential semi-permeability of the membrane concerning radon diffusion.

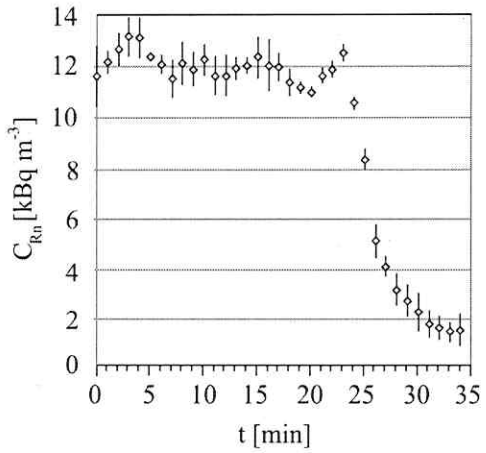

Figure 3-13: Decrease in radon activity concentration as f (t) (mean values from four experiments).

Before including the membrane tubing in the closed circuit air stream the radon activity concentration in the system was about 12 kBq m^{-3}. Homogeneity in radon activity concentration was guaranteed by circling the air through the system for 23 minutes. The data displayed in Figure 3-13 confirm that there was no leakage in the closed system; the activity concentration stays at a constant level of 12 ± 0.52 kBq m^{-3} over that time. Subsequently the air stream was lead through the membrane tubing by switching the gate valves as described above. As it can be seen the activity concentration drops immediately. Radon leaves the system via diffusion through the wall of the membrane tubing and enters the fume hood where the equipment was placed. Since the fume hood was closed and its ventilation switched off, radon activity concentration builds up in the air around the membrane tubing until activity concentration equilibrium is reached (ca. 1.5 kBq m^{-3}).

As it can be seen in Figure 3-13 activity concentration equilibrium has established after about 10 minutes, a time which is correspondent to the time that was needed to reach activity concentration equilibrium in the reverse experiments discussed above (a). Hence, it can be stated that radon diffusion through the membrane does not depend on the direction of the radon activity concentration gradient across the membrane, i.e., no inside → outside/outside → inside anisotropy concerning radon diffusion has to be taken into account.

3.2.4.2 Test of the radon extraction module

(d) Radon extraction module test with increasing activity concentrations

The results of the first laboratory experiment with the radon extraction module, which focussed on its performance in case of continuously increasing radon activity concentrations, are illustrated in Figure 3-14.

The radon-in-water activity concentrations achieved by means of the extraction module for the four activity concentration steps applied are 0.3 ± 0.03, 4.7 ± 0.2, 9.8 ± 0.3, and 15.2 ± 0.2 Bq l^{-1}, respectively. The values show low uncertainties and are in good agreement with the respective values determined by means of LSC (amounting to 0.4 ± 0.02, 4.4 ± 0.2, 9.7 ± 0.5, and 14.9 ± 0.8 Bq l^{-1}, respectively, as shown in Figure 3-14). The results confirm the 100 % efficiency of the membrane concerning radon transfer through it.

Since the RAD-7 was used as radon-in-air monitor, the response time to the abrupt changes in radon activity concentration in the water is about 50 minutes at each step, as discussed above.

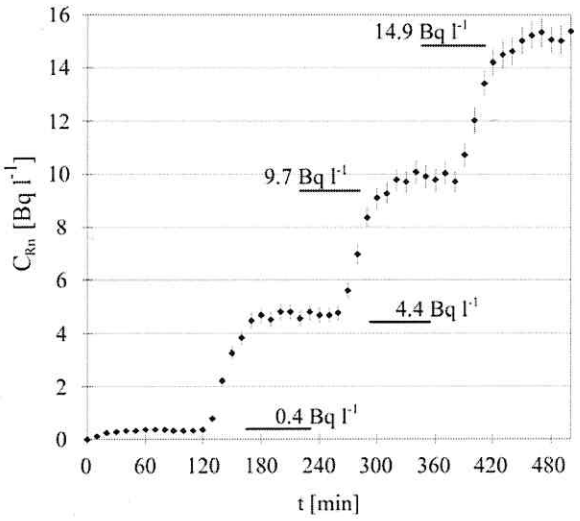

Figure 3-14: Increase in radon activity concentrations as f (t) in four steps; activity concentrations determined by LSC are also given partitioning.

(e) Radon extraction module test with decreasing activity concentrations

The second laboratory experiment with the radon extraction module focussed on the continuous detection of abruptly decreasing aqueous radon activity concentrations. The respective results are displayed in Figure 3-15.

As it can be seen in Figure 3-15 the abrupt increase in radon activity concentration at the beginning of the experiment, caused by putting the radon extraction module into a 100 litre water volume showing a radon activity concentration of 6 kBq m^{-3} (at t_0), was detected with a response time of about 50 min (from t_0 to t_1). The equilibration time is in accordance with the results of the first laboratory experiment with the extraction module focussing on activity concentration increase (d). However, in contrast to the determined water → air equilibration time, air → water equilibration (from t_2 to t_3) took about four times as long to reach the new equilibrium activity concentration of about 3.4 kBq m^{-3} in the gas phase. According to the results of the air/air experiments (c) such different performance is not due to a potential anisotropic permeability of the membrane material.

A possible reason for the delay determined for air → water equilibration can be, that according to common model assumptions on mass transfer across hydrophobic and microporous polymer membranes, a stagnant aqueous boundary layer is established at the outside of the membrane tubing during the experiment. An estimation based on reasonable assumptions (for the diffusion coefficients of radon in water and air and on the membrane and boundary layer thickness) yields an air → water transport resistance, which is three to four orders of magnitude larger compared to that for the diffusion through air-filled membrane pores and adjacent stationary air films. A pressure dependence of the radon permeability can also contribute to the delay on radon migration from the air stream inside the tubing to the outer water reservoir. Nörenberg et al. (2001) have found in their studies of pressure-dependent permeation of the noble gases from helium to xenon through polypropylene membranes that capillary condensation and adsorption to the inner polymer surface can occur especially for the heavier molecules krypton and xenon already at a partial pressure of ~10^{-8} Pa. A more detailed study is needed in order to clarify the respective experimental findings.

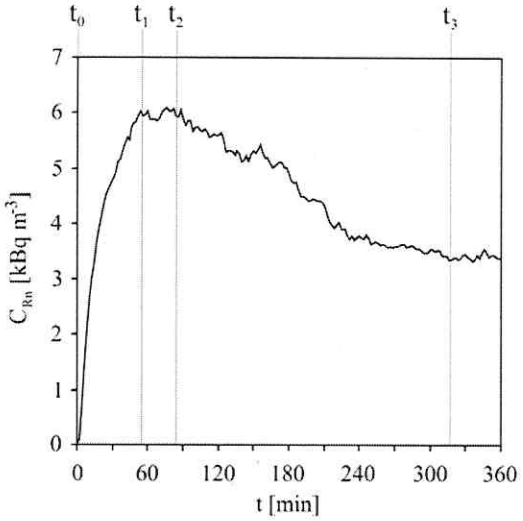

Figure 3-15: Decrease in radon activity concentration as f (t).

(f) Field test of the radon extraction module

The results of the field experiment are shown in Figure 3-16. The radon-in-water activity concentrations determined in-situ at four depths in the lake by means of the radon extraction module are 46 ± 15, 55 ± 8, 61 ± 11, and 49 ± 20 Bq m^{-3}, respectively. The values show higher uncertainties than the laboratory results discussed above (d), which is probably due to the much lower radon activity concentrations present in the lake giving rise to worse counting statistics and to a slight drift of the boat despite its fixation by anchor. However, it can be seen that all determined activity concentrations fall into a comparably narrow range of activity concentrations around 50 Bq m^{-3}, which confirms the good mixing of the water body. The homogeneity of the water body was also indicated by the values determined for electrical conductivity, pH, and temperature, as mentioned above.

The activity concentrations detected in-situ with the radon extraction module are in good agreement with the values determined from discrete samples taken from the four depths. The respective samples analyzed in the laboratory by means of the technique described by Lee and Kim (2006) show radon activity concentrations of 48 ± 14, 39 ± 12, 50 ± 11, and 56 ± 12 Bq m^{-3}, confirming again the 100 % efficiency of the membrane material concerning diffusive radon transfer. Laboratory analysis of the sample taken from 4 m depth revealed a slightly lower activity concentration than it was determined in-situ with the radon extraction module. The reason for that might be some radon loss during sampling and sample handling.

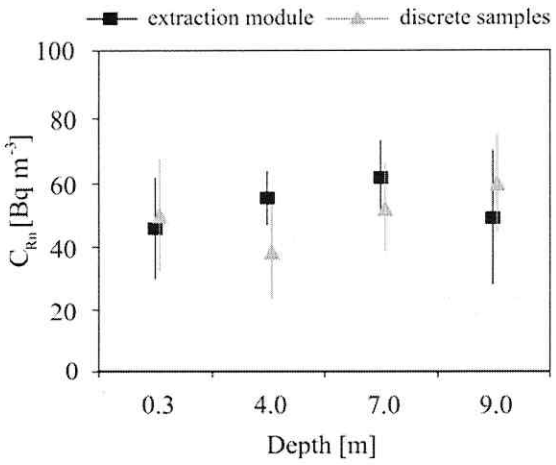

Figure 3-16: Radon activity concentrations in four depths in a lake determined by means of the radon extraction module.

3.2.5 Conclusion

The laboratory and field experiments show that the radon extraction module principally allows a straightforward determination of low radon-in-water activity concentrations. It can be concluded that the developed device proved to be a powerful tool for in-situ determination of radon activity concentrations in open water bodies. Besides the immediate availability of the results, the main advantage of in-situ determination of radon activity concentrations is the avoidance of significant radon losses from the water sample to be examined. However, due to the potential "memory effect" resulting from the delayed air → water transfer of radon compared to water → air transfer (cf. Figure 3-15) a continuous measurement of radon activity concentrations is not possible if concentration changes are to be expected to occur within about 4 hours. Due to the apparent time delay of air → water transfer of radon the equipment must be flushed after each measurement by exchanging about two detection chamber volumes of air in order to get rid of the radon remaining in the system. That procedure takes about 5 minutes only.

4 Application of radon for tracing groundwater discharge into lakes

4.1 Using radon for tracing groundwater discharge into a meromictic lake

4.1.1 Introduction

In the presented case study, the quantification of the overall groundwater discharge into a lignite mining lake was assessed by using radon as a natural geochemical tracer. The chosen study site was a meromictic lake, i.e., a water body that is divided horizontally into two separate layers – the upper mixolimnion (with seasonal mixing) and the lower monimolimnion (without seasonal mixing). For the estimation of groundwater discharge rates into the lake a simple box model including all radon input and output terms related to each layer was applied.

The study discussed in the following section has been published in a modified form as:

Schmidt, A., Schubert, M. (2007). Using radon-222 for tracing groundwater discharge into an open-pit lignite mining lake – a case study. *Isotopes in Environmental and Health Studies* 43: 387-400.

4.1.2 Basic concept

In order to apply naturally occurring radon as a tracer for the estimation of groundwater discharge into a lake, it is necessary to relate the radon inventory of the lake water body to the groundwater discharge rate. This requires the consideration of all radon input and output terms with regard to the lake water body. Given that the studied lake lacks any noteworthy connection to an open watercourse radon input terms are limited to (1) groundwater discharge (benthic advective radon input), (2) in-situ radon production from decaying radium-226 dissolved in the water column, and (3) input via diffusion or physical mixing (bioturbation, sediment resuspension) of radon by radium-226 decay in the sediments. The output terms include (1) radon decay, (2) radon loss to the atmosphere (degassing), and (3) subsurface outflow (benthic advective radon output). A simple box model can be used to illustrate this approach (Figure 4-1).

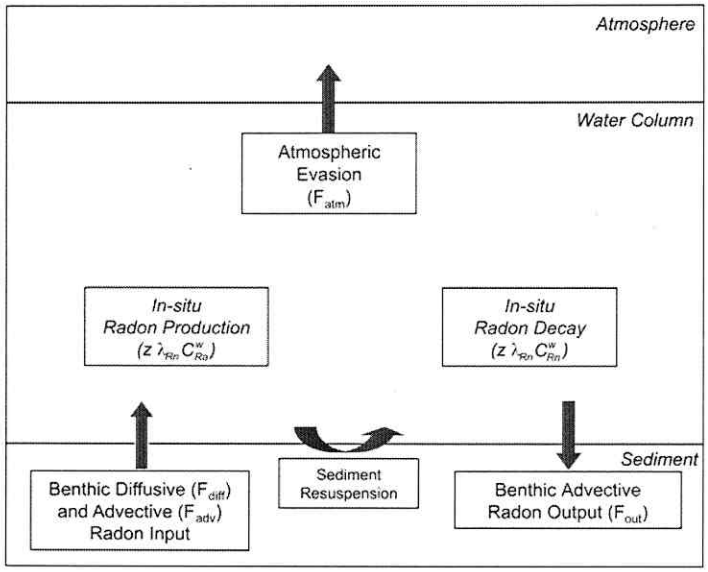

Figure 4-1: Simple box model showing possible input and output terms supporting the radon inventory of a lake water body; F_{adv}-input is the desired result of this study.

In consideration of Figure 4-1, a one-dimensional model can be applied for quantitative description of a respective steady-state system (Eq. 4-1, Corbett et al. 2000).

$$(F_{adv} + F_{diff} + C^{w}_{Ra}\ \lambda_{Rn}\ z) - (F_{atm} + C^{w}_{Rn}\ \lambda_{Rn}\ z + F_{out}) = 0 \qquad \text{Eq. 4-1}$$

F_{adv}	advective radon flux, sediment → water	[Bq m^{-2} s^{-1}]
F_{diff}	diffusive radon flux, sediment → water	[Bq m^{-2} s^{-1}]
C^{w}_{Ra}	radium-226 activity concentration - water	[Bq m^{-3}]
λ_{Rn}	radon decay constant	[s^{-1}]
z	height of the water column	[m]
F_{atm}	radon flux, water → atmosphere	[Bq m^{-2} s^{-1}]
C^{w}_{Rn}	radon activity concentration - water	[Bq m^{-3}]
F_{out}	advective radon output, water → sediment	[Bq m^{-2} s^{-1}]

In Eq. 4-1 the terms ($C^{w}_{Ra}\ \lambda_{Rn}\ z$) and ($C^{w}_{Rn}\ \lambda_{Rn}\ z$) quantify the radon production by radium-226 decay and the decay of radon, respectively, within the water column. The radon decay constant (λ_{Rn}) amounts to 2.1×10^{-6} s^{-1} (cf. Eq. 2-3 and Table 2-3).

The approach neglects the release of radon into the lake water via sediment-resuspension because the respective input is, in most cases, insignificantly small (Weyhenmeyer 1998). Furthermore, the output of radon with the subsurface lake water outflow (benthic advective radon output, F_{out}; Figure 4-1) is neglected. Stringer (2004) showed in a case study that less than 1 % of the complete radon output flux is caused by this process. Hence, although the magnitude of this parameter may vary between different lake environments (and different hydrological systems) this output term of radon is in general negligible compared to the other fluxes investigated.

The radon inventory of a lake water body (I) is taken as the total activity concentration in the water column per square metre surface area [Bq m^{-2}]. As shown in Figure 4-1 and Eq. 4-1, this radon inventory is supported by benthic radon fluxes and in-situ production. Since only the benthic radon inputs F_{adv} and F_{diff} are of interest in this particular study, these two input processes of radon must be examined separately. The portion of the radon inventory of a lake water body, which is supported by benthic radon fluxes (and not supported by in-situ production) is referred to as excess-inventory (I^{Ex}). Once I^{Ex} has been measured, the total benthic radon flux ($F_{total} = F_{adv} + F_{diff}$) into the water body that is required to support I^{Ex} can be determined by applying Eq. 4-2 (Burnett and Dulaiova 2003).

$$F_{total} = F_{atm} + (C^{w}_{Rn}\,\lambda_{Rn} z) - (C^{w}_{Ra}\,\lambda_{Rn}\, z) = \frac{I^{ex}\lambda_{Rn}}{1-e^{-\lambda_{Rn} t}} \qquad \text{Eq. 4-2}$$

To quantify the individual radon input and output terms on the basis of the radon inventory of a lake a steady-state situation over at least five radon half-lifes (20 days) must be assumed. In this case, F_{total} equals the excess radon inventory multiplied by the radon decay constant (Eq. 4-2).

The advective radon flux (F_{adv}) from the sediment (i.e., the aquifer) into the lake water body term is directly linked to groundwater discharge. With the aim of separating F_{adv} from F_{total} in order to quantitatively assess the groundwater discharge, all other radon input and output terms have to be quantified. In the following sections, the single source and sink terms referred to in Eq. 4-1 and Eq. 4-2 are briefly described.

In-situ radon production and decay

The production of radon [Bq s^{-1}] within a water column with a certain height (z in [m]) and a given base area [m^2] depends on the radium-226 activity concentration (C^w_{Ra}) [Bq m^{-3}] in the water and can be represented as (C^w_{Ra} λ_{Rn} z) as given in Eq. 4-1. Likewise, the decay of radon within the water column depends on the radon activity concentration in the water and can be expressed as (C^w_{Rn} λ_{Rn} z) [Bq m^{-2} s^{-1}]. C^w_{Ra} and C^w_{Rn} can easily be determined as shown later.

Atmospheric loss

The flux of radon from an open water body into the atmosphere is governed by diffusion due to the radon activity concentration gradient at the water/air interface and by turbulent transfer at the water surface. It can be quantified using an empirical equation presented by Macintyre et al. (1995, Eq. 4-3).

$$F_{atm} = \upsilon \left(C^w_{Rn} - k_{w/air}\, C^{atm}_{Rn} \right) \qquad \text{Eq. 4-3}$$

F_{atm}	radon flux, water → atmosphere	[Bq m^{-2} d^{-1}]
υ	radon transfer velocity	[cm h^{-1}]
C^w_{Rn}	radon activity concentration - water	[Bq m^{-3}]
C^{atm}_{Rn}	radon activity concentration - atmosphere	[Bq m^{-3}]
$k_{w/air}$	partition coefficient	[-]

The partition coefficient of radon can be calculated with an empirical equation presented by Weigel (1978; cf. Eq. 2-10 and section 2.1.4) or can be taken from the extensive data collection published by Clever (1979).

The radon transfer velocity (v) is governed by wind speed and water currents (Borges et al. 2004). For its estimation the following empiric equation can be used (Macintyre et al. 1995).

$$v_{600} = 0.45\, u_{10}^{1.6} \left(\frac{Sc_{Rn}}{600} \right)^{-\frac{2}{3}} \qquad \text{Eq. 4-4}$$

u_{10}	wind speed in 10 m height	[m s^{-1}]
Sc_{Rn}	Schmidt number	[-]

The Schmidt number of radon is defined as the ratio of the kinematic viscosity of water (1.0043×10^{-6} m^2 s^{-1} at 20°C and 101.325 kPa) and the radon molecular diffusion coefficient in water (1.16×10^{-9} m^2 s^{-1} at 20°C). In order to compare Schmidt numbers of different gases, Schmidt numbers are generally standardized by dividing them by the Schmidt number of CO_2 at 20°C, which equals to 600. The subscript "600" in v_{600} refers to this standardization.

Benthic radon input

Radon input from the lake floor includes both, diffusive flux from the sediment and advective flux with the groundwater as described above. In order to calculate F_{adv}, the contribution of diffusion, F_{diff}, must be quantified. To assess F_{diff} batch experiments can be performed where bottom sediments and ambient lake water are kept in a closed system for at least five radon half-lives in order to simulate radon diffusion from the sediment into the overlying water at the sediment/water interface (Corbett et al. 1998). Radon activity concentrations in the pore water and in the overlying water are then measured. The diffusive flux of radon from the sediment into the overlying water can be estimated using a depth-independent equation introduced by Martens et al. (1980, Eq. 4-5).

$$F_{diff} = (\lambda D_s)^{0.5} \left(C_{Rn}^{pw} - C_{Rn}^{w} \right) \qquad \text{Eq. 4-5}$$

F_{diff}	diffusive radon flux, sediment → water	[Bq m^{-2} d^{-1}]
D_s	radon diffusion coefficient - sediment	[-]
C_{Rn}^{pw}	radon activity concentration - pore water	[Bq m^{-3}]
C_{Rn}^{w}	radon activity concentration - surface water	[Bq m^{-3}]

The radon diffusion coefficient (D_S) can be calculated using Eq. 2-17 and Eq. 2-18 (cf. section 2.2.3). After quantification of all individual source and sink terms as discussed above, Eq. 4-1 can be solved for the advective radon flux from the sediment into the lake water body (F_{adv}). The mean groundwater discharge velocity necessary to support that advective flux can be obtained according to Eq. 4-6 and can be converted into discharge units [$m^3\ s^{-1}$], related to the surface of the lake.

$$v_{gw} = \frac{F_{adv}}{C_{Rn}^{pw}} \qquad \text{Eq. 4-6}$$

v_{gw}	groundwater velocity	[$m\ s^{-1}$]
F_{adv}	advective radon flux, sediment → water	[$Bq\ m^{-2}\ d^{-1}$]
C_{Rn}^{pw}	radon activity concentration - pore water	[$Bq\ m^{-3}$]

One limitation of the described method is the requirement that F_{adv} and the respective estimates of v_{gw} are considered uniform across the lake bed, i.e., the groundwater discharge rate is likely underestimated in some locations and overestimated in others. Point sources such as springs are integrated together with areas where little or no groundwater discharge is occurring. However, since the overall groundwater discharge into a lake is the desired result rather than the actual location of discharge, this limitation is not of relevance for this study.

4.1.3 Study area

The case study was carried out on a mining lake (Lake Waldsee, 51°37'14"N, 14°34'17"E) located in the lignite mining district of Lusatia in eastern Germany (Figure 4-2a). The lake is situated in the western part of the Muskauer Faltenbogen, an ice-pushed ridge of a moraine formed by the Middle Pleistocene Elster-glacial. This glaciation caused strong tectonic deformations, which results in a heterogeneous and disturbed geology.

The lake is meromictic, i.e., its water body is divided into two horizontal layers: the upper mixolimnion with seasonal overturn and the lower monimolimnion, which is excluded from seasonal mixing, and thus from contact to the atmosphere. The two

layers are separated by the metalimnion. Since the monimolimnion shows only limited exchange of colloidal and dissolved matter with the mixolimnion across that interface, it develops physical and chemical properties different to the mixolimnion (Boehrer and Schultze 2008). Generally the most significant properties found in a monimolimnion are (1) anoxic conditions, (2) the enrichment of microbial decay products in the sediment, and (3) the occurrence of hydrogen sulfide triggering the precipitation of metal sulfides (Boehrer and Schultze 2006).

The investigated lake has a maximum depth of about 4.5 m, a surface area of about 3 400 m^2 and a volume of about 7 200 m^3 (Figure 4-2b). There is no surface drainage into the lake. Hence (apart from run-off water and precipitation), the only possible pathway for water inflow is groundwater discharge. At the northern edge of the lake, a small creek drains water from the lake during the wet season. However, during the sampling campaigns presented here that outflow was dry.

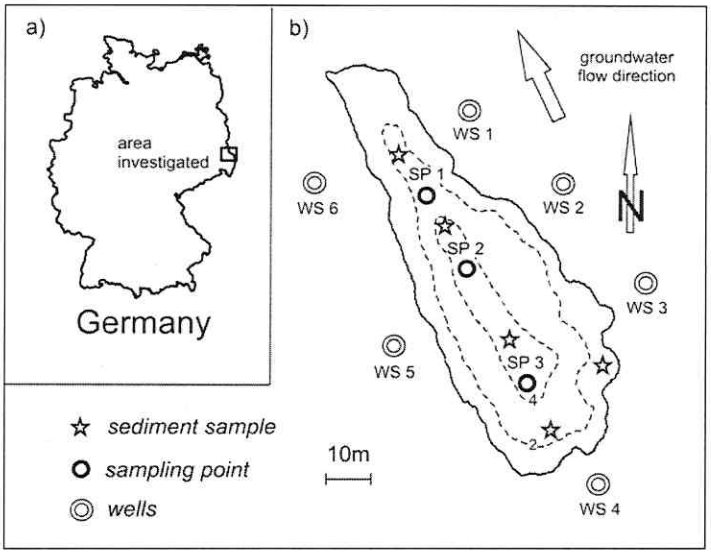

Figure 4-2: a) Location of the study area; b) Lake Waldsee with groundwater wells (WS) and lake water sampling points (SP); dashed lines indicate contour lines of lake water depth [m]. Stars show sediment sampling points: < 2 m depth = MIX 1, > 2 m depth = MON 1 – 4, with increasing numbers from SE to NW.

Six temporary groundwater monitoring wells with diameters of 2.54 cm and depths from 4 to 7 m were installed at a distance of about 10 m from the lake shore (WS 1 – WS 6, Figure 4-2b). To allow representative groundwater sampling, all wells were screened between 2 m and their base. However, representative groundwater sampling

was found to be generally difficult. Due to poor well development, two of the wells (WS 3 and WS 5) could not be used for groundwater sampling at all. In the other four wells, the groundwater table was found at very different depths, indicating a quite heterogeneous geological environment in the aquifer.

Three fixed sampling points were established on the lake (SP 1 – SP 3, Figure 4-2b). In a preliminary survey, similar depth profiles for all measured parameters (temperature, pH, electrical conductivity, radon activity concentration) were determined at the three points. Therefore, the sampling point SP 2, which is located in the centre of the lake, was considered representative for the whole lake water body.

4.1.4 Material and Methods

4.1.4.1 Sampling

Sampling was performed in October and December 2006. Lake water samples were collected at sampling point SP 2. Temperature, electrical conductivity, and pH profiles were taken at the same location (Figure 4-2b).

Groundwater monitoring wells (WS 1, 2, 4, 6) were sampled during the October campaign using a peristaltic pump (12.25, Eijkelkamp). The well sampling protocol began with removing the stagnant water from the wells before the samples (6 litre each) were collected. The wells were purged long enough to displace at least three well volumes of water. Temperature, pH, and electrical conductivity were monitored continuously until steady-state conditions were reached in the pump stream, using a WTW Multi 340i probe (Nova Analytics Company).

Lake sediment samples were obtained from five different locations (Figure 4-2b) using a standard sediment corer made from PVC (polyvinyl chloride) pipes 60 cm in length and 10 cm in diameter. One sample was taken from the mixolimnion zone (MIX 1), while the other four were taken from the monimolimnion zone (MON 1 – 4).

4.1.4.2 Methods used

All water samples were collected in 6 litre HDPE-bottles designed for radon-in-water activity concentration measurements. Sample bottles were equipped with a three port screw-on-cap (Stringer and Burnett 2004). Through one of the ports, the water sample

(6 litre) was filled into the bottle from the bottom up without much turbulence. Contact of the water with the outside air was strictly prevented in order to avoid radon loss by degassing. The other two ports were connected to the radon-in-air monitor such that one port is linked to its outlet and the other port is connected to its inlet.

Radon measurement was done by purging radon from each of the bottled water samples into a closed air loop (Lee and Kim 2006). The circulating air, which enters the water sample via a bubble stone attached to the end of the inlet tube, purges radon from the water sample until radon activity concentration equilibrium is reached between the water and air. After equilibrium is reached, the radon activity concentration in the air loop is measured by means of a radon-in-air monitor. In the presented study, a RAD-7 radon-in-air Monitor was used. The air loop which was maintained at a flow rate of about 1 l min^{-1} included a desiccant column to ensure low moisture content of the recirculating air (< 10 %). The RAD-7 has been described in detail in section 3.1.

All samples were measured twice. The first analysis was done within a few hours after sampling to determine the total radon activity concentration in the lake water body. The resulting total radon activity concentrations were decay-corrected back to the time of sampling. A second analysis was performed after 30 days (i.e., eight radon half-lives) after sampling to determine the radon activity concentration that is supported by radium-226 dissolved in the water sample. Excess radon activity concentrations were taken as the difference between the total radon activity concentration determined initially and the radon activity concentration supported by dissolved radium-226 determined after 30 days.

Batch experiments with lake water and sediments were carried out in order to quantitatively assess the diffusive radon flux from the sediment into the water column and to determine the radon activity concentration representative for infiltrating groundwater (Corbett et al. 1998). Sediment cores of about 40 cm in length and 10 cm in diameter, including a volume of about one litre of overlying lake water, were kept still over a period of 30 days in the (sealed) PVC pipes in which they had been collected. After this period, the pore water and the overlying water were separated (preventing air contact) and the respective radon activity concentrations were measured using liquid scintillation counting (Tri-Carb 2770 TR/SL, Canerra-Packard, Freyer at al. 1997).

To estimate radon fluxes into the atmosphere, the atmospheric radon activity concentration at the study site was measured continuously at ten–minute intervals just

above the ground surface close to the lake shore with a portable radon-in-air monitor (AlphaGuard, Genitron Instruments). The AlphaGuard has been described in detail in section 3.2.

Temperature, pH, and electrical conductivity profiles in the lake were measured in-situ at sampling point SP 2 using an YSI 6820 probe (YSI Hydrodata Ltd). Wind velocity was determined using a stationary wind speed sensor (Wind Speed Sensor 2740, Aanderaa Instruments) installed on the lake at sampling point SP 2. Wind speed was recorded every ten minutes.

4.1.5 Results and discussion

4.1.5.1 pH, electrical conductivity, and temperature depth profiles

As expected for a meromictic lake, the permanent stratification of the water body results in typical pH, electrical conductivity, and temperature profiles as shown in Figure 4-3. The thickness of the metalimnion is approximately 0.3 m, starting at a depth of about 1.2 m. However, the actual depth and thickness of the metalimnion vary seasonally.

Both the mixolimnion and monimolimnion show slightly acidic pH values with the monimolimnion being more acidic than the mixolimnion. However, pH conditions in the two layers do not differ considerably from each other. Values range from 5.6 to 6.7 and 5.6 to 6.2 in October and from 5.8 to 6.7 and 5.8 to 6.1 in December for the mixolimnion and monimolimnion, respectively. During both sampling campaigns the lowest pH values were found in the metalimnion (Figure 4-3).

The electrical conductivities measured within the mixolimnion and the monimolimnion were found to be nearly constant within each layer. However, electrical conductivities measured in the mixolimnion are significantly lower than those found in the monimolimnion, confirming the stable stratification of the water body. Mixolimnion values were found to be 380 and 304 $\mu S\ cm^{-1}$ in October and December, respectively, electrical conductivities in the monimolimnion were 770 and 666 $\mu S\ cm^{-1}$ in October and December, respectively (Figure 4-3).

The temperature profiles indicate a thermal stratification of the lake. Water temperatures within the mixolimnion were constant at 11.7°C (October) and 4.5°C (December), indicating effective water mixing above the metalimnion. In December, the temperature in the monimolimnion is constant with depth but at a value of 6.8°C significantly lower

than in October. The October profile below the metalimnion shows a slight temperature increase to reach a maximum at about 2 m below the lake surface (13.0°C) and then a decrease with depth until it reaches its minimum value at the sediment surface (9.3°C).

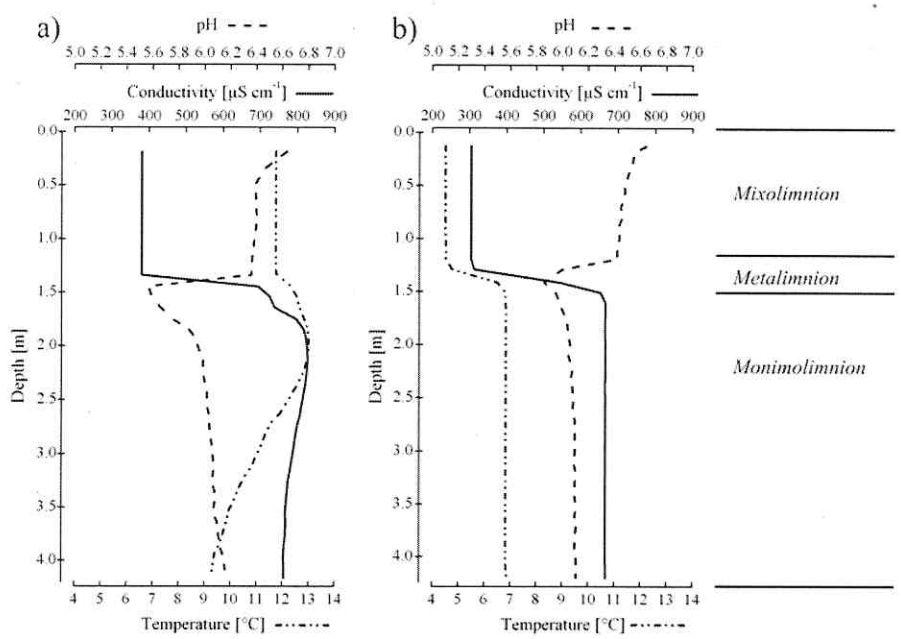

Figure 4-3: Depth profiles of pH, electrical conductivity, and temperature at sampling point SP 2 during a) the October and b) the December 2006 sampling.

4.1.5.2 Excess radon profiles

The radon depth profiles measured within the lake during the two sampling campaigns revealed significant excess radon activity concentrations (Rn_{ex}; Figure 4-4).

The excess radon measured over the complete profiles was about twice as high in October (22.3 ± 9.3 Bq m^{-3}) as in December (12.1 ± 4.9 Bq m^{-3}). Since the diffusive benthic flux can be assumed to be constant over time (at least during the sampling period), the observed differences in the mean excess radon activity concentrations indicating significantly higher groundwater discharge rates in October.

Since excess radon was observed in the mixolimnion as well as in the monimolimnion, benthic fluxes must be expected in both water masses. The sediment material collected from the mixolimnion zone (MIX 1) was found to be a fine grained sand with a k_f value of about 10^{-4} m s^{-1}. The sediment from the monimolimnion zone (MON 1 – 4) was a silty clay with a small fraction of fine sand; the k_f value is around 10^{-6} m s^{-1}.

During the October campaign excess radon showed steady activity concentrations of around 16.0 ± 2.2 Bq m^{-3} from the lake surface down to a depth of 3 m. The only exception is the sample taken 1 m below the surface, just above the metalimnion with a significantly higher value of 25.0 ± 7.3 Bq m^{-3}. Near the sediment, the excess radon activity concentration increases, reaching its maximum value above the sediment surface (43.7 ± 10.7 Bq m^{-3}). This trend corresponds to the temperature gradient found in the monimolimnion in October and can be explained by moderate groundwater discharge to the bottom of the lake in spite of the rather low hydraulic conductivity of the sediment material found there.

As mentioned above excess radon activity concentrations determined during the December campaign are generally lower than those measured in October (by about 55 %). The sample taken at 1.5 m, which shows a very low excess radon activity concentration of 1.0 ± 0.2 Bq m^{-3}, was probably collected from the metalimnion. This rather thin layer is isolated from the rest of the lake water body with regard to material transport. The only noteworthy radon source in the metalimnion is from decay of dissolved radium-226. Hence, hardly any excess radon is present. Excluding the very low value measured at 1.5 m, excess radon activity concentrations average about 14.0 ± 2.7 Bq m^{-3}, a value comparable to the activity concentration found in the upper part of the lake in October (< 3 m). In general, the excess radon activity concentrations are more constant in December than in October. The significant spike of excess radon observed close to the sediment in October was not found in December, which suggests that the groundwater discharge at the bottom of the lake had (at least temporarily) halted. This indicates that F_{adv} and hence groundwater discharge is variable over time.

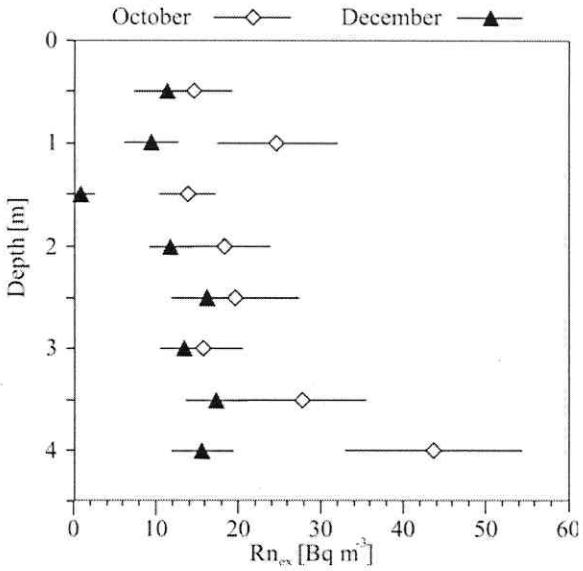

Figure 4-4: Excess radon depth profiles determined during the two sampling campaigns.

Because of the strong meromixis and the negligible diffusion length of radon in water, the mixolimnion and monimolimnion must be considered separate water masses with regard to their excess radon inventories. Total benthic radon fluxes were calculated with Eq. 4-2 assuming steady state conditions. All representative data for mixolimnion and monimolimnion are summarized in Table 4-1. It must be pointed out that the F_{total} values given for the mixolimnion do not yet include atmospheric evasion losses. The respective correction for this process will be discussed in section 4.1.5.5.

Table 4-1: Excess radon inventories and total benthic radon fluxes ($F_{total} = F_{adv} + F_{diff}$) determined in the mixolimnion (MIX) and the monimolimnion (MON) during the two sampling campaigns.

Location	Water column [m]	I^{ex} October [Bq m^{-2}]	I^{ex} December [Bq m^{-2}]	F_{total} October [Bq m^{-2} d^{-1}]	F_{total} December [Bq m^{-2} d^{-1}]
MIX	1.2	21.3 ± 6.1	14.8 ± 4.0	3.9 ± 1.1	2.7 ± 0.7
MON	2.9	72.7 ± 21.3	42.0 ± 9.3	13.2 ± 3.9	7.6 ± 1.7

4.1.5.3 Radon activity concentration of the discharging groundwater

Radon activity concentrations in groundwater wells were measured during the October sampling. Around the northern part of the lake, activity concentrations vary between 4.2 ± 0.2 kBq m^{-3} (WS 2) and 7.7 ± 0.4 kBq m^{-3} (WS 1). At the southern tip of the lake,

however, an activity concentration of only 80 ± 20 Bq m^{-3} (WS 4) was found. Since the local groundwater flow direction is reported to be to the north roughly parallel to the lake axis (Kupetz 1997, Rascher et al. 2000) lake water dilution in WS 4 can be ruled out. Hence, the wide activity concentration range found in groundwater wells within such short distances must be explained by the very complex geological setting in this area as described in the literature (Kupetz 1997, Rascher at al. 2000). One effect of this complex geology is highly variable specific radium-226 activities of the aquifer material. The complex geological setting is also evident by the fact that the depths of the groundwater table in the four sampled wells differed by a few decimetres over distances of about 30 m, indicating poor hydrological connection between them.

In order to ensure representative radon activity concentrations for the groundwater endmember, pore water radon activity concentrations from sediment equilibration batch experiments (discussed in the following section) were used to assess the groundwater discharge instead of using the radon activity concentrations determined in the groundwater wells. The pore water radon activity concentrations determined from batch experiments can be taken as representative for discharging groundwater because the thickness of the sediment layer has been determined during sediment sampling with > 40 cm. Therefore, it can be assumed that the groundwater remains in the sediment matrix long enough to reach secular equilibrium between radium-226 and radon.

4.1.5.4 Diffusive benthic fluxes

The diffusive radon fluxes were determined using the sediment cores collected from the lake (cf. section 4.1.4.1 and 4.1.4.2, Figure 4-2b). Water samples to determine radon activity concentrations in the overlying water column were taken directly from the sealed sediment cores after 30 days for equilibration. The mean radon activity concentration supported by diffusive radon flux (C_{Rn}^{w}) found for the monimolimnion was 36.6 ± 7.3 Bq m^{-3}. The sample taken from the mixolimnion showed a lower diffusion-supported value of 22.3 ± 4.0 Bq m^{-3}.

Pore water radon activity concentrations (C_{Rn}^{pw}) obtained by the batch experiments varied between 1.0 ± 0.05 kBq m^{-3} and 2.0 ± 0.1 kBq m^{-3}, with a mean activity concentration of 1.73 ± 0.49 kBq m^{-3} for the monimolimnion. The sediment sample taken from the mixolimnion showed a lower activity concentration of 0.6 ± 0.03 kBq m^{-3}. All data are summarized in Table 4-2.

Table 4-2: Radon activity concentrations determined during batch experiments with sediment samples taken from the mixolimnion (MIX) and the monimolimnion (MON) and respective diffusive radon fluxes.

Location	C_{Rn}^{w} [Bq m^{-3}]	C_{Rn}^{pw} [kBq m^{-3}]	F_{diff} [Bq m^{-2} d^{-1}]
MIX 1	22.3 ± 4	0.6 ± 0.03	4.1 ± 0.5
MON 1	47.7 ± 10	2.0 ± 0.1	13.9 ± 0.7
MON 2	22.3 ± 4	1.0 ± 0.5	7.0 ± 0.4
MON 3	33.4 ± 7	1.9 ± 0.1	13.3 ± 0.7
MON 4	43.1 ± 9	2.0 ± 0.1	14.0 ± 0.7

The diffusive radon flux associated with each sampling location was calculated using Eq. 4-5. The estimated diffusive fluxes from the lake sediment into the water column are 4.1 ± 0.4 Bq m^{-2} d^{-1} for the mixolimnion and 12.0 ± 1.2 Bq m^{-2} d^{-1} for the monimolimnion.

The ratio of sediment surface/water volume is of importance for assessing the relevance of diffusive radon input to the water column. In Figure 4-5 this relation is plotted. While the ratio in the mixolimnion (≤ 1.2 m) is less than 0.02, it is significantly higher and increasing with depth throughout the monimolimnion (≥ 1.5 m). Therefore, it can be assumed that diffusive radon input into the lake is of hardly any relevance in the mixolimnion compared to the monimolimnion.

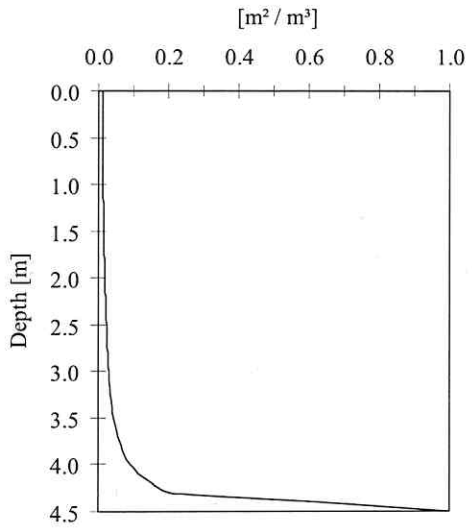

Figure 4-5: Sediment surface area [m²] vs. water volume [m³] as a function of depth.

4.1.5.5 Atmospheric evasion

Due to the stable stratification of the lake, radon loss via atmospheric evasion is only relevant for the mixolimnion. Atmospheric radon activity concentrations near the lake were determined to be 6.6 ± 3.8 Bq m^{-3} and 3.8 ± 3.9 Bq m^{-3} for October and December, respectively. Wind speed was averaged for each sampling period and showed values of 0.24 m s^{-1} for October and 0.76 m s^{-1} for December. For the calculation of F_{atm} Eq. 4-3 was employed and the calculated fluxes were 0.1 ± 0.05 Bq m^{-2} d^{-1} for October and 0.5 ± 0.17 Bq m^{-2} d^{-1} for December.

4.1.5.6 Radon budget and estimation of groundwater discharge

Applying Eq. 4-1, input and output fluxes of radon were estimated for the lake in October and December 2006. All data used to obtain these fluxes and all results are summarized in Table 4-3 and in Table 4-4, respectively.

In order to estimate groundwater discharge based on the radon balance, the radon activity concentrations determined by the sediment equilibrium batch experiments are assigned to the discharging groundwater (cf. Eq. 4-6 and Table 4-2). Assuming groundwater uniformly seeps into the lake over the entire lake bed, the data collected during the October campaign suggest an advective velocity of 0.66 ± 0.19 cm d^{-1} for the mixolimnion and 0.06 ± 0.06 cm d^{-1} for the monimolimnion. For December, the mixolimnion showed a value of 0.53 ± 0.13 cm d^{-1}, but for the monimolimnion radon inventory was balanced by benthic diffusive flux only. Therefore, no groundwater discharge has been found in the monimolimnion in December.

The total volume of groundwater input into the lake for October was estimated at 18.9 ± 5.4 m^3 d^{-1} for the mixolimnion and 0.7 ± 0.7 m^3 d^{-1} for the monimolimnion. For December, the groundwater discharge into the mixolimnion was 15.0 ± 3.7 m^3 d^{-1}. Based on the water volume of the mixolimnion (5 900 m^3) and the monimolimnion (1 300 m^3), the residence time of lake water varies between 0.9 and 1.1 years for the mixolimnion and 5.3 years for the monimolimnion. The significantly shorter residence time of lake water in the mixolimnion agrees with the observed precipitation and run-off water inputs and the lake water discharge from the mixolimnion via a temporary creek during the wet season.

Table 4-3: Parameters used for calculations to estimate groundwater discharge into Lake Waldsee in October and December 2006.

Symbol	Parameter	Unit	Value
C_{Rn}^{w}	Radon activity conc., overlying water – Mixolimnion	[Bq m^{-3}]	22.3 ± 4.0
	Radon activity conc., overlying water – Monimolimnion	[Bq m^{-3}]	36.6 ± 7.3
C_{Rn}^{pw}	Radon activity conc., pore water fluid – Mixolimnion	[Bq m^{-3}]	600 ± 30
	Radon activity conc., pore water fluid – Monimolimnion	[Bq m^{-3}]	1725 ± 90
Φ	Sediment porosity	[-]	0.9
October			
u_{10}	Wind speed	[m s^{-1}]	0.24
T	Temperature – Mixolimnion	[°C]	11.7
	Temperature – Monimolimnion	[°C]	11.4
υ	Gas transfer velocity	[m s^{-1}]	9.5×10^{-8}
k	Partition coefficient – Mixolimnion	[-]	0.33
	Partition coefficient – Monimolimnion	[-]	0.33
Sc	Schmidt number – Mixolimnion	[-]	926
	Schmidt number – Monimolimnion	[-]	934
Ds	Radon sediment diffusion coefficient – Mixolimnion	[m^2 d^{-1}]	7.2×10^{-5}
	Radon sediment diffusion coefficient – Monimolimnion	[m^2 d^{-1}]	7.2×10^{-5}
December			
u_{10}	Wind speed	[m s^{-1}]	0.76
T	Temperature – Mixolimnion	[°C]	4.8
	Temperature – Monimolimnion	[°C]	6.9
υ	Gas transfer velocity	[m s^{-1}]	5.3×10^{-7}
k	Partition coefficient – Mixolimnion	[-]	0.42
	Partition coefficient – Monimolimnion	[-]	0.39
Sc	Schmidt number – Mixolimnion	[-]	1128
	Schmidt number – Monimolimnion	[-]	1061
Ds	Radon sediment diffusion coefficient – Mixolimnion	[m^2 d^{-1}]	5.9×10^{-5}
	Radon sediment diffusion coefficient – Monimolimnion	[m^2 d^{-1}]	6.3×10^{-5}

Table 4-4: Input and output fluxes of radon for Lake Waldsee.

Parameter		October [Bq m^{-2} d^{-1}]	December [Bq m^{-2} d^{-1}]
output			
F_{atm}	Mixolimnion	0.1 ± 0.05	0.5 ± 0.2
$z \lambda_{Rn} C_{Rn}^{w}$	Mixolimnion	8.2 ± 2.2	4.2 ± 1.4
	Monimolimnion	22.5 ± 3.9	15.4 ± 3.4
input			
$z \lambda_{Rn} C_{Ra}^{w}$	Mixolimnion	4.3 ± 1.3	1.5 ± 0.8
	Monimolimnion	9.3 ± 3.3	7.8 ± 3.0
F_{diff}	Monimolimnion	12.0 ± 2.5	12.0 ± 2.5
F_{adv}	Mixolimnion	4.0 ± 1.7	3.2 ± 1.0
	Monimolimnion	1.2 ± 0.3	--

4.1.6 Conclusion

One of the main purposes of the case study discussed above was to confirm the applicability of naturally occurring radon as a geochemical tracer for investigating groundwater discharge into lakes.

A meromictic lake, i.e., a water body that is divided horizontally into two separate layers, the upper mixolimnion (with seasonal mixing) and the lower monimolimnion (without seasonal mixing), was chosen for the on-site survey. During two sampling campaigns groundwater discharge rates could be qualified and quantified separately for the mixolimnion and the monimolimnion using radon as a tracer. The results allow the conclusion that the presented method has high potential for being used as fast and straightforward measure even at low groundwater discharge rates.

4.2 Using radon for tracing groundwater discharge into a dimictic lake

4.2.1 Introduction

A case study was carried out with the aim to practically test whether estimates of groundwater discharge rates into lakes can be made via an uncomplicated and straightforward technique using radon as a naturally occurring groundwater tracer. As the investigation site a dimictic lake was chosen, i.e., a lake where the water body is subject to biannual changes in stratification (Boehrer and Schultze 2008). During spring and autumn the water body is well mixed, during summer and winter the water body shows (thermal) stratification.

In order to evaluate changes in the spatial and temporal radon patterns in the lake sampling campaigns were conducted during different stages of stratification. It was hypothesized that if a lake is well mixed and the radon activity concentration of the discharging groundwater is known, only a few water samples are necessary to calculate the radon inventory and finally to estimate groundwater discharge rates to the lake.

The study discussed in the following section has been published in a modified form as:

Schmidt, A., Stringer, C. E., Haferkorn, U., Schubert, M. (2008). Quantification of groundwater discharge into lakes using radon-222 as naturally occurring tracer. *Environmental Geology*, doi: 10.1007/s00254-008-1186-3.

4.2.2 Study area

The presented study was carried out at Lake Ammelshainer See (51°17'51"N, 12°36'30"E), a dredging lake located in the eastern part of Germany, about 25 km east of Leipzig (Figure 4-6a). The lake is situated in the southern part of the Leipzig Lowland; a landscape characterized by tertiary and quaternary sediments (Eissmann and Litt 1994).

Lake Ammelshainer See has an average depth of about 10 m and a maximum depth of about 24 m. Its surface covers an area of around 5.3×10^5 m^2; the entire water volume is approximately 5.6×10^6 m^3 (Figure 4-6b). There is no noteworthy input or output of surface water. Hence, the only relevant water sources are precipitation and groundwater. The local groundwater discharges into the lake mainly from a north-eastern direction (Haferkorn et al. 2003).

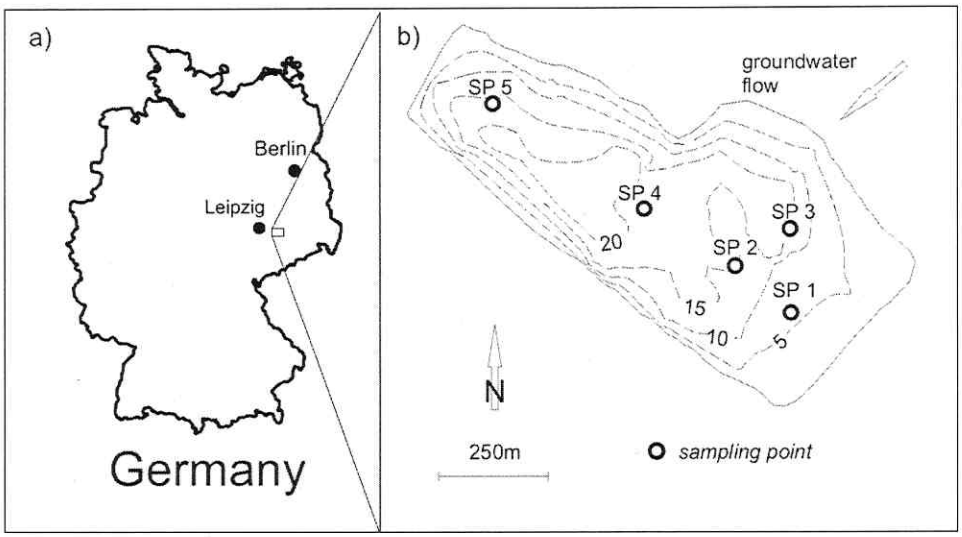

Figure 4-6: a) Location of the investigation area; b) Lake "Ammelshainer See" with sampling points (SP); drawn through line indicates lake boundary, dashed lines indicate contour lines of lake water depth [m].

The phreatic aquifer in the study area consists of river sediments (Mulde Terrace) deposited in late Pleistocene and has a thickness of about 20 m. The river sediments consist mainly of coarse sands and gravels, which were exploited in numerous pits. Today, many of these former mining pits are lakes, like Lake Ammelshainer See, which are fed by the mentioned aquifer.

4.2.3 Material and Methods

4.2.3.1 Modeling approach

For quantitatively assessing the groundwater discharge rate into the lake by using radon as a geochemical tracer the same box model discussed in section 4.1.2 can be applied. The model considers all radon source and sink terms related to a water column in the surface water body represented by a sampling point (Corbett et al. 1997) and assumes steady-state conditions with respect to all radon fluxes. Compared to Eq. 4-1 the equation used here (Eq. 4-7), is slightly modified: the term $\lambda_{222}I_{226}$ represents the radon input from decaying radium-226 that is dissolved in the water (secular equilibrium between radium and radon is assumed) and the term $\lambda_{222}I_{222}$ quantifies the total radon decay within the considered water column.

$$F_{adv} + F_{diff} + \lambda_{222} I_{226} - F_{atm} - \lambda_{222} I_{222} = 0 \qquad \text{Eq. 4-7}$$

The quantification of F_{adv} is the desired result of the investigation, since the advective radon flux at the sediment/water interface is directly linked to the groundwater flow velocity and to the radon activity concentration of the discharging groundwater. Hence, by dividing F_{adv} by the radon activity concentration of the groundwater, the groundwater flow velocity is obtained (cf. Eq. 4-6).

4.2.3.2 Sampling and measurement

On-site activities

Five sampling points (SP 1 – SP 5) with different water depths (SP 1: 7 m; SP 2, 3, 5: 15 m; SP 4: 17 m) were defined on the lake (Figure 4-6b). Water sampling was performed during two field campaigns, which were scheduled at the beginning of April and at the end of May 2007, i.e., during different mixing stages of the lake. The lake water table between the two sampling campaigns remained constant.

Water samples were taken from different depths at all five sampling points using a peristaltic pump, allowing the recording of depth radon activity concentration profiles. All water samples were collected in special 6 litre HDPE-bottles designed for radon-in-water activity concentration measurement ensuring minimum radon loss by degassing (Stringer and Burnett 2004).

Sediment samples were taken via a sediment corer at each of the sampling points during the April campaign. The specific activity of radium-226 in the sediment was measured via gamma spectrometry (HPGe Coaxial low energy detector).

Temperature, pH, and electrical conductivity profiles were measured in-situ in the water columns at all five sampling points down to the lake bottom using a KLL-Q probe (Seba Hydrometry GmbH). Wind speed data for each sampling campaign were obtained from a weather station located at the western side of the lake (Leipzig-Holzhausen) supervised by the DWD (Deutscher Wetterdienst, German weather service). Atmospheric radon activity concentration was monitored using the AlphaGuard.

Laboratory measurements

Radon measurement of lake water samples was carried out using a method described by Lee and Kim (2006), using a RAD-7. The radon-in-air monitor RAD-7 has been discussed in detail in section 3.1. The HDPE-sample bottles were connected to the RAD-7 and the internal air pump of the radon-monitor was used for re-circulating a closed air loop through the 6 litre water sample, purging radon from the water into the air loop. After reaching equilibrium between water, air, and radon progeny attached to the PIPS detector (~ 50 min) the radon activity concentration measured in the air loop was used for calculating the initial radon-in-water activity concentration of the respective sample.

All samples were measured twice. The first analysis was done within a few hours after sampling and the resulting activity concentrations were decay-corrected back to the time of sampling. With the aim to determine the radon activity concentration that is supported by radium-226 dissolved in the water a second analysis was performed 30 days later, i.e., after eight radon half-lives had passed during which the bottles were kept closed. The difference between the results of the first and the second analysis represents the excess radon activity of each sample. Excess radon activity concentrations were used for further calculation.

In order to quantitatively assess the diffusive radon flux (F_{diff}) from the sediment into the water column, batch experiments with lake water and lake sediments taken at the five sampling points were carried out. The respective experimental approach has been described by Corbett et al. (1998). In short, 150 g of sediment and 600 ml of lake water were put into a stoppered glass flask and then shaken continuously using an overhead shaker. After reaching secular decay equilibrium between sediment radium-226 and water radon after 30 days (i.e., eight radon half-lives), water from the flasks (500 ml) was transferred into a glass bottle (with special care that no radon is degassing) and analyzed using the AlphaGuard as described by Schubert et al. (2006).

4.2.3.3 Hydrologic studies based on Darcy's law

A hydrodynamic-numerical groundwater flow- and particle tracking model (PCGEOFIM®, Müller et al. 2003) based on Darcy's law (cf. section 2.2.3) was used to simulate the groundwater flow system in the vicinity of Lake Ammelshainer See.

PCGEOFIM® is based on finite volume elements (125 × 125 m grid), i.e., the geometry, the hydrogeological aquifer properties, and the boundary conditions are described within these finite volume elements. On the basis of the digitalized hollow form of Lake Ammelshainer See horizontal and vertical linkages between the connected aquifer and the water body were established. This kind of processing of hollow forms within a model allows the exactly acquisition of changes in the storage and, hence, an exactly balancing of static and dynamic changes in the water volume of Lake Ammelshainer See.

Regarding to the results of the hydrodynamic-numerical modeling the mean groundwater flow velocity in the vicinity of the lake varies between 22 and 29 cm d^{-1}. The resulting volumetric groundwater discharge into the lake is in the range of 116 600 – 153 700 m^3 d^{-1}.

4.2.4 Results and discussion

4.2.4.1 pH, electrical conductivity, and temperature depth profiles

The three measured water parameters indicate that the water body was well mixed during the April sampling campaign. Figure 4-7a exemplifies the results recorded at sampling point SP 4. At all other sampling points comparable patterns were observed. Temperature, electrical conductivity, and pH show values of 8.1 ± 0.15°C, 780 ± 4 µS cm^{-1} and 7.7 ± 0.1, respectively, which are all virtually constant over the whole vertical profile.

During the May sampling campaign (Figure 4-7b), temperature was found to be constant only down to a water depth of around 8 m (20 ± 0.15°C), below which it is sharply decreasing to about 10 ± 0.15°C at a depth of around 12 m. Further down, the temperature is still decreasing, but with a less steep gradient. It reaches around 8 ± 0.15°C at the sediment surface (17 m). The measured temperature profile indicates that the lake showed a thermal stratification during the May campaign dividing the water body into an upper well mixed epilimnion (0 – 8 m) and a deeper hypolimnion (> 12 m), which is excluded from mixing processes and hence from atmospheric contact. Both layers are separated by a thermocline (8 – 12 m).

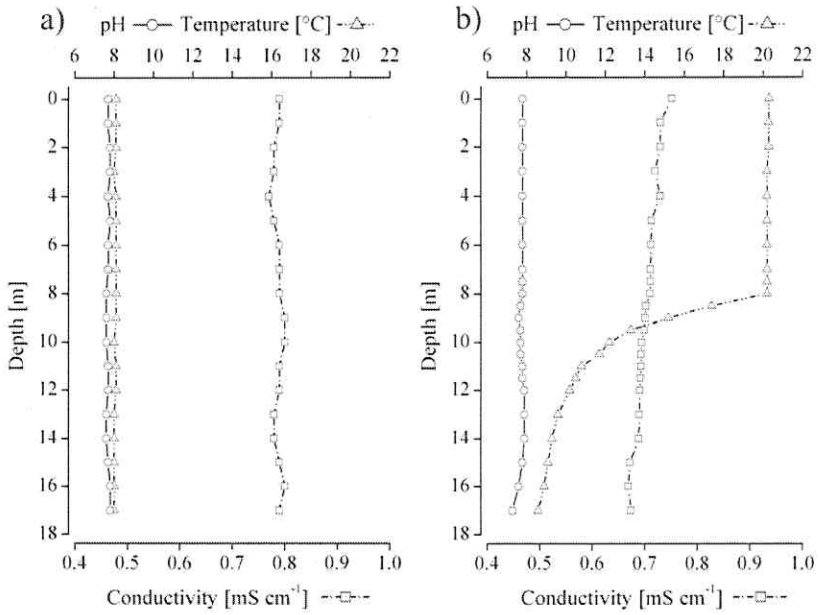

Figure 4-7: Representative vertical profiles of pH, temperature, and electrical conductivity measured during (a) April and (b) May 2007 at SP 4 (cf. Figure 4-6b).

In contrast to the temperature profile pH and electrical conductivity values are nearly constant over the whole water column also in May. Where pH values are in the same range as in early April, electrical conductivity is slightly lower (700 ± 4 µS cm^{-1}). The values indicate that no significant change in water chemistry occurs during changing of the mixing stages of the lake.

4.2.4.2 Excess radon profiles

Excess radon profiles are shown for all five sampling points in Figure 4-8 (April) and Figure 4-9 (May). Table 4-5 and Table 4-6 summarize the average excess radon values and the resulting radon inventories of the water columns represented by each sampling point for the April and May campaign, respectively.

As shown in Figure 4-7a, no stratification of the lake water body was indicated by pH, temperature, and electrical conductivity in April. The same is reflected by the excess radon depth profiles, which do not show major gradients (Figure 4-8). Radon inventories representative for the complete water columns at each sampling point during the April campaign are given in Table 4-5. The values vary in a small range between 363 and 436 Bq m^{-2} (based on the average water depth of about 10 m).

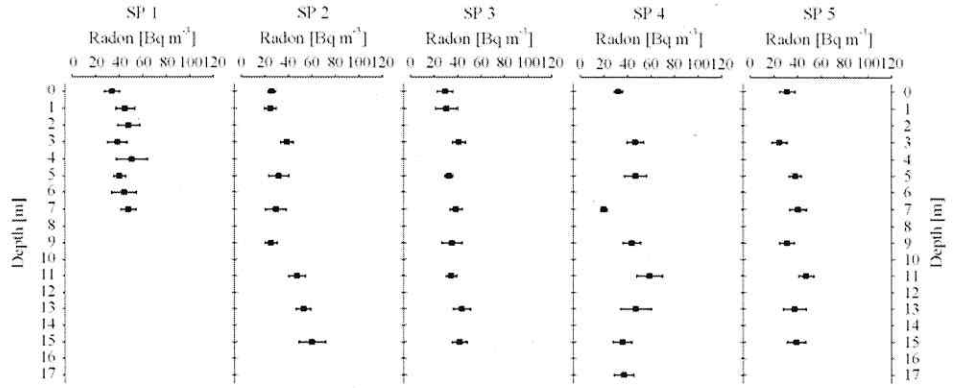

Figure 4-8: Excess radon depth profiles at each sampling point during the April campaign. Uncertainties are at the 2σ level and based on counting statistics.

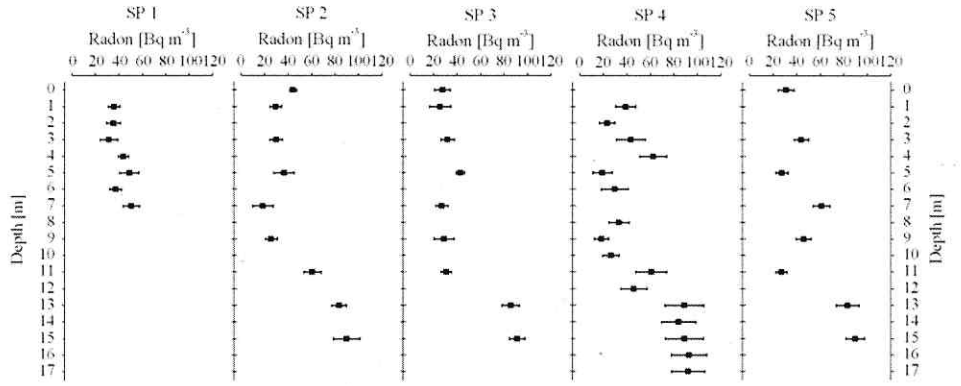

Figure 4-9: Excess radon depth profiles at each sampling point during the May campaign. Uncertainties are at the 2σ level and based on counting statistics.

During the May campaign the lake shows a thermal stratification (Figure 4-7b), which is also illustrated by the radon activity concentration (Figure 4-9). As shown in Figure 4-7, pH, and electrical conductivity and hence the water chemistry of the lake water does not change during different mixing stages. Thus, it can be inferred that a potential groundwater discharge influences the whole surface water body and not only a single water mass (neither epilimnion nor hypolimnion). Hence, for the further calculations the lake is considered as being well mixed in relation to the radon activity concentration, i.e., the average excess radon values and the according radon inventories are related to the whole lake water body. The values obtained (again based on the average water depth of about 10 m) are summarized in Table 4-6; they range between 304 and 405 Bq m^{-2}. The fact that the radon inventories determined during both sampling campaigns vary for each campaign in a very small range confirms the hypothesis, that just a few water

samples are necessary to calculate the radon inventory of the lake water with sufficient accuracy.

Table 4-5: Average excess radon activity concentrations for the water columns at each sampling point and resulting excess radon inventories (based on the average water depth of about 10 m) during the April sampling campaign.

SP	Average excess radon activity concentration [Bq m^{-3}]	Radon inventory [Bq m^{-2}]
1	43.6 ± 5.6	435.9 ± 56.3
2	37.2 ± 8.4	371.8 ± 84.5
3	36.3 ± 5.1	362.6 ± 50.9
4	40.9 ± 9.5	408.7 ± 94.6
5	36.3 ± 6.9	362.8 ± 69.5

Table 4-6: Average excess radon activity concentrations for the water columns at each sampling point and resulting excess radon inventories (based on the average water depth of about 10 m) during the May sampling campaign.

SP	Average excess radon activity concentration [Bq m^{-3}]	Radon inventory [Bq m^{-2}]
1	40.5 ± 7.4	404.7 ± 73.6
2	34.9 ± 13.9	349.3 ± 139.4
3	30.4 ± 5.7	304.2 ± 57.2
4	36.5 ± 15.4	365.5 ± 153.6
5	39.3 ± 13.4	393.2 ± 134.2

4.2.4.3 Radon activity concentration of the discharging groundwater

A key parameter for determining advection rates is the radon activity concentration of the groundwater discharging into the lake (Burnett et al. 2007). Groundwater samples can be taken for analysis from monitoring wells situated close to the lake under investigation. However, it has to be kept in mind that after about 20 days (i.e., five radon half-lives) decay equilibrium between the radon activity concentration of the groundwater and the aquifer matrix is virtually reached (97 %). Hence, if there is no evidence of direct spring inputs (like in the study discussed) and if a substantial sediment layer is found at the lake's bottom and if the groundwater flow velocity is slow enough to allow groundwater/sediment contact of more than 20 days, radon activity concentrations determined in groundwater wells surrounding the lake are not necessarily representative for the discharging water.

The thickness of the sediments was determined via depth sonar during the hydrographic surveying of the lake. It is increasing from a few centimetres in the littoral zone to more than two metres in the deepest parts of the lake. At the north-eastern shoreline, where groundwater discharge is known to occur, sediment thickness reaches a few decimetres already in the very shallow parts of the lake and increases to more than 2.5 m at SP 3 (Figure 4-2b). The sediment is mainly fine sand with faintly silt contingent with silt distribution slightly increasing towards the deeper parts of the lake. Hence, batch experiments (n = 5) with sediments from the north-eastern part of the lake were carried out with the aim to determine the radon equilibrium activity concentration of the discharging pore water (Corbett et al. 1998). The respective pore water equilibrium activity concentrations were found to be in a small range between 300 ± 24 and 330 ± 28 Bq m^{-3}. The mean value of this range, 316 ± 12.9 Bq m^{-3}, was used for any further calculations.

4.2.4.4 Diffusive benthic fluxes

As mentioned above, the advective radon flux has to be distinguished from the diffusive radon input from the sediment into the lake water body. Burnett et al. (2003b) used data from various environments to derive an empirical equation (Eq. 4-8) relating the specific radium-226 activity of the sediment (expressed in dpm g^{-1}) to the diffusive flux from the sediment into the water column (expressed in dpm m^{-2} d^{-1}).

$$F_{diff} = 495\ A_{Ra} + 18.2 \qquad \text{Eq. 4-8}$$

F_{diff}	radon flux, sediment → surface water	[Bq m^{-2} d^{-1}]
A_{Ra}	specific radium-226 activity - sediment	[Bq kg^{-1}]

The measured specific radium-226 activity of sediment samples from the sampling points and the resulting benthic diffusive fluxes obtained by using Eq. 4-8 are shown in Table 4-7 (values are recalculated to SI-units).

Considering the distribution of the sampling points on the lake the average value of all determined fluxes (43.6 ± 32.6 Bq m^{-2} d^{-1}) was used as representative value for further calculations in order to estimate the overall diffusive radon input into the lake water.

Table 4-7: Measured specific radium-226 activities of lake sediments and calculated benthic diffusive fluxes.

SP	Radium-226 [Bq kg^{-1}]	Diffusive radon flux [Bq m^{-2} d^{-1}]
1	14 ± 2	7.2 ± 1.3
2	155 ± 9	77.0 ± 4.8
3	159 ± 9	79.0 ± 4.8
4	168 ± 9	83.5 ± 4.8
5	161 ± 9	80.0 ± 4.8

4.2.4.5 Atmospheric evasion

Gas exchange across the water/air interface may be a significant sink for radon. Radon flux to the atmosphere (F_{atm}) depends on turbulent transfer and on molecular diffusion generated by the activity concentration gradient at the water/air interface (Macintyre et al. 1995; cf. Eq. 4-3 and section 4.1.2).

During both sampling campaigns the atmospheric radon activity concentration was monitored at the southern end of the lake using the AlphaGuard. The activity concentrations averaged at 5.7 ± 2.4 Bq m^{-3} and 2.8 ± 2.5 Bq m^{-3} for April and May, respectively. The resulting atmospheric fluxes are summarized in Table 4-8.

4.2.4.6 Radon budget and estimation of groundwater discharge

All relevant data, the resulting advective radon fluxes, and groundwater discharge rates for each sampling point and both sampling campaigns are summarized in Table 4-8. For the April campaign the groundwater discharge rates representative for the sampling points vary between 16.0 ± 5.3 and 22.1 ± 7.2 cm d^{-1}. For the May campaign the groundwater discharge rates vary between 14.0 ± 4.4 and 22.6 ± 7.9 cm d^{-1}. Under consideration of uncertainties (2σ-error) no gradients exists between the five sampling points.

For the calculation of the volumetric groundwater discharge into the lake the surface of the considered water body has to be taken into account. The calculated discharge rates were related to the lake surface area (530 000 m^2) for both campaigns. Considering the water volume of the lake, and the volumetric groundwater discharge the residence time of the lake water can be calculated as follows:

$$t_{Rt} = \frac{V_L}{V_{GD}} \qquad \text{Eq. 4-9}$$

t_{Rt}	water residence time	$[d^{-1}]$
V_L	water volume of the lake	$[m^3]$
V_{GD}	volumetric groundwater discharge	$[m^3\ d^{-1}]$

The resulting values, together with the determined values for volumetric groundwater discharge, are summarized in Table 4-9.

Table 4-8: Radon fluxes and groundwater (GW) discharge rates for the April and May sampling campaign. As radon activity concentration for the groundwater endmember 316 ± 12.9 Bq m^{-3} was used (cf. section 4.2.4.3). Note: $\lambda_{222}I_{222}$ represents the decay of the total radon activity concentration.

SP	$\lambda_{222}I_{222}$	F_{atm}	$\lambda_{222}I_{226}$	F_{diff}	F_{adv}	GW-discharge rate
			[Bq m^{-2} d^{-1}]			[cm d^{-1}]
April 2007 campaign						
1	108.9 ± 20.4	34.7 ± 7.1	30.0 ± 5.1		70.0 ± 19.4	22.1 ± 7.2
2	103.4 ± 16.8	29.3 ± 5.7	36.1 ± 4.6		53.0 ± 15.0	16.8 ± 5.8
3	96.0 ± 16.9	28.6 ± 5.2	30.4 ± 5.7	43.6 ± 3.0	50.6 ± 13.4	16.0 ± 5.3
4	110.5 ± 17.1	32.4 ± 6.6	36.5 ± 2.9		62.8 ± 17.8	19.9 ± 6.7
5	101.2 ± 16.5	28.6 ± 5.8	35.5 ± 4.0		50.6 ± 15.4	16.0 ± 5.9
May 2007 campaign						
1	105.5 ± 11.1	14.4 ± 0.1	32.2 ± 5.0		44.1 ± 10.4	14.0 ± 4.4
2	101.8 ± 12.2	16.6 ± 0.2	17.8 ± 2.6		57.0 ± 11.8	18.0 ± 4.9
3	93.5 ± 11.4	15.5 ± 0.2	15.2 ± 3.3	43.6 ± 3.0	50.1 ± 10.8	15.9 ± 4.5
4	114.4 ± 20.4	19.1 ± 0.3	18.4 ± 1.4		71.5 ± 21.6	22.6 ± 7.9
5	109.6 ± 12.2	18.4 ± 0.2	17.2 ± 2.0		67.2 ± 11.7	21.3 ± 4.9

As shown in Table 4-9 the groundwater discharge determined at the five sampling locations vary between about 84 845 and 117 381 m^3 d^{-1} for the April campaign. The overall groundwater discharge for the May campaign range within 73 982 and 119 927 m^3 d^{-1}. In consideration of the uncertainties all determined values are within the same range. A mean value, which includes all determined groundwater discharge rates amounts to 96 268 ± 14 495 and 97 258 ± 19 159 m^3 d^{-1}, for April and May, respectively.

Table 4-9: Groundwater discharge and lake water residence times for the April and May sampling campaign.

SP	Volumetric groundwater discharge [m^3 d^{-1}]	Water residence time [d]
April 2007 campaign		
1	117 381 ± 38 308	47.7 ± 11.7
2	88 927 ± 30 827	63.0 ± 16.2
3	84 845 ± 28 191	66.0 ± 16.5
4	105 280 ± 35 638	53.2 ± 13.5
5	84 905 ± 31 481	66.0 ± 17.8
May 2007 campaign		
1	73 982 ± 23 281	75.7 ± 18.1
2	95 645 ± 25 716	58.5 ± 12.4
3	84 094 ± 23 979	66.6 ± 14.8
4	119 927 ± 41 929	46.7 ± 12.1
5	112 643 ± 25 759	49.7 ± 9.3

These groundwater discharge values are slightly lower than the volumetric groundwater discharge rates based on the groundwater flow model Darcy's law (cf. section 4.2.3.3). This can be explained with the limitation of the used groundwater model, e.g., (1) the hydraulic conductivity was estimated and may not reflect the average conditions for the actual groundwater flow path considered, (2) the groundwater flow conditions used may not reflect truly conditions and (3) flow net analysis cannot account for spatial variability and other local factors which influence groundwater discharge rates. In general, the mentioned factors lead to a higher estimation of groundwater flow velocities and, hence, to higher groundwater discharge rates.

As also shown in Table 4-9 the residence time of the lake water varies between 47.7 ± 11.7 and 66.0 ± 17.8 days for the April and 46.7 ± 12.1 and 75.7 ± 18.1 days for the May campaign.

Lake Ammelshainer See is situated in a water protection area and this region is intensively used for drinking water supply for the City of Leipzig. Thus, the high groundwater flow velocity in the vicinity and the short water residence time of Lake Ammelshainer See are caused by the related activities.

4.2.5 Summary and Conclusion

This study was carried out with the aim to examine the applicability of naturally occurring radon as a geochemical tracer for the investigation of groundwater discharge into lakes. The results from the radon method are within a good agreement with discharge rates obtained from a conventional hydrodynamic-numerical groundwater flow model based on Darcy's law. It could be shown that in case of a lake with a size and shape of Lake Ammelshainer See (530 000 m^2) reasonable groundwater discharge estimates can be made by collecting and analyzing just a few water samples. Thus, the use of radon as a naturally occurring tracer allows the easy, fast, and inexpensive assessment of groundwater/lake water interaction and the prediction of the future development of the respective water resources.

5 Conclusions for the use of radon as a natural geochemical tracer for study of groundwater discharge into lakes

The overall purpose of the presented study was testing the applicability of the naturally occurring radionuclide radon-222 as a geochemical tracer for the investigation of groundwater discharge into lakes.

Radon is predestinated for its utilization as groundwater indicator because of its ubiquitous occurrence making it a geochemical tracer, because of its noble gas configuration leading to its biologically and chemically inert behavior, and due to its short half-life resulting in substantially lower radon activity concentrations in surface waters compared to groundwater.

The methodical approach of using radon as a tracer in the given context is based on balancing the geochemical budget related to a specific lake water body quantitatively for all radon input and output terms.

In the presented work the method was successfully applied for assessing groundwater discharge into a dimictic and a meromictic lake, i.e., into two essentially different lake environments. As a result it was shown that radon allows qualitative and quantitative estimation of groundwater discharge rates for both, discrete water layers as well as for whole water bodies.

Attaining information on groundwater discharge rates is essential for the calculation of water residence times and hence for predicting the future development of the studied surface water resource. Thus, the assessment of water budgets of lakes, in particular of systems with limited input and output via surface water, i.e., groundwater seepage lakes, greatly benefits from the application of the radon method.

One of the main advantages of the described approach to estimating groundwater discharge rates is the fact that a lake water column generally tends to integrate the radon signal that comes into the water body via various seeps and springs. This has the advantage of smoothing out small-scale variations in groundwater discharge and allows the interpretation of rather large spatial heterogeneities that are associated with groundwater pathways.

In general, it can be stated that the use of radon as a naturally occurring geochemical

tracer admits a fast, straightforward, and inexpensive assessment of groundwater discharge rates into lakes.

In the given context radon-222 is a powerful tool for the assessment of hydrological processes, which occur within a time frame of up to 16 days (four radon half-lives). However, processes that take longer (e.g. very slow groundwater discharge into lake water bodies with restricted water circulation) cannot be examined using solely radon as a geochemical tracer. In that case other tracer techniques have to be employed additionally. As one option the use of the four naturally occurring radium isotopes, showing half-lives between 3.6 days and 1 600 years, in combination with radon-222 could provide a tool for the investigation of such hydrological processes. In future studies this approach will be tested.

Bibliography

Abdelouas, A., Lutze, W., Nuttall, E. (1998). Chemical reactions of uranium in ground water at a mill tailing site. *Journal of Contaminant Hydrology* 34: 343-361.

Almeida, R. M. R., Lauria, D. C., Ferreira, A. C., Sracek, O. (2004). Groundwater radon, radium and uranium concentrations in Regiao dos Lagos, Rio de Janeiro state, Brazil. *Journal of Environmental Radioactivity* 73: 323-334.

Andrews, J. N., Wood, D. F. (1972). Mechanism of radon release in rock matrices and entry into groundwaters. *Transactions of the Institution of Mining and Metallurgy* B81: 198-209.

Avrorin, V. V., Krasikova, R. N., Nefedov, V. D., Toropova, M. A. (1981). Production of higher fluorides and oxides of radon. *Radiokhimiya* 23: 879-883.

Ball, T. K., Cameron, D. G., Colman, T. B., Roberts, P. D. (1991). Behavior of radon in the geological environment - A review. *Quarterly Journal of Engineering Geology* 24: 169-182.

Barretto, P. M. C. (1975). Radon-222 emanation characteristics of rocks and minerals. *Radon in Uranium Mining*. IAEA. Wien: 129-150.

Barton, A. F. M. (1991). CRC Handbook of Solubility Parameters and Other Cohesion Parameters, CRC Press Boca Raton, Ann Arbor, Boston, London: 739p.

Blodau, C. (2006). A review of acidity generation and consumption in acidic coal mine lakes and their watersheds. *Science of the Total Environment* 369: 307-332.

Bocanegra, R., Hopke, P. K. (1988). Radon adsorption on activated carbon and the effect of some airborne contaminants. *Science of the Total Environment* 76(2-3): 193-202.

Boehrer, B., Schultze, M. (2006). On the relevance of meromixis in mine pit lakes. Proceedings of the 7th International Congress on Acid Rock Drainage (ICARD), 27th-29th March, St. Louis, USA.

Boehrer, B., Schultze, M. (2008). Stratification of lakes. *Reviews of Geophysics*: in press. doi: 10.1029/2007RG000210.

Bonotto, D. M., Andrews, J. N. (1997). The implications of laboratory ^{222}Rn flux

measurements to the radioactivity in groundwater: the case of a karstic limestone aquifer. *Applied Geochemistry* 12: 715-726.

Borges, A. V., Delille, B., Schiettecatte, L. S., Gazeau, F., Abril, G., Frankignoulle, M. (2004). Gas transfer velocities of CO_2 in three European estuaries (Randers Fjord, Scheldt, and Thames). *Limnology and Oceanography* 49: 1630-1641.

Bossus, D. A. W. (1984). Emanating power and specific surface area. *Radiation Protection Dosimetry* 7: 73-76.

Burnett, W. C., Kim, G., Lane-Smith, D. (2001). A continuous radon monitor for assessment of ^{222}Rn in coastal ocean waters. *Journal of Radioanalytical and Nuclear Chemistry* 249(1): 167-172.

Burnett, W. C., Bokuniewicz, H., Huettel, M., Moore, W. S., Taniguchi, M. (2003a). Groundwater and pore water inputs to the coastal zone. *Biogeochemistry* 66: 3-33.

Burnett, W. C., Cable, J. E., Corbett, D. R. (2003b). Radon tracing of submarine groundwater discharge in coastal environments. *Land and Marine Hydrogeology*. M. Taniguchi, K. Wang, T. Gamo (Eds.). Elsevier: 25-43.

Burnett, W. C., Dulaiova, H. (2003). Estimating the dynamics of groundwater input into the coastal zone via continuous radon-222 measurements. *Journal of Environmental Radioactivity* 69: 21-35.

Burnett, W. C., Aggarwal, P. K., Aureli, A., Bokuniewicz, H., Cable, J. E., Charette, M. A., Kontar, E., Krupa, S., Kulkarni, K. M., Loveless, A., Moore, W. S., Oberdorfer, J. A., Oliveira, J., Ozyurt, N., Povinec, P., Privitera, A. M. G., Rajar, R., Ramassur, R. T., Scholten, J., Stieglitz, T., Taniguchi, M., Turner, J. V. (2006). Quantifying submarine groundwater discharge in the coastal zone via multiple methods. *Science of the Total Environment* 367: 498-543.

Burnett, W. C., Dulaiova, H. (2006). Radon as a tracer of submarine groundwater discharge into a boat basin in Donnalucata, Sicily. *Continental Shelf Research* 26(7): 862-873.

Burnett, W. C., Santos, I. R., Weinstein, Y., Swarzenski, P. W., Herut, B. (2007). Remaining uncertainties in the use of Rn-222 as a quantitative tracer of submarine groundwater discharge. *A New focus on groundwater-seawater interactions*. W.

Sanford, C. Langevin, M. Polemio, P. Povinec (Eds.). Perugia, Italy, IAHS Publ. 312: 109-118.

Burnett, W. C., Peterson, R., Moore, W. S., de Oliveira, J. (2008). Radon and radium isotopes as tracers of submarine groundwater discharge - Results from the Ubatuba Brazil SGD assessment intercomparison. *Estuarine Coastal and Shelf Science* 76: 501-511.

Cable, J. E., Burnett, W. C., Chanton, J. P., Weatherly, G. L. (1996). Estimating groundwater discharge into the northeastern Gulf of Mexico using radon-222. *Earth and Planetary Science Letters* 144: 591-604.

Cable, J. E. and Martin, J. B. (2008). In situ evaluation of nearshore marine and fresh pore water transport into Flamengo Bay, Brazil. *Estuarine Coastal and Shelf Science* 76: 473-483.

Cecil, L. D., Green, J. R. (1999). Radon-222. *Environmental tracers in subsurface hydrogeology*. P. Cook, A. Herczeg (Eds.). Boston, Kluwer: 175-195.

Chanton, J. P., Burnett W. C., Dulaiova, H., Corbett, D. R., Taniguchi, M. (2003). Seepage rate variability in Florida Bay driven by Atlantic tidal height. *Biogeochemistry* 66: 187-202.

Clever, H. L. (1979). Solubility data series, Volume 2: Krypton, Xenon and Radon – gas solubilities. *International Union of Pure and Applied Chemistry*. H. L. Clever, Pergamon Press; Oxford/UK.

Cohen, B. L., Nason, R. (1986). A diffusion barrier charcoal adsorption collector for measuring Rn concentrations in indoor air. *Health Physics* 50: 457–463.

Cook, P. G., Solomon, D. K., Plummer, L. N., Busenberg, E., Schiff, S. L. (1995). Chlorofluorocarbons as tracers of groundwater transport processes in a shallow, silty sand aquifer. *Water Resources Research* 31: 425-434.

Cook, P. G., Favreau, G., Dighton, J. C., Tickell, S. (2003). Determining natural groundwater influx to a tropical river using radon, chlorofluorocarbons and ionic environmental tracers. *Journal of Hydrology* 277: 74-88.

Cook, P. G., Lamontagne, S., Berhane, D., Clark, J. F. (2006). Quantifying groundwater

discharge to Cockburn River, southeastern Australia, using dissolved gas tracers Rn-222 and SF_6. *Water Resources Research* 42: W10411.

Corbett, D. R., Burnett, W. C., Cable, P. H., Clark, S. B. (1997). Radon tracing of groundwater input into Par Pond, Savannah River Site. *Journal of Hydrology* 203(1-4): 209-227.

Corbett, D. R., Burnett, W. C., Cable, P. H., Clark, S. B. (1998). A multiple approach to the determination of radon fluxes from sediments. *Journal of Radioanalytical and Nuclear Chemistry* 236: 247-252.

Corbett, D. R., Dillon, K., Burnett, W. C., Chanton, J. (2000). Estimating the groundwater contribution into Florida Bay via natural tracers, ^{222}Rn and CH_4. *Limnology and Oceanography* 45: 1546-1557.

Cothern, C. R. (1987). Properties. *Environmental Radon*. C. R. Cothern, J. E. Smith Jr. (Eds.). New York, Plenum Press. 35: 1-30.

Craig, H. (1969). Abyssal carbon and radiocarbon in the pacific. *Journal of Geophysical Research* 74: 5491-5506.

Crusius, J., Koopmans, D., Bratton, J. F., Charette, M. A., Kroeger, K., Henderson, P., Ryckman, L., Halloran, K., Coleman, J. A. (2005). Submarine groundwater discharge to a small estuary estimated from radon and salinity measurements and a box model. *Biogeosciences* 2: 141-157.

De Jong, P., Van Dijk, W., De Vries, W., Van der Graaf, E. R., Roelofs, L. M. M. (2005). Interlaboratory comparison of three methods for the determination of the radon exhalation rate of building materials. *Health Physics* 88: 59-64.

Durridge Company, Inc. (2000). RAD7 radon detector - Owner's manual: 77p.

Eissmann, L., Litt, T. (1994). Klassische Quartärfolge Mitteldeutschlands von der Elsterzeit bis zum Holozän unter besonderer Berücksichtigung der Stratigraphie, Paläoökologie und Vorgeschichte. *Altenburger Naturwissenschaftliche Forschungen* 7: 250-356.

Ellins, K. K., Roman-Mas, A., Lee, R. W. (1990). Using ^{222}Rn to examine groundwater/surface discharge interaction in the Rio Grande de Manati, Puerto

Rico. *Journal of Hydrology* 115(1-4): 319-341.

Evangelou, V. P., Zhang, Y. L. (1995). A review: pyrite oxidation mechanism and acid mine drainage prevention. *Environmental Science & Technology* 25: 141-199.

Ferry, C., Richon, P., Beneito, A., Cabrera, J., Sabroux, J.-C. (2002). An experimental method for measuring the radon-222 emanation factor in rocks. *Radiation Measurements* 35: 579-583.

Freeze, R. A., Cherry, J. A. (1979). Groundwater. Englewood Cliffs: 604p.

Freyer, K., Treutler, H. C., Dehnert, J., Nestler, W. (1997). Sampling and measurement of radon-222 in water. *Journal of Environmental Radioactivity* 37(3): 327-337.

Freyer, K., Treutler, H. C., Just, G., Philipsborn, v. H. (2003). Optimization of time resolution and detection limit for online measurements of ^{222}Rn in water. *Journal of Radioanalytical and Nuclear Chemistry* 257: 129-132.

Gallagher, D. L., Dietrich, A. M., Reay, W. G., Hayes, M. C., Simmons, G. M. (1996). Ground water discharge of agricultural pesticides and nutrients to estuarine surface water. *Ground Water Monitoring and Remediation* 16: 118-129.

Gandy, C. J., Smith, J. W. N., Jaris, A. P. (2007). Attenuation of mining-derived pollutants in the hyporheic zone: A review. *Science of the Total Environment* 373: 435-446.

Gaul, W. C., Underhill, D. W. (2005). Dynamic adsorption of radon by activated carbon. *Health Physics* 88: 371-378.

Genitron Instruments (2002). Bedienungsanleitung, Mobiler Radon-Monitor "AlphaGUARD": 40p.

Gibson, J. J., Prepas, E. E., McEachern, P. (2002). Quantitative comparison of lake throughflow, residency, and catchment runoff using stable isotopes: modelling and results from a regional survey of Boreal lakes. *Journal of Hydrology* 262: 128-144.

Gooddy, D. C., Darling, W. G., Abesser, C., Lapworth, D. J. (2006). Using chlorofluorocarbons (CFCs) and sulphur hexafluoride (SF_6) to characterise groundwater movement and residence time in a lowland Chalk catchment. *Journal*

of Hydrology 330: 44-52.

Göttlicher, J., Gasharova, B. (2000). Interactions of iron and sulfur bearing solid phase with water in surface coal mining pits and acidic mining lakes. *Applied Mineralogy in Research, Economy, Technology, Ecology and Culture*. D. Rammlmair (Ed.). Rotterdam, Balkema: 557-560.

Greenman, D. J., Rose, A. W. (1996). Factors controlling the emanation of radon and thoron in soils of the eastern U.S.A. *Chemical Geology* 129: 1-14.

Haferkorn, U., Müller, K., Mellentin, U., Fahl, J. (2003). Möglichkeiten und Grenzen der Stofftransportmodellierung (Nitrat) am Beispiel des Parthegebietes. *UFZ-Bericht*: 14p.

Hagerthey, S. E., Kerfoot, W. C. (1998). Groundwater flow influences the biomass and nutrient ratios of epibenthic algae in a north temperate seepage lake. *Limnology and Oceanography* 43: 1227-1242.

Harvey, F. E., Rudolph, D. L., Frape, S. K. (2000). Estimating ground water flux into large lakes: Application in the Hamilton Harbor, western Lake Ontario. *Ground Water* 38(4): 550-565.

Hayashi, M., Rosenberry, D. O. (2002). Effects of ground water exchange on the hydrology and ecology of surface water. *Ground Water* 40: 309-316.

Hildebrand, J. (1929). Solubility. XII. Regular solutions. *Journal of American Chemical Society* 51: 66-80.

Hoehn, E., von Gunten, H. R. (1989). Radon in groundwater: a tool to assess infiltration from surface waters to aquifers. *Water Resources Research* 25: 1795-1803.

Hohener, P., Surbeck, H. (2004). ^{222}Radon as a tracer for nonaqueous phase liqiud in the vadose zone: experiments and analytical model. *Vadose Zone Journal* 3: 1276-1285.

Iversen, N., Jørgsen, B. B. (1993). Diffusion coefficients of sulfate and methane in marine sediments: Influence of porosity. *Geochimica et Cosmochimica Acta* 57: 571-578.

Jensen, K. H., Bitsch, K., Bjerg, P. L. (1993). Large-scale dispersion experiments in a

sandy aquifer in Denmark - observed tracer movements and numerical-analyses. *Water Resources Research* 29: 673-696.

Key, R. M., Brewer, R. L., Stockwell, J. H., Guinasso, N. L., Schink, D. R. (1979). Some improved techniques for measuring radon and radium in marine sediments and in seawater. *Marine Chemistry* 7: 251-264.

Kishel, H. F., Gerla, P. J. (2002). Characteristics of preferential flow and groundwater discharge to Shingobee Lake, Minnesota, USA. *Hydrological Processes* 16: 1921-1934.

Kluge, T., Ilmberger, J., von Rohden, C., Aeschbach-Hertig, W. (2007). Tracing and quantifying groundwater inflow into lakes using a simple method for radon-222 analysis. *Hydrology and Earth System Sciences* 11: 1621-1631.

Knöller, K., Strauch, G. (2002). The application of stable isotopes for assessing the hydrological, sulfur, and iron balances of acidic mining lake ML111 (Lusatia, Germany) as a basis for biotechnological remediation. *Water, Air, and Soil Pollution: Focus* 2: 3-14.

Knöller, K., Fauville, A., Mayer, B., Strauch, G., Friese, K., Veizer, J. (2004). Sulfur cycling in an acid mining lake and its vicinity in Lusatia, Germany. *Chemical Geology* 204: 303-323.

Kraemer, T. F. (2005). Radium isotopes in Cayuga Lake, New York: Indicators of inflow and mixing processes. *Limnology and Oceanography* 50(1): 158-168.

Krishnaswami, S., Seidemann, D. E. (1988). Comparative study of ^{222}Rn, ^{40}Ar, ^{39}Ar and ^{37}Ar leakage from rocks and minerals: Implications for the role of nanopores in gas transport through natural silicates. *Geochimica et Cosmochimica Acta* 52: 655-658.

Kupetz, M. (1997). Geologischer Bau und Genese der Stauchendmoräne Muskauer Faltenbogen. *Brandenburgische Geowiss. Beitr* 4: 1-20.

Lau, S., Schubert, M. and Meißner, R. (2004). Ein neues Verfahren zur Lokalisierung von Bodenkontaminationen durch Mineralöle. *Wasserwirtschaft*, 4: 27-30.

Lee, D. R. (1977). A device for measuring seepage flux in lake and estuaries. *Limnology*

and Oceanography 22(1): 140-147.

Lee, J. M., Kim, G. (2006). A simple and rapid method for analyzing radon in coastal and ground waters using a radon-in-air monitor. *Journal of Environmental Radioactivity* 89(3): 219-228.

Macintyre, S., Wanninkhof, R., Chanton, J. P. (1995). Trace gas exchange across the air-water interface in freshwater and coastal marine environments. *Methods in Ecology- Biogenic Trace Gases: Measuring Emissions from Soil and Water*. P. A. Matson, R. C. Harriss (Eds.). Cambridge, Mass., Blackwell Science: 52-97.

Maerki, M., Wehrli, B., Dinkel, C., Muller, B. (2004). The influence of tortuosity on molecular diffusion in freshwater sediments of high porosity. *Geochimica et Cosmochimica Acta* 68: 1519-1528.

Maraziotis, E. A. (1996). Effects of intraparticle porosity on the radon emanation coefficient. *Environmental Science & Technology* 30: 2441-2448.

Martens, C. S., Kipphut, G. W., Klump, J. V. (1980). Sediment-water chemical exchange in the coastal zone traced by in situ radon-222 flux measurements. *Science* 208: 285-288.

Mathieu, G. G., Biscaye, P. E., Lupton, R. A., Hammond, D. E. (1988). System for measurement of Rn-222 at low-levels in natural-waters. *Health Physics* 55(6): 989-992.

McCoy, C. A., Corbett, D. R., McKee, B. A. and Top, Z. (2007). An evaluation of submarine groundwater discharge along the continental shelf of Louisiana using a multiple tracer approach. *Journal of Geophysical Research-Oceans* 112: C03013

Menditto, A., Patriarca, M., Magnusson, B. (2007). Understanding the meaning of accuracy, trueness and precision. *Accreditation and Quality Assurance* 12: 45-47.

Michel, J. (1987). Sources. *Environmental Radon*. C. R. Cothern, J. E. Smith Jr. (Eds.) New York, Plenum Press. 35: 81-130.

Moore, W. S. (1996). Large groundwater inputs to coastal environments revealed by ^{226}Ra enrichments. *Nature* 380: 612-614.

Moore, W. S. (2006). The role of submarine groundwater discharge in coastal

biogeochemistry. *Journal of Geochemical Exploration* 88(1-3): 389-393.

Müller, M., Sames, D., Mansel, H. (2003). PCGEOFIM - A Finite Volume Model for More? MODFLOW and More 2003: Understanding through Modelling, International Ground Water Modeling Center (IGWMC), Colorado School of Mines, Golden, Colorado.

Mullinger, N. J., Binley, A. M., Pates, J. M., Crook, N. P. (2007). Radon in chalk streams: spatial and temporal variation of groundwater sources in the Pang and Lambourn catchments, UK. *Journal of Hydrology* 339: 172-182.

Nazaroff, W. W., Moed, B. A., Sextro, R. G. (1988). Soil as a Source of Indoor Radon: Generation, Migration, and Entry. *RADON AND ITS DECAY PRODUCTS IN INDOOR AIR*. W. W. Nazaroff, A. V. Nero (Eds.). New York/USA, John Wiley & Sons: 57-112.

Nazaroff, W. W. (1992). Radon transport from soil to air. *Reviews of Geophysics* 30(2): 137-160.

Nörenberg, H., Burlakov, V. M., Kosmella, H. J., Smith, G. D. W., Briggs, G. A. D., Miyamoto, T., Tsukahara, Y. (2001). Pressure-dependent permeation of noble gases (He, Ne, Ar, Kr, Xe) through thin membranes of oriented polypropylene (OPP) studied by mass spectrometry. *Polymer* 42: 10021-10026.

Pates, J. M., Mullinger, N. J. (2007). Determination of Rn-222 in fresh water: Development of a robust method of analysis by alpha/beta separation liquid scintillation spectrometry. *Applied Radiation and Isotopes* 65(1): 92-103.

Peng, T.-H., Takahashi, T., Broecker, W. S. (1974). Surface radon measurements in the north pacific ocean station papa. *Journal of Geophysical Research* 79(12): 1772-1780.

Porcelli, D., Swarzenski, P. W. (2003). The behavior of U- and Th-series nuclides in groundwater. *Reviews in Mineralogy and Geochemistry*. B. Bourdon, G. M. Henderson, C. C. Lundstrom, S. P. Turner (Eds.). Geochemical Society Mineralogical Society of America. 52: 317-361.

Prausnitz, J. M., Lichtenthaler, R. N., de Azevedo, E. G. (1986). Molecular thermodynamics of fluid-phase equilibria. Englewood Cliffs, New Jersey, PTR

Prentice-Hall, Inc. 860p.

Przylibski, T. A. (2000). Estimating the radon emanation coefficient from crystalline rocks into groundwater. *Applied Radiation and Isotopes* 53(3): 473-479.

Purtscheller, F., Pirchl, T., Sieder, G., Stingl, V., Tessadri, T., Brunner, P., Ennemoser, O., Schneider, P. (1995). Radon emanation from giant landslides of Koefels (Tyrol, Austria) and Langtang-Himal (Nepal). *Environmental Geology* 26(1): 32-38.

Rama, Moore, W. S. (1984). Mechanism of transport of U-Th series radioisotopes from solids into ground water. *Geochimica et Cosmochimica Acta* 48: 395-399.

Rascher, J., Meier, J., Kupetz, M. (2000). Der Geopark Muskauer Faltenbogen – Grundlagen, Stand, Perspektiven. *Geowiss. Mitt. Thüringen, Beiheft* 10: 75-85.

Reinstorf, F., Strauch, G., Schirmer, K., Glaser, H. R., Moder, M., Wennrich, R., Osenbruck, K., Schirmer, M. (2008). Mass fluxes and spatial trends of xenobiotics in the waters of the city of Halle, Germany. *Environmental Pollution* 152(2): 452-460.

Rona, E. (1917). Diffusionsgröße and Atomdurchmesser der Radiumemanation. *Zeitschrift für physikalische Chemie* 92: 213-218.

Santos, I. R., Burnett, W., Chanton, J. P., Mwashote, B., Suryaputra, I. G. N. A., Dittmar, T. (2008a). Nutrient biogeochemistry in a Gulf of Mexico subterranean estuary and groundwater-derived fluxes to the coastal ocean. *Limnology and Oceanography* 53: 705-718.

Santos, I. R., Niencheski, F., Burnett, W., Peterson, R., Chanton, J., Andrade, C. F., Milani, I. B., Schmidt, A., Knoeller, K. (2008b). Tracing anthropogenically-driven groundwater discharge into a coastal lagoon from southern Brazil. *Journal of Hydrology*: in press. doi: 10.1016/j.jhydrol.2008.02.010.

Scatchard, G. (1931). Equilibria in non-electrolyte solutions in relation to the vapor pressures and densities of the components. *Chemical Review* 8: 321-333.

Schlüter, M., Sauter, E. J., Andersen, C. E., Dahlgaard, H., Dando, P. R. (2004). Spatial distribution and budget for submarine groundwater discharge in Eckernforde Bay

(Western Baltic Sea). *Limnology and Oceanography* 49(1): 157-167.

Schmidt, A., Schubert, M. (2007). Using radon-222 for tracing groundwater discharge into an open-pit lignite mining lake - a case study. *Isotopes in Environmental and Health Studies* 43(4): 387-400.

Schmidt, A., Stringer, C. E., Haferkorn, U., Schubert, M. (2008). Quantification of groundwater discharge into lakes using radon-222. *Environmental Geology*: in press. doi: 10.1007/s00254-008-1186-3.

Schneider, R. L., Negley, T. L., Wafer, C. (2005). Factors influencing groundwater seepage in a large, mesotrophic lake in New York. *Journal of Hydrology* 310(1-4): 1-16.

Schubert, M. (2006). Radon in Bodenluft und Grundwasser als natürlicher Tracer zur Beantwortung umweltrelavanter und geowissenschaftlicher Fragestellungen. Institut für Geophysik und Geologie, Universität Leipzig. Leipzig, Habilitation: 227p.

Schubert, M., Bürkin, W., Peña, P., Lopez, A., Balcázar, M. (2006). On-site determination of the radon concentration in water samples: methodical background and results from laboratory studies and a field-scale test. *Radiation Measurements* 41: 492-497.

Schubert, M., Lehmann, K., Paschke, A. (2007a). The partition coefficient of radon between water and fuel oil model mixtures and its use for the assessment of subsurface NAPL contamination. *Science of the Total Environment* 376: 306-316.

Schubert, M., Paschke, A., Lau, S., Geyer, W., Knöller, K. (2007b). Radon as a naturally occurring tracer for the assessment of residual NAPL contamination of aquifers. *Environmental Pollution* 145: 920-927.

Schubert, M., Schmidt, A., Paschke, A., Lopez, A., Balcázar, M. (2008). In situ determination of radon in surface water bodies by means of a hydrophobic membrane tubing. *Radiation Measurements* 43: 111-120.

Schumann, R. R., Gundersen, L. C. S. (1996). GEOLOGIC AND CLIMATIC CONTROLS ON THE RADON EMANATION COEFFICIENT. *Environmental International* 22(1): 439-446.

Sebestyen, S. D. and Schneider, R. L. (2001). Dynamic temporal patterns of nearshore seepage flux in a headwater Adirondack lake. *Journal of Hydrology* 247: 137-150.

Sebestyen, S. D., Schneider, R. L. (2004). Seepage patterns, pore water, and aquatic plants: hydrological and biogeochemical relationships in lakes. *Biogeochemistry* 68(3): 383-409.

Semkow, T. M., Parekh, P. P. (1990). The role of radium distribution and porosity in radon emantion from solids. *Geophysical Research Letters* 17: 837-840.

Semkow, T. M. (1991). Fractal model of radon emanation from solids. *Physical Review Letters* 66(23): 3012-3015.

Semprini, L., Hopkins, O. S., Tasker, B. R. (2000). Laboratory, field and modeling studies of radon-222 as a natural tracer for monitoring NAPL contamination. *Transport in Porous Media* 38: 223-240.

Shaw, R. D., Prepas, E. E. (1990a). Groundwater-lake interactions: I. Accuracy of seepage meter estimates of lake seepage. *Journal of Hydrology* 119(1-4): 105-120.

Shaw, R. D., Prepas, E. E. (1990b). Groundwater-lake interactions: II. Nearshore seepage patterns and the contribution of ground water to lakes in central Alberta. *Journal of Hydrology* 119(1-4): 121-136.

Shaw, R. D., Shaw, J. F. H., Fricker, H., Prepas, E. E. (1990c). An integrated approach to quantify groundwater transport of phosphorus to Narrow Lake, Alberta. *Limnology and Oceanography* 35: 870-886.

Stein, L. (1983). The chemistry of radon. *Radiochimica Acta* 32: 163-171.

Steinberg, M., Manowitz, B. (1959). Recovery of fission product noble gases. *Industrial & Engineering Chemistry Research* 51(1): 47-50.

Stieglitz, T. (2005). Submarine groundwater discharge into the near-shore zone of the Great Barrier Reef, Australia. *Marine Pollution Bulletin* 51(1-4): 51-59.

Stringer, C. (2004). Assessment of groundwater discharge to Lake Barco via radon tracing. Department of Oceanography, Florida State University. Tallahassee. Master Thesis: 58p.

Stringer, C., Burnett, W. C. (2004). Sample bottle design improvements for radon

emanation analysis of natural waters. *Health Physics* 87: 642-646.

Sun, H., Semkow, T. M. (1998). Mobilization of thorium, radium and radon radionuclides in ground water by successive alpha-recoils. *Journal of Hydrology* 205: 126-136.

Surbeck, H. (1996). A Radon-in-Water Monitor Based on Fast Gas Transfer Membranes. International Conference on Technologically Enhanced Natural Radioactivity (TENR) caused by Non-Uranium Mining, Szczyrk, Poland.

Swarzenski, P. W., Orem, W. H., McPherson, B. F., Baskaran, M., Wan, Y. (2006). Biogeochemical transport in the Loxahatchee River estuary, Florida: The role of submarine groundwater discharge. *Marine Chemistry* 101(3-4): 248-265.

Swarzenski, P. W. (2007). U/Th series radionuclides as coastal groundwater tracers. *Chemical Reviews* 107(2): 663-674.

Swarzenski, P. W., Reich, C., Kroeger, K. D., Baskaran, M. (2007). Ra and Rn isotopes as natural tracers of submarine groundwater discharge in Tampa Bay, Florida. *Marine Chemistry* 104(1-2): 69-84.

Taniguchi, M., Burnett, W. C., Dulaiova, H., Kontar, E. A., Povinec, P. P., Moore, W. S. (2006). Submarine groundwater discharge measured by seepage meters in Sicilian coastal waters. *Continental Shelf Research* 26(7): 835-842.

Tanner, A. B. (1964). Radon migration in the ground: A review. *Proceedings of the International Symposium on the Natural Radiation Environment*. J. A. S. Adams, W. M. Lowder (Eds.). University of Chicago Press: 161-181.

Tanner, A. B. (1980). Radon Migration in the Ground: A Supplementary Review. Proceedings of the International Symposium on the Natural Radiation Environment 3, Conf-780422; US Department of Commerce, National Technical Information Service, Springfield/Il/USA.

Treutler, H. C., Just, G., Schubert, M., Weiß, H. (2007). Radon as tracer for the determination of mean residence times of groundwater in decontamination reactors. *Journal of Radioanalytical and Nuclear Chemistry* 272: 583-588.

Tuccimei, P., Salvati, R., Capelli, G., Delitala, M. C., Primavera, P. (2005).

Groundwater fluxes into a submerged sinkhole area, Central Italy, using radon and water chemistry. *Applied Geochemistry* 20: 1831-1847.

Turner, J. E. (2007). Atoms, Radiation, and Radiation Protection. Weinheim, Wiley-VCH: 585p.

Ullman, W. J., Aller, R. C. (1982). Diffusions coefficients in nearshore marine sediments. *Limnology and Oceanography* 27(3): 552-556.

Van Rees, K. C. J., Sudicky, E. A., Rao, P. S., Reddy, K. R. (1991). Evaluation of laboratory techniques for measuring diffusion coefficients in sediments. *Environmental Science & Technology* 25(9): 1605-1611.

Weigel, F. (1978). Radon. *Chemiker-Zeitung* 102(9): 287-299.

Weinstein, Y., Burnett, W. C., Swarzenski, P. W., Shalem, Y., Yechieli, Y., Herut, B. (2007). Role of aquifer heterogeneity in fresh groundwater discharge and seawater recycling: An example from the Carmel coast, Israel. *Journal of Geophysical Research-Oceans* 112(C12).

Weyhenmeyer, G. (1998). Resuspension in lakes and its ecological impact - a review. *Arch. Hydrobiol. Spec. Issues Advanc. Limnol.*, 51: 185-200.

Wiegel, S., Aulinger, A., Brockmeyer, R., Harms, H., Loffler, J., Reincke, H., Schmidt, R., Stachel, B., von Tumpling, W., Wanke, A. (2004). Pharmaceuticals in the river Elbe and its tributaries. *Chemosphere* 57(2): 107-126.

Wilkening, M. (1990). Radon in the environment. Amsterdam, Elsevier: 137p.

Wu, Y., Wen, X., Zhang, Y. (2004). Analysis of the exchange of groundwater and river water by using Radon-222 in the middle Heihe Basin of northwestern China. *Environmental Geology* 45: 647-653.

Yehdegho, B., Rozanski, K., Zojer, H., Stichler, W. (1997). Interaction of dredging lakes with the adjacent groundwater field: An isotope study. *Journal of Hydrology* 192(1-4): 247-270.

Zektser, I. S., Loaiciga, H. A. (1993). Groundwater fluxes in the global hydrologic-cycle - past, present and future. *Journal of Hydrology* 144(1-4): 405-427.

Ich versichere, dass ich die von mir vorgelegte Dissertation selbständig angefertigt, die benutzten Quellen und Hilfsmittel vollständig angegeben und die Stellen der Arbeit – einschließlich Tabellen, Karten und Abbildungen –, die anderen Werken im Wortlaut oder dem Sinn nach entnommen sind, in jedem Einzelfall als Entlehnung kenntlich gemacht habe; dass diese Dissertation noch keiner anderen Fakultät oder Universität zur Prüfung vorgelegen hat; dass sie – abgesehen von unten angegebenen Teilpublikationen – noch nicht veröffentlicht worden ist sowie, dass ich eine solche Veröffentlichung vor Abschluss des Promotionsverfahrens nicht vornehmen werde. Die Bestimmungen der Promotionsordnung sind mir bekannt. Die von mir vorgelegte Dissertation ist von Professor Dr. Martin Melles betreut worden.

Teilpublikationen

Schmidt, A., Schlueter, M., Melles, M., Schubert, M. (2008). Continuous and discrete on-site detection of radon-222 in ground- and surface waters by means of an extraction module. *Applied Radiation and Isotopes,* doi:10.1016/j.apradiso.2008.05.005.

Schmidt, A., Stringer, C. E., Haferkorn, U., Schubert, M. (2008). Quantification of groundwater discharge into lakes using radon-222 as naturally occurring tracer. *Environmental Geology*, doi: 10.1007/s00254-008-1186-3.

Schubert, M., Schmidt, A., Paschke, A., Lopez, A., Balcázar, M. (2008). In situ determination of radon in surface water bodies by means of a hydrophobic membrane tubing. *Radiation Measurements*, 43, 111-120.

Schmidt, A., Schubert, M. (2007). Using radon-222 for tracing groundwater discharge into an open-pit lignite mining lake – a case study. *Isotopes in Environmental and Health Studies,* 43/4, 387-400.

Schmidt, A., Schubert, M. (2007). Using ^{222}Rn as environmental tracer for assessing groundwater/surface water interaction. *Geochimica et Cosmochimica Acta,* 71/15, A894.

Leipzig, 27. Juni 2008